Phase Space topology of Chaos: Theory and Applications

Denisse Sciamarella

Max Planck Institute for the Physics of Complex Systems

Phase Space topology of Chaos: Theory and Applications

Denisse Sciamarella (IFAEC-CNRS)

IFAECI Institut Franco-Argentin d'Études sur le Climat et ses Impacts

cnrs IRD CONICET Universidad de Buenos Aires

International Seminar & Workshop, October 12th 2023
MPIPKS Dresden

Institut Franco-Argentin d'Etudes sur le Climat et ses Impacts

INSTITUT FRANCO-ARGENTIN D'ÉTUDES SUR LE CLIMAT ET SES IMPACTS
INSTITUTO FRANCO-ARGENTINO DE ESTUDIOS SOBRE EL CLIMA Y SUS IMPACTOS

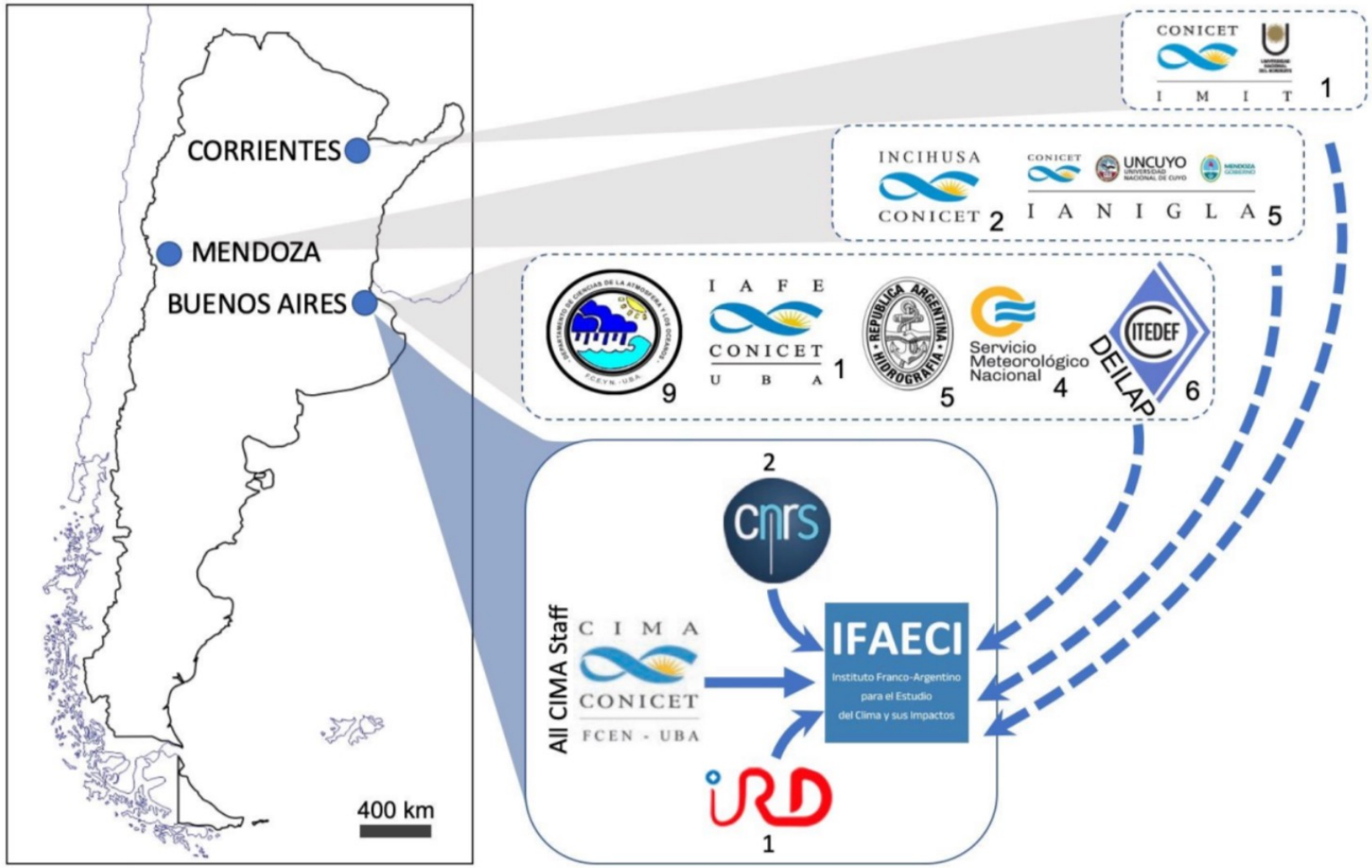

Max Planck Institute for the Physics of Complex Systems

Institut Franco-Argentin d'Etudes sur le Climat et ses Impacts

🇫🇷 ifaeci.cnrs.fr
🇦🇷 ifaeci.cima.fcen.uba.ar

IRL 3351 (CNRS)
UMI 262 (IRD)

~ 210 people
73 permanent staff
(2 CNRS researchers, 1 délégation IRD)
63 PhD students
67 Master students
7 étudiants de maîtrise
+ stagiaires (Ecole Polytechnique)

Regional hub for the Climate Sciences in South America

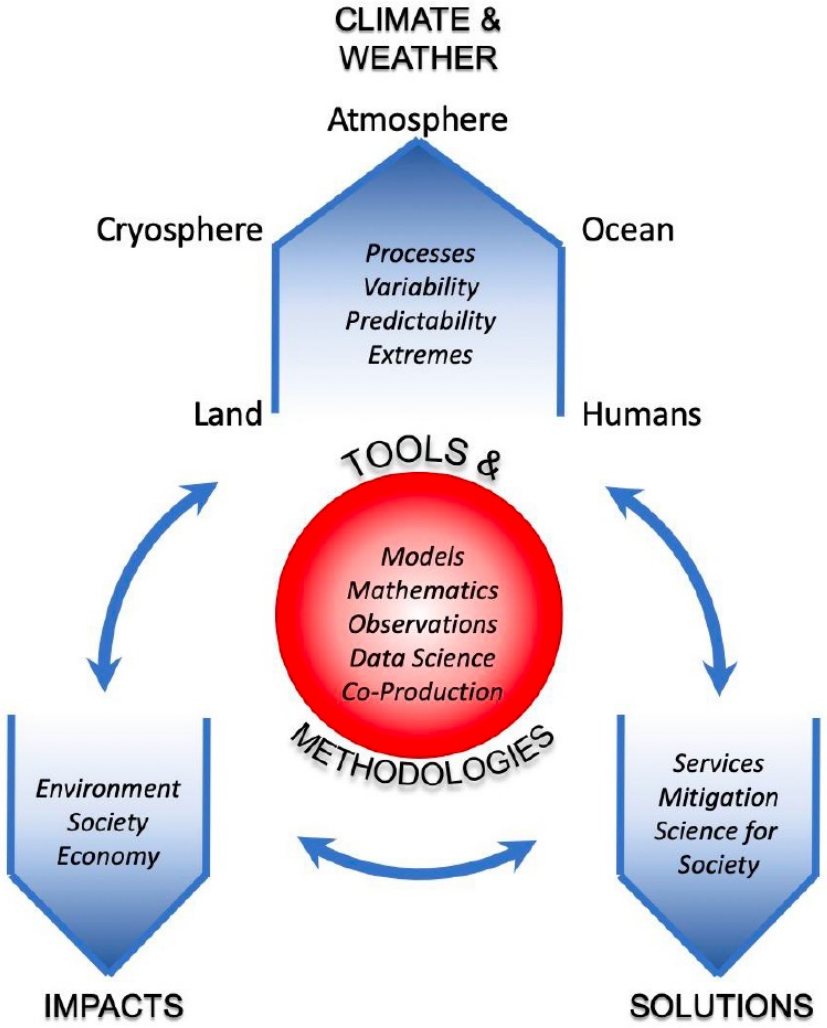

Max Planck Institute for the Physics of Complex Systems

TOOLS & METHODOLOGIES
Models
Mathematics
Observations
Data Science
Co-Production

Topology as a theoretical and data analysis tool for understanding the fundamental processes underlying the dynamics of complex systems.

This paper is based on the invited talks given by the two authors in an online series on "Perspectives on climate sciences: From historical developments to research frontiers".

Nonlin. Processes Geophys., 30, 399–434, 2023
https://doi.org/10.5194/npg-30-399-2023

Nonlinear Processes in Geophysics
Open Access
EGU

Review article

Review article: Dynamical systems, algebraic topology and the climate sciences

Michael Ghil[1,2,3] **and Denisse Sciamarella**[4,5,6]

[1]Geosciences Department and Laboratoire de Météorologie Dynamique (CNRS and IPSL), École Normale Supérieure and PSL University, 75231 Paris CEDEX 05, France
[2]Department of Atmospheric & Oceanic Sciences, University of California at Los Angeles, Los Angeles, CA 90095-1567, USA
[3]Departments of Mathematics and of Finance, Imperial College London, London, SW7 2BX, UK
[4]Institut Franco-Argentin d'Études sur le Climat et ses Impacts (IFAECI) International Reseach Laboratory 3351 (CNRS – IRD – CONICET – UBA) C1428EGA, Buenos Aires, Argentina
[5]Facultad de Ciencias Exactas y Naturales, Universidad de Buenos Aires, Buenos Aires, Argentina
[6]Centre National de la Recherche Scientifique, 75794 Paris CEDEX 16, France

Correspondence: Michael Ghil (ghil@atmos.ucla.edu) and Denisse Sciamarella (denisse.sciamarella@cnrs.fr)

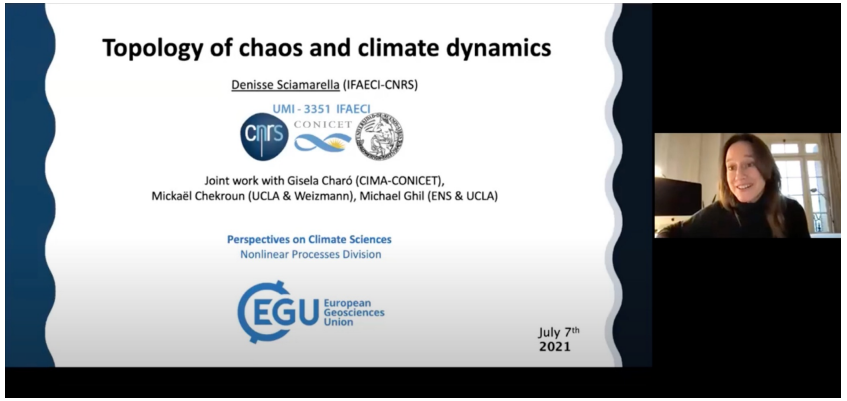

Max Planck Institute for the Physics of Complex Systems

Phase Space Topology of chaos: Theory and Applications

Introduction

- What is chaos topology?

Methods

- Isopleths, branched manifolds, cell complexes, homologies.

Applications

- Lagrangian analysis, Climate dynamics.

Templex

- Why and how was it conceived? How is it computed?

Random templex

- How is it defined? How does it encode topological tipping points?

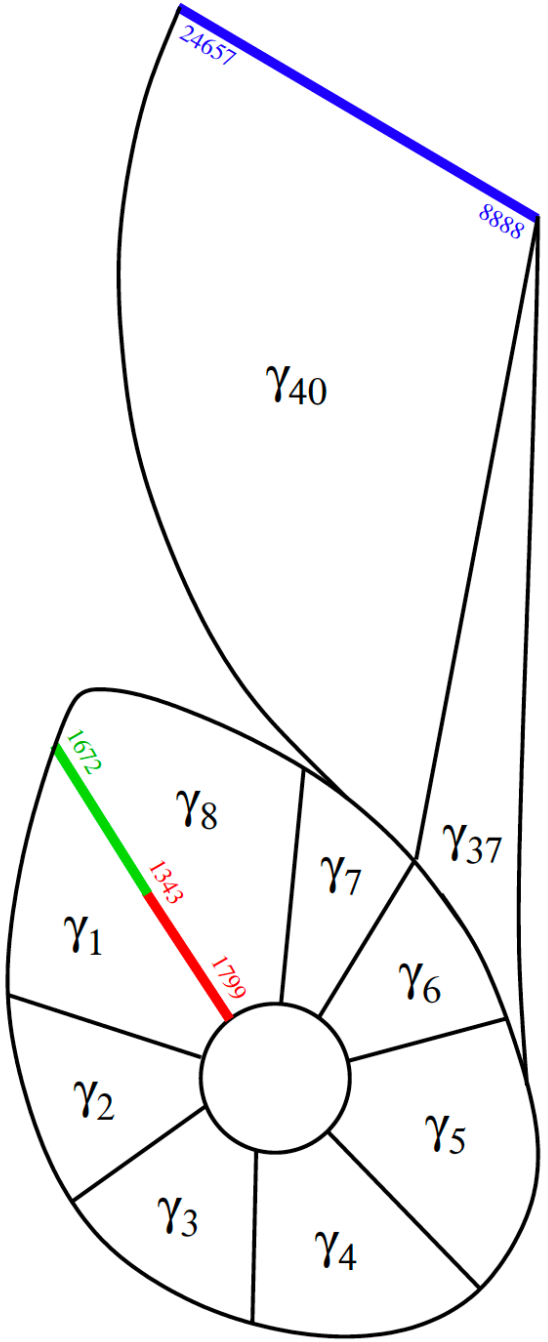

Introduction

- What is chaos topology and why is it important?

Topological chaos considers the problem of how fluid particle trajectories are entangled in physical space during a mixing experiment.

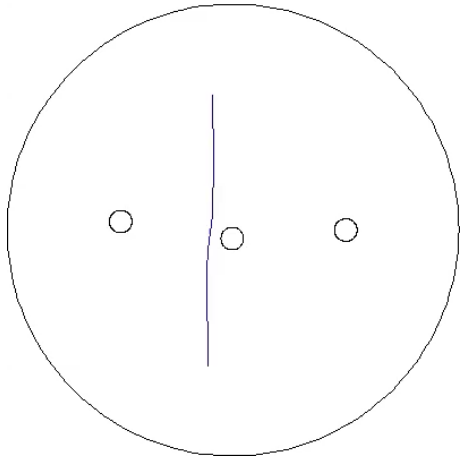

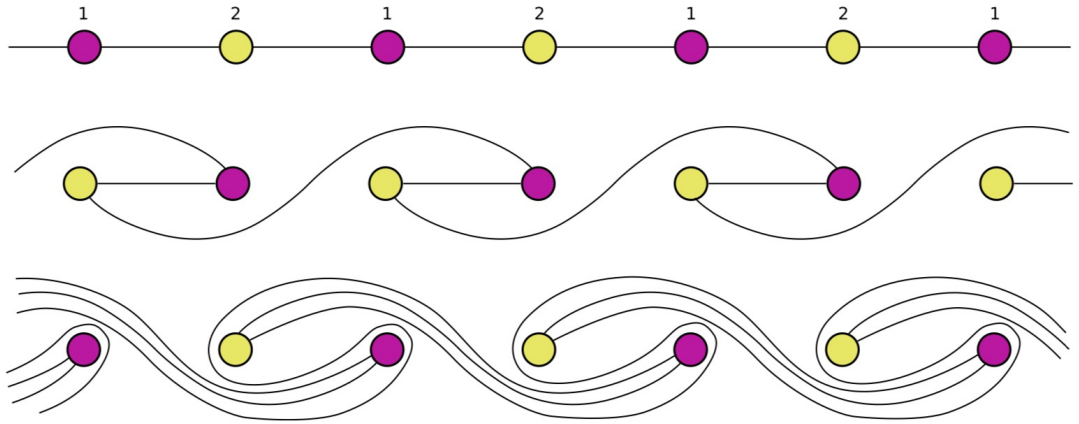

Topological mixing with ghost rods
Gouillart, *et al*. PRE 73, 036311 (2006)

It generally relies on the periodic motion of obstacles in a two-dimensional flow in order to form nontrivial braids. This motion generates exponential stretching of material lines, and hence efficient mixing.

Introduction

- What is chaos topology and why is it important?

Chaos topology (or topology of chaos) considers the problem of how *n*-dimensional trajectories/point-clouds are topologically structured in state space.

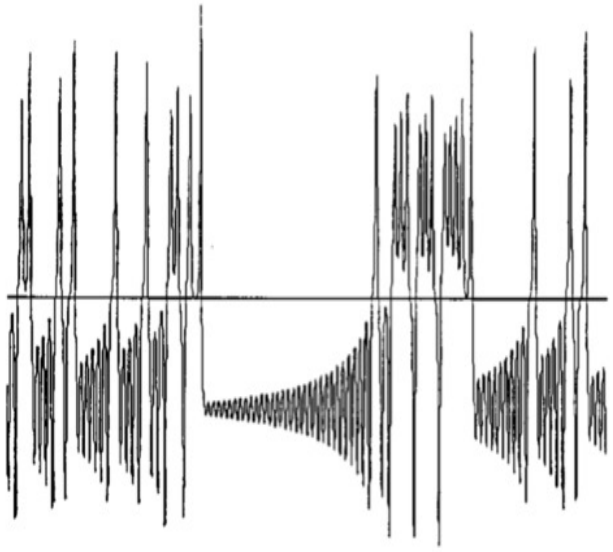

Optically pumped molecular laser run under a resonance-operating condition.

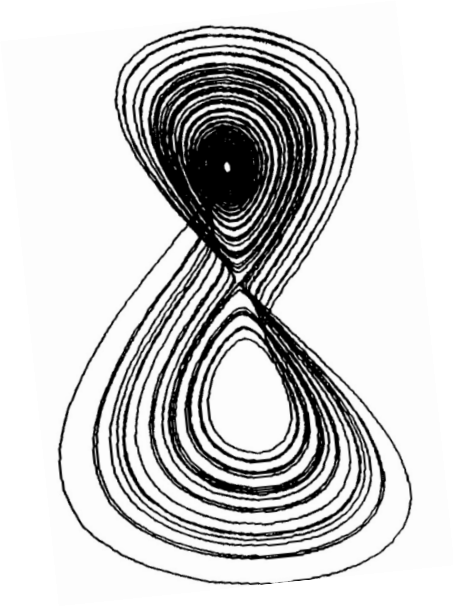

Embedding projection onto a plane.

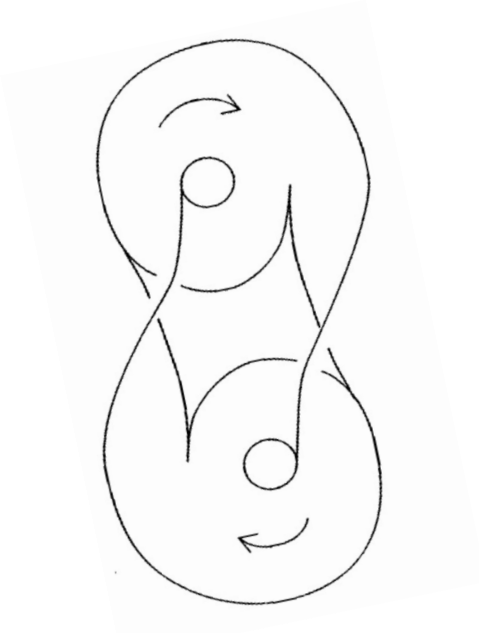

Branched manifold.

R. Gilmore, Reviews of Modern Physics, Vol. 70, No. 4, October 1998

Introduction

- What is chaos topology and why is it important?

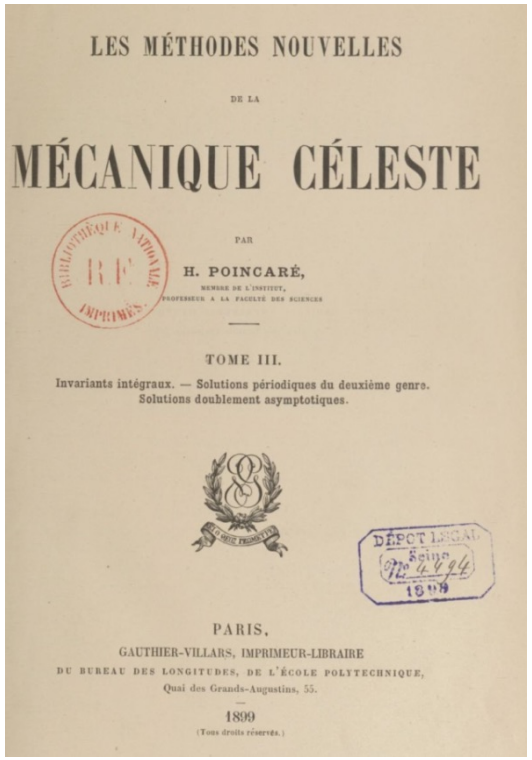
LES MÉTHODES NOUVELLES

DE LA

MÉCANIQUE CÉLESTE

PAR

H. POINCARÉ,

MEMBRE DE L'INSTITUT,
PROFESSEUR A LA FACULTÉ DES SCIENCES

TOME III.

Invariants intégraux. — Solutions périodiques du deuxième genre.
Solutions doublement asymptotiques.

PARIS,
GAUTHIER-VILLARS, IMPRIMEUR-LIBRAIRE
DU BUREAU DES LONGITUDES, DE L'ÉCOLE POLYTECHNIQUE,
Quai des Grands-Augustins, 55.

1899

The origins of « chaos » theory can be found in the pioneering works of Henri Poincaré towards the end of the XIX century concerning the old and difficult problem of the stability of the Solar System.

"Analysis Situs" is a seminal mathematics paper that he published in 1895 with five supplements that followed between 1899 and 1904.

These papers provided the first systematic treatment of topology and introduced the use of algebraic structures to study topological spaces, founding the field of algebraic topology.

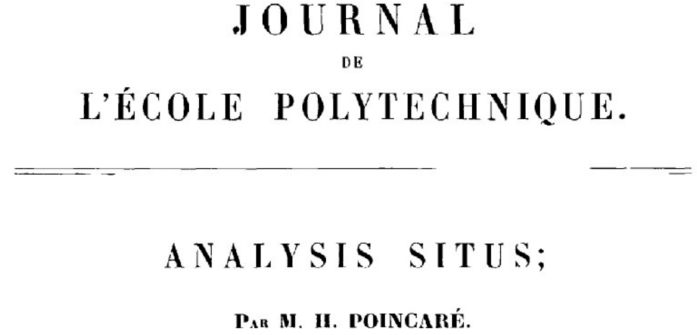
JOURNAL
DE
L'ÉCOLE POLYTECHNIQUE.

ANALYSIS SITUS;

PAR M. H. POINCARÉ.

Poincaré introduced the concept of homology, that we are going to encounter further and thoroughly in this presentation.

Introduction

- What is chaos topology and why is it important?

The first methods to reconstruct phase space from experimental time series and to study geometric structures significance in that space appear in 1980.

VOLUME 45, NUMBER 9 PHYSICAL REVIEW LETTERS 1 SEPTEMBER 1980

Geometry from a Time Series

N. H. Packard, J. P. Crutchfield, J. D. Farmer, and R. S. Shaw
Dynamical Systems Collective, Physics Department, University of California, Santa Cruz, California 95064
(Received 13 November 1979)

It is shown how the existence of low-dimensional chaotic dynamical systems describing turbulent fluid flow might be determined experimentally. Techniques are outlined for reconstructing phase-space pictures from the observation of a single coordinate of any dissipative dynamical system, and for determining the dimensionality of the system's attractor. These techniques are applied to a well-known simple three-dimensional chaotic dynamical system.

PACS numbers: 47.25.-c

Introduction

- What is chaos topology and why is it important?

Geometric methods continue to be used, e.g., to understand datasets of Lagrangian trajectories.

Understanding the geometry of transport: Diffusion maps for Lagrangian trajectory data unravel coherent sets

Cite as: Chaos **27**, 035804 (2017); https://doi.org/10.1063/1.4971788
Submitted: 20 March 2016 . Accepted: 18 July 2016 . Published Online: 22 February 2017

Ralf Banisch, and Péter Koltai

But is geometry the *best* lens we can use to classify data according to underlying differences in dynamics?

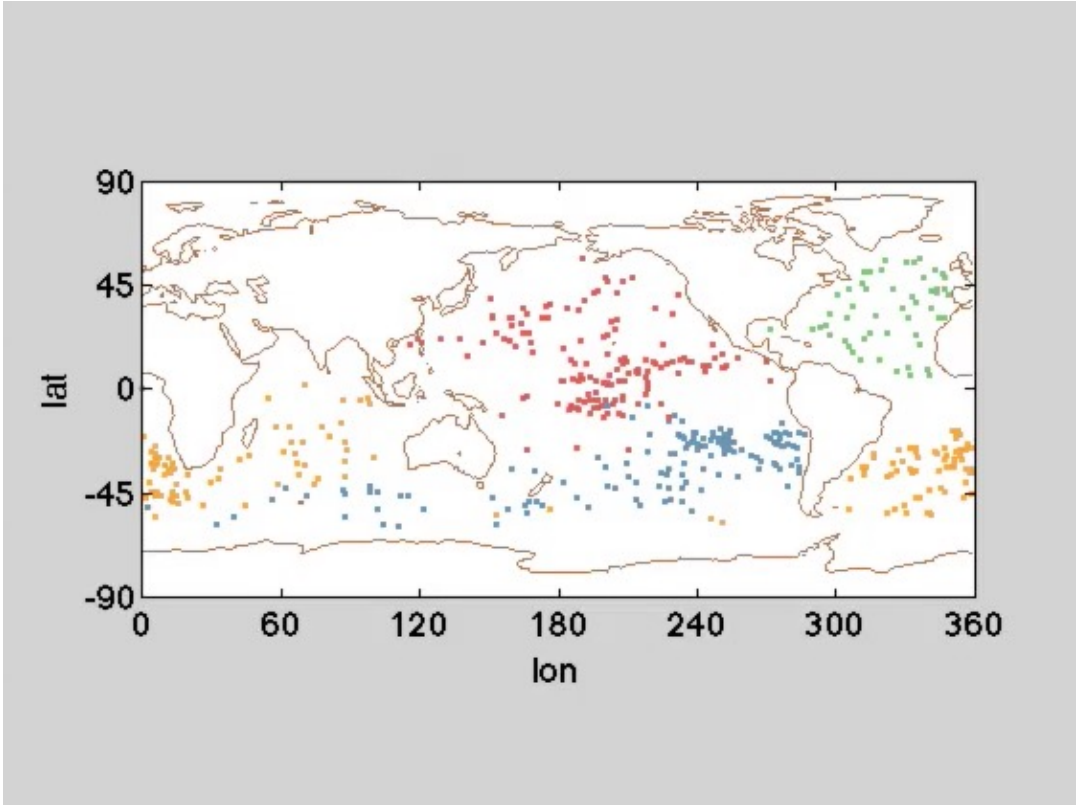

Introduction

- What is chaos topology and why is it important?

Invariants in phase space can be of different types:

a) Metric: dimensions of various types, e.g., correlation dimension (Grassberger & Procaccia, 1983), multifractal scaling functions (Halsey et al., 1986).

b) Dynamic: Lyapunov exponents (Oseledec, 1968; Wolf et al., 1985), as discussed by Eckmann & Ruelle (1985) and by Abarbanel et al. (1993).

c) Topological: linking numbers, relative rotation rates, Conway polynomials, Branched Manifolds (Birman & Williams, 1983).

Invariants (a) and (b) do not provide information on how to model the system's dynamics, while (c) actually does!

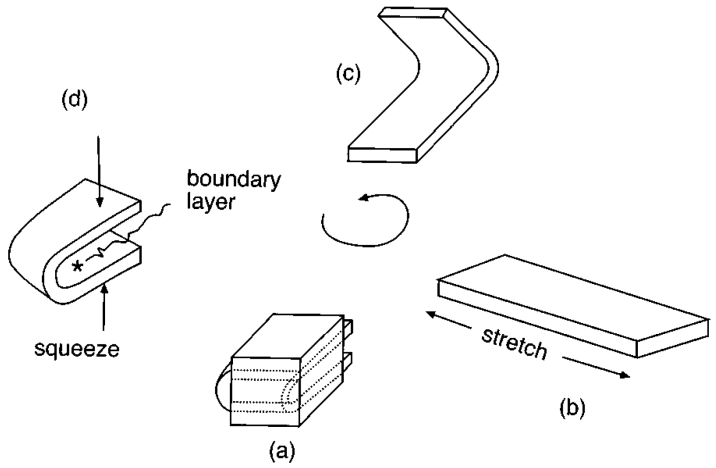

R. Gilmore, *Reviews of Modern Physics*, Vol. 70(4), October 1998

Introduction

- What is chaos topology and why is it important?

Topology is concerned with the properties of a geometric object that are preserved under continuous deformations, such as stretching, twisting, crumpling, and bending; that is, without closing holes, opening holes, gluing, or passing through itself. The animated image shows a continuous deformation of a mug into a doughnut: both objects are topologically equivalent.

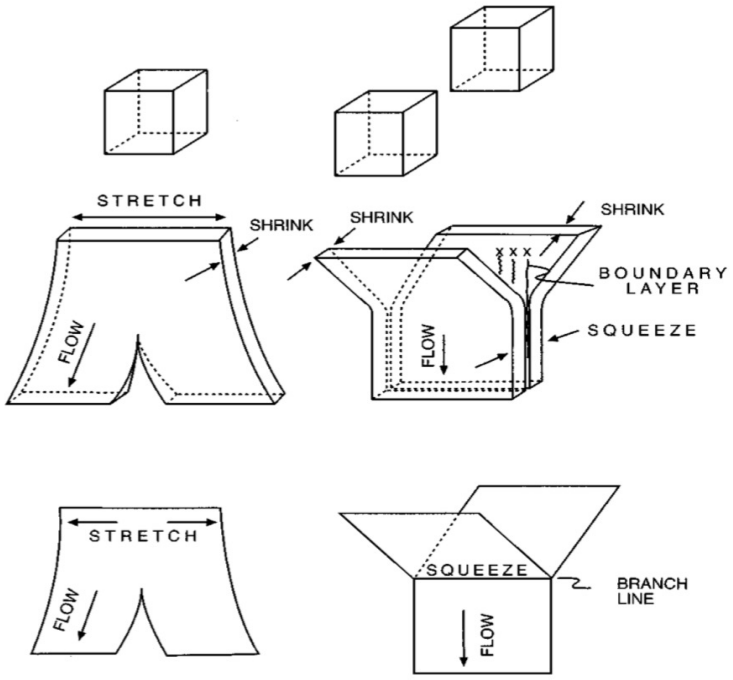

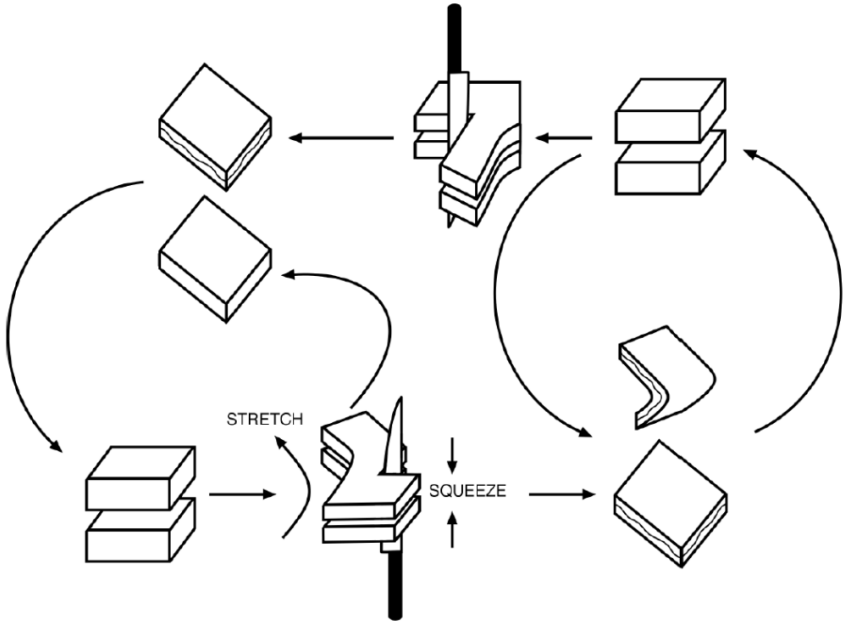

Gilmore & Lefranc. *The Topology of Chaos: Alice in Stretch and Squeezeland*. Wiley-Interscience, 2002.

The “recipe” to “knead” the Lorenz’63 attractor is a sequence of steps that are topological in nature.

Introduction

- What is chaos topology and why is it important?

The advantage of using topology, instead of geometry or fractality, to describe chaos lies in the fact that topology provides information about the stretching, folding, tearing or squeezing mechanisms that act in phase space to shape the flow.

Geometry may differ, but if the underlying dynamics is equivalent, the topology should be the same.

Unveiling the topology <=> Unveiling the dynamics

Methods

- Isopleths, branched manifolds, knot-holders, cell complexes, homologies

Henri Poincaré first described the way in which a dynamical system's properties depend upon its topology.

The concept of branched manifold, introduced by Robert F. Williams in 1974, was anticipated in Edward Lorenz's famous 1963 paper: on page 20, he remarks that the trajectory 'lives' on a surface and describes the architecture of the attractor in terms of "isopleths."

EXPANDING ATTRACTORS

by R. F. WILLIAMS

TABLE OF CONTENTS

Publ. Math. IHES, v. 43 (1974), p. 169–203

Deterministic Nonperiodic Flow[1]

EDWARD N. LORENZ

Massachusetts Institute of Technology

(Manuscript received 18 November 1962, in revised form 7 January 1963)

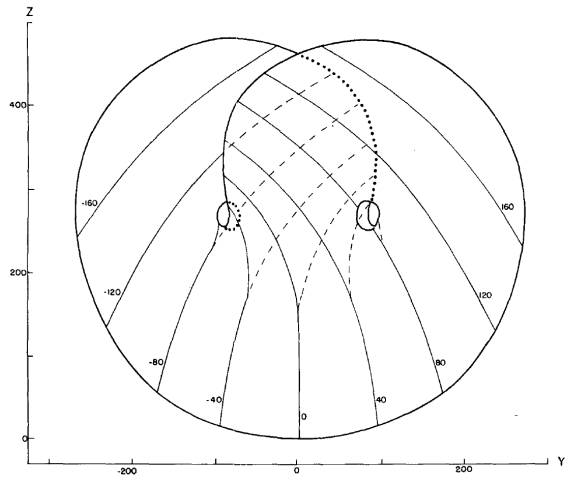

FIG. 3. Isopleths of X as a function of Y and Z (thin solid curves), and isopleths of the lower of two values of X, where two values occur (dashed curves), for approximate surfaces formed by all points on limiting trajectories. Heavy solid curve, and extensions as dotted curves, indicate natural boundaries of surfaces.

Methods

- Isopleths, branched manifolds, knot-holders, cell complexes, homologies

With Joan Birman, Robert F. Williams used branched manifolds to classify chaotic attractors in terms of the way periodic orbits are "knotted" in dynamical systems.

Topology Vol. 22, No. 1, pp. 47–82, 1983
Printed in Great Britain.

0040–9383/83/010047–36$03.00/0
Pergamon Press Ltd.

KNOTTED PERIODIC ORBITS IN DYNAMICAL SYSTEMS—I: LORENZ'S EQUATIONS

JOAN S. BIRMAN† and R. F. WILLIAMS‡

(*Received* 31 *March* 1980)

§1. INTRODUCTION

THIS PAPER is the first in a series which will study the following problem. We investigate a system of ordinary differential equations which determines a flow on the 3-sphere S^3 (or $\mathbb{R}^3$ or ultimately on other 3-manifolds), and which has one or perhaps many periodic orbits. We ask: can these orbits be knotted? What types of knots can occur? What are the implications?

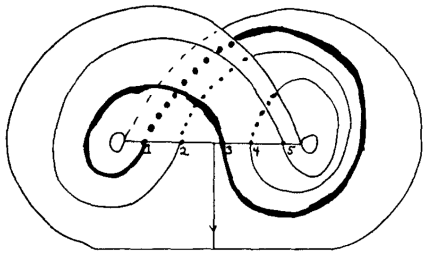

The set of unstable periodic orbits (UPOs) of the Lorenz attractor lie on a "Branched Manifold", i.e. on a 2-manifold or surface with the property that each point has a neighbourhood that is homoeomorphic to either a full 2-ball or a half 2-ball.

Birman & Williams discovered that systems whose branched manifolds have the same topology are dynamically equivalent.

Methods

- Isopleths, branched manifolds, knot-holders, cell complexes, homologies

Is there a "table of elements" for the different dynamics?

Dynamical system	ODEs	Parameters	Branched manifold
Rossler	$\dot{x} = -y - z$ $\dot{y} = x + ay$ $\dot{z} = b + z(x - c)$	$(a, b, c) = (2.0, 4.0, 0.398)$	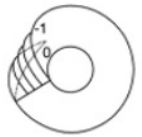
Duffing	$\dot{x} = y$ $\dot{y} = -\delta y - x^3 + x + A\sin(\omega t)$	$(\delta, A, \omega) = (0.4, 0.4, 1.0)$	
van der Pol	$\dot{x} = by + (c - dy^2)x$ $\dot{y} = -x + A\sin(\omega t)$	(b, c, d, A, ω) $=$ $(0.7, 1.0, 10.0, 0.25, \pi/2)$	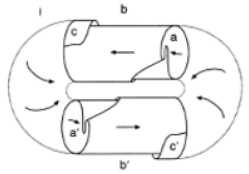
Lorenz	$\dot{x} = -\sigma x + \sigma y$ $\dot{y} = Rx - y - xz$ $\dot{z} = -bz + xy$	$(R, \sigma, b) = (26.0, 10.0, 8/3)$	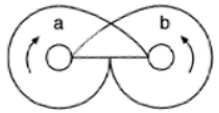

Gilmore & Lefranc. *The Topology of Chaos: Alice in Stretch and Squeezeland*. Wiley-Interscience, 2002.

Methods

- Isopleths, branched manifolds, knot-holders, cell complexes, homologies

In the late 90s, it was possible to determine whether or not two three-dimensional (3-D) dissipative dynamical systems are equivalent by using knot theory.

Topological analysis of chaotic dynamical systems

Robert Gilmore

Department of Physics & Atmospheric Science, Drexel University, Philadelphia, Pennsylvania 19104

Topological methods have recently been developed for the analysis of dissipative dynamical systems that operate in the chaotic regime. They were originally developed for three-dimensional dissipative dynamical systems, but they are applicable to all "low-dimensional" dynamical systems. These are systems for which the flow rapidly relaxes to a three-dimensional subspace of phase space. Equivalently, the associated attractor has Lyapunov dimension $d_L<3$. Topological methods supplement methods previously developed to determine the values of metric and dynamical invariants. However, topological methods possess three additional features: they describe how to model the dynamics; they allow validation of the models so developed; and the topological invariants are robust under changes in control-parameter values. The topological-analysis procedure depends on identifying the stretching and squeezing mechanisms that act to create a strange attractor and organize all the unstable periodic orbits in this attractor in a unique way. The stretching and squeezing mechanisms are represented by a caricature, a branched manifold, which is also called a template or a knot holder. This turns out to be a version of the dynamical system in the limit of infinite dissipation. This topological structure is identified by a set of integer invariants. One of the truly remarkable results of the topological-analysis procedure is that these integer invariants can be extracted from a chaotic time series. Furthermore, self-consistency checks can be used to confirm the integer values. These integers can be used to determine whether or not two dynamical systems are equivalent; in particular, they can determine whether a model developed from time-series data is an accurate representation of a physical system. Conversely, these integers can be used to provide a model for the dynamical mechanisms that generate chaotic data. In fact, the author has constructed a doubly discrete classification of strange attractors. The underlying branched manifold provides one discrete classification. Each branched manifold has an "unfolding" or perturbation in which some subset of orbits is removed. The remaining orbits are determined by a basis set of orbits that forces the presence of all remaining orbits. Branched manifolds and basis sets of orbits provide this doubly discrete classification of strange attractors. In this review the author describes the steps that have been developed to implement the topological-analysis procedure. In addition, the author illustrates how to apply this procedure by carrying out the analysis of several experimental data sets. The results obtained for several other experimental time series that exhibit chaotic behavior are also described. [S0034-6861(98)00304-3]

Reviews of Modern Physics, Vol. 70, No. 4, October 1998

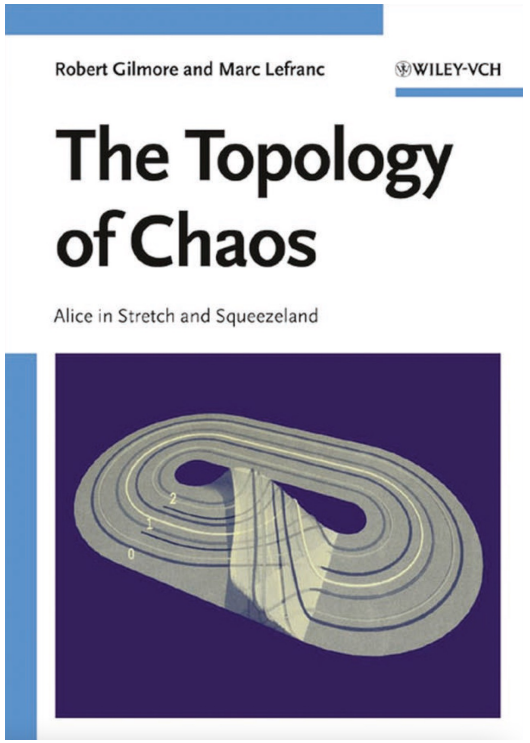

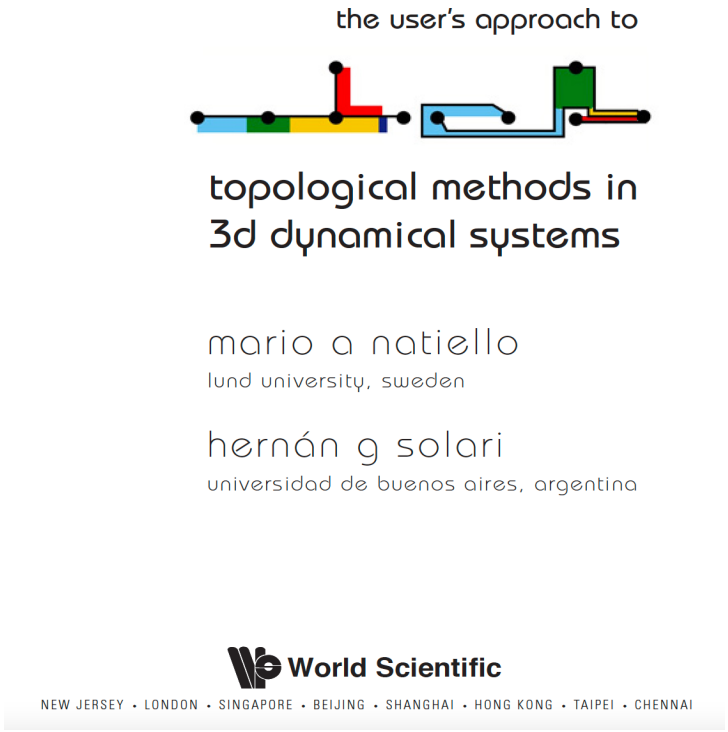

Methods

Computing topological invariants using **knots**…

3D trajectory set

Knot invariants

- Isopleths, branched manifolds, knot-holders, cell complexes, homologies

1) Approximate trajectories by closed curves.

2) Find a topological representation for the orbit structure.

3) Obtain an algebraic description for the topological structure.

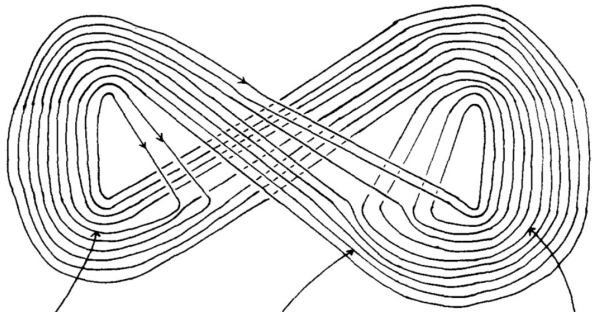

1 2 3

1

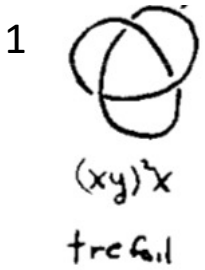

2

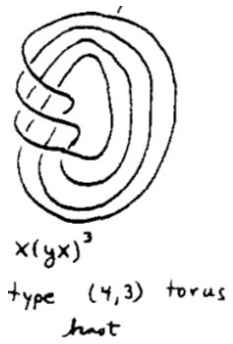

3

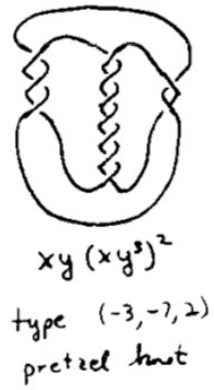

1) Close-return method – time series, though, must be long and noise free.

2) Knot theory – knot ≡ orbit in three dimensions.

3) Knot invariants – *e.g.*, linking numbers, Conway polynomials.

Knotted periodic orbits in dynamical systems. Topology: Vol.22. No. I,pp.47~81. 1983

Methods

- Isopleths, branched manifolds, knot-holders, cell complexes, homologies

Knot information for a chaotic attractor can be condensed in a knot-holder or template.

A chaotic attractor is an invariant set under the action of a flow. For strongly dissipative systems, this invariant set can be described strips that lodge the knots along the attractor.

The different branches discriminate the different paths followed by the flow determining the (fictive) boundaries between the different strips.

Typically, a strip is defined between a splitting chart and a joining chart where the strips are joined (squeezed) into a single strip.

All the non-trivial dynamical processes are captured between the splitting and the joining chart, ended by a
joining line, which corresponds to a Poincaré section.

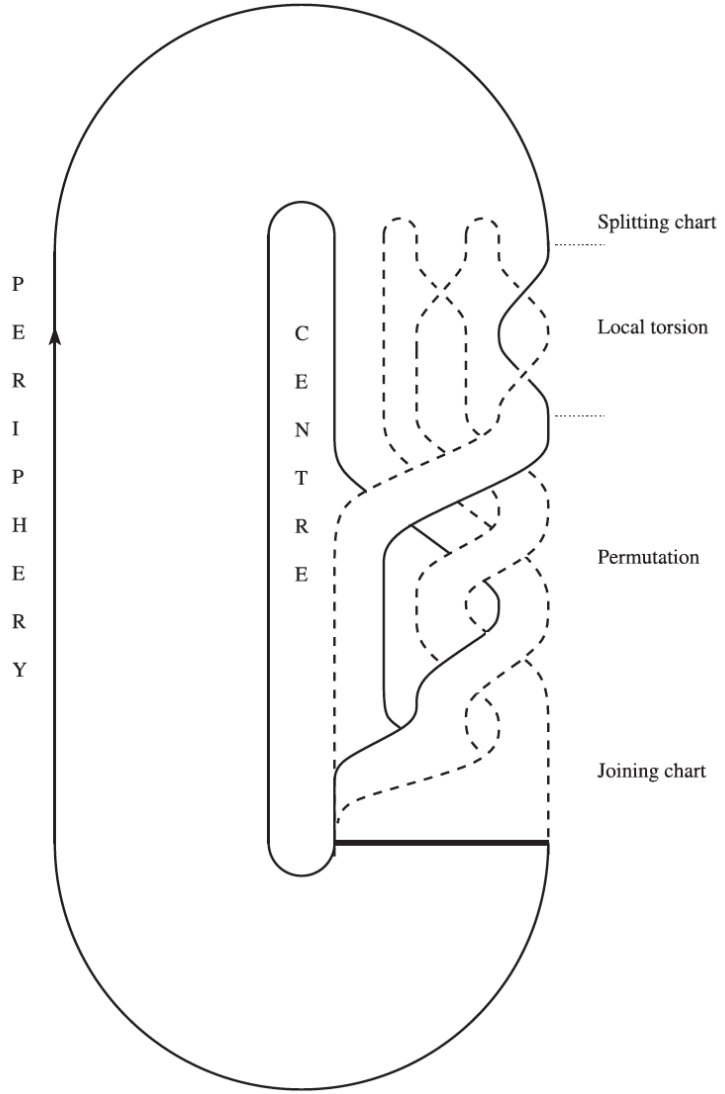

Methods

- Isopleths, branched manifolds, knot-holders, cell complexes, homologies

ELSEVIER

Chaos, Solitons & Fractals
Volume 13, Issue 5, April 2002, Pages 1099-1113

Should all the species of a food chain be counted to investigate the global dynamics?

Christophe Letellier [a], Luis A. Aguirre [b], Jean Maquet [a], M.A. Aziz-Alaoui [c]

ELSEVIER

Biosystems
Volume 158, August 2017, Pages 17-30

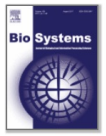

How tumor growth can be influenced by delayed interactions between cancer cells and the microenvironment?

Dibakar Ghosh [a], Subhas Khajanchi [b], Sylvain Mangiarotti [c], Fabrice Denis [d], Syamal K. Dana [e], Christophe Letellier [f]

ELSEVIER

Chaos, Solitons & Fractals
Volume 13, Issue 1, January 2002, Pages 95-107

Analysis of the dynamics of a realistic ecological model

Christophe Letellier [a], M.A. Aziz-Alaoui [b]

Springer Link

Published: 30 March 2008

Forecasting the Time Series of Sunspot Numbers

L. A. Aguirre, C. Letellier & J. Maquet

Solar Physics **249**, 103–120 (2008) | Cite this article

Methods

- Isopleths, branched manifolds, knot-holders, cell complexes, homologies

What's wrong with templates? They are very difficult to construct… they imply the reconstruction of Unstable Periodic Orbits (UPOs) and besides, they are no longer meaningful if a fourth dimension in phase space is involved, since they unknot….

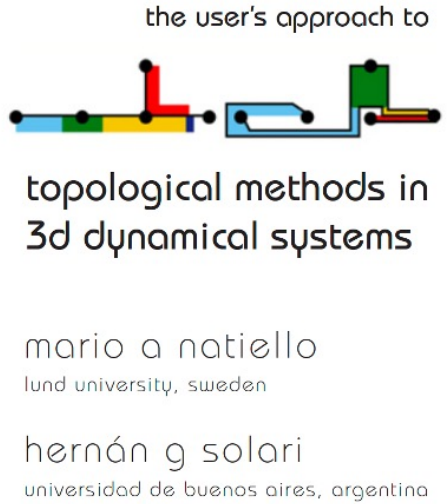

Chapter 7

A braided view of a knotty story

Mario Natiello
Matematikcentrum-LTH, Lunds Universitet
Box 118, 221 00 Lund, Sverige

Hernán Solari
Departmento de Física, Facultad de Ciencias Exactas y Naturales
Universidad de Buenos Aires, Argentina

Periodic orbits of 3-d dynamical systems admitting a Poincaré section can be described as braids. This characterisation can be transported to the Poincaré section and Poincaré map, resulting in the braid type. Information from braid types allows to estimate bounds for the topological entropy of the map while revealing detailed orbit information from the original system, such as the orbits that are necessarily present along with the given one(s) and their organisation. We review this characterisation with some examples –from a user-friendly perspective–, focusing on systems whose Poincaré section is homotopic to a disc.

6.6.3 ***Homology groups***

Still, we may want to understand the topological properties of the set of periodic orbits hidden in our data. We need some "braidless" method (in the sense that knots "dissolve" into trivial objects in higher dimensions) and one method that appears to jump at hand is to consider the homology groups associated to our data [Muldoon et al. 1993, Sciamarella and Mindlin 1999; 2001].

Methods

- Isopleths, branched manifolds, knot-holders, cell complexes, homologies

Physica D 65 (1993) 1–16
North-Holland

SDI: 0167-2789(92)00026-1

1993

PHYSICA D

Topology from time series

M.R. Muldoon[a], R.S. MacKay[a], J.P. Huke[b] and D.S. Broomhead[b]
[a]*Nonlinear Systems Laboratory, Mathematics Institute, University of Warwick, Coventry CV4 7AL, United Kingdom*
[b]*DRA at RSRE, Malvern, St. Andrew's Road, Great Malvern, Worcestershire WR14 3PS, United Kingdom*

Received 15 August 1992
Revised manuscript received 13 November 1992
Accepted 23 November 1992
Communicated by G. Ahlers

We describe methods for the study of topological pro
systems. We explain how to compute such invariants as the
and suggest a number of potential applications.

1999

VOLUME 82, NUMBER 7 PHYSICAL REVIEW LETTERS 15 FEBRUARY 1999

Topological Structure of Chaotic Flows from Human Speech Data

Denisse Sciamarella and G. B. Mindlin
Departamento de Física, FCEN, Universidad de Buenos Aires, Pab I, Ciudad Universitaria, cp 1428, Buenos Aires, Argentina
(Received 7 July 1998)

We report the analysis of branched manifolds through homolog
applicability of the topological approach to the analysis of human sp
cases are discussed. [S0031-9007(99)08424-0]

PACS numbers: 47.52.+j, 02.40.Sf, 43.72.+q

2001

PHYSICAL REVIEW E, VOLUME 64, 036209

Unveiling the topological structure of chaotic flows from data

Denisse Sciamarella and G. B. Mindlin
Departamento de Física, Facultad de Ciencias Exactas y Naturales, Universidad de Buenos Aires, Pab I, Ciudad Universitaria, Casilla de Correo 1428, Buenos Aires, Argentina
(Received 13 December 2000; published 21 August 2001)

We report the analysis of branched manifolds through homologies, in order to extend the range of applicability of the topological approach to the analysis of chaotic data. Analytic and numerical cases are discussed.

DOI: 10.1103/PhysRevE.64.036209 PACS number(s): 05.45.Pq, 47.52.+j, 02.40.Sf

Methods

- Isopleths, branched manifolds, knot-holders, cell complexes, homologies

Computing topology using knot theory

3-D trajectory set

Knot invariants

RESTRICTIONS

- Precision and length of time series must be good enough for orbits in phase space to be reconstructed accurately …
- Phase space dimension cannot be higher than three, since knots or braids unknot …

Computing topology using homologies

n-D point-cloud

Homologies

HOMOLOGY GROUPS

- Time series can be shorter and noisy since the method is independent of the reconstruction of trajectories in phase space (no periodic orbit).
- Applicable in *n* dimensions: the method is knotless and braidless.

Methods

- Branched Manifold Analysis through Homologies (BraMAH)

  Acronym first used in Charó, Artana & Sciamarella,
  Physica D 405 (2020) 132371

Sanskrit: ब्रह्मा, Romanized: Brahmā or Bramāh

Brahmā is a Hindu god, referred to as "the Creator" within the Trimurti, the trinity of supreme divinity. He is associated with knowledge and creation.

Brahmā is traditionally depicted with four faces and four arms. Each face of his points to a cardinal direction. His hands hold no weapons, one of his hands holds mālā (Sanskrit: माला) symbolizing time. As we shall see, time will lead us to the templex.

Unlike other complexes, the BraMAH cell complex is constructed to fit on a branched manifold.

Methods

Computing topological invariants using **homologies**

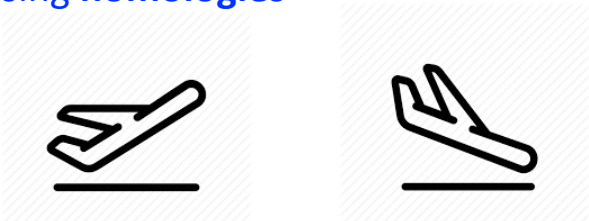

*n*D point-cloud — Homologies

- Branched Manifold Analysis through Homologies (BraMAH)

1) Approximate points as lying on a branched manifold.

2) Find a topological representation for the branched manifold.

3) Obtain an algebraic description of the topological structure.

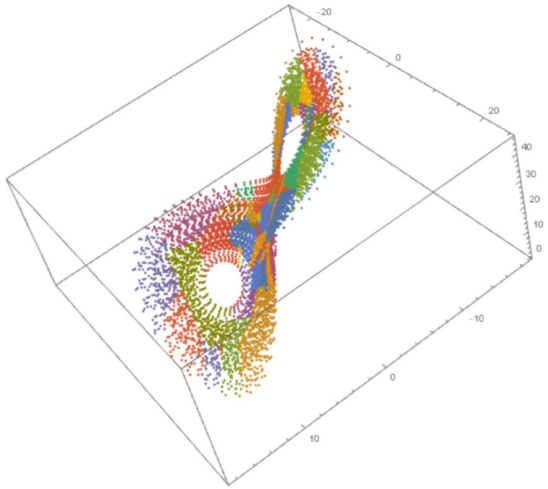

BraMAH COMPLEX construction

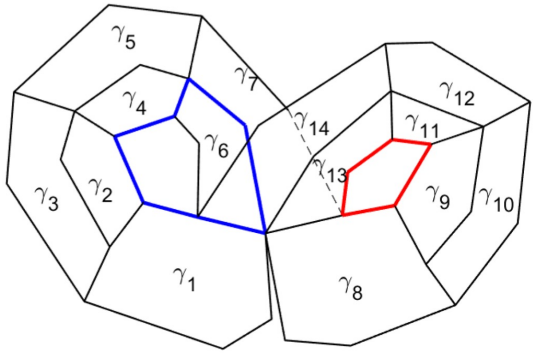

HOMOLOGY GROUP computation

$$H_0 \approx Z^1;$$
$$H_1 \approx Z^2;$$
$$H_2 \approx 0$$

1) Local approximation by *d*-disks => short and noisy time series *can* be handled.

2) Build a cell complex keeping track of the gluing prescriptions => *3*D+ *can* be handled.

3) Compute homologies and orientability properties of the cell complex => the structure can be identified.

Methods

- Branched Manifold Analysis through Homologies (BraMAH)

A **patch** is a set of points $\{x_i\}$ around an arbitrary point x_0 , that is locally homeomorphic to the interior of a disk in d dimensions ($d \leq n$)

Point-cloud decomposition into patches

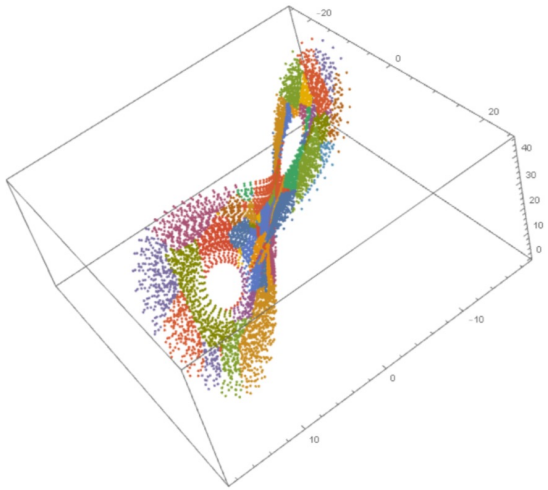

A patch is a good approximation of a hyperplane of dimension d in a space of dimension n if the square roots of d among the n second moments of $\{x_i\}$ decrease linearly with R while $(n–d)$ decrease as lower powers of R.

$X_{i,j} = (x_{i,j} - x_{0,j}) \Rightarrow$

find N_1 such that d among n singular values of $X_{i,j}$ vary linearly with N

Patches are used to construct the cells in the cell complex

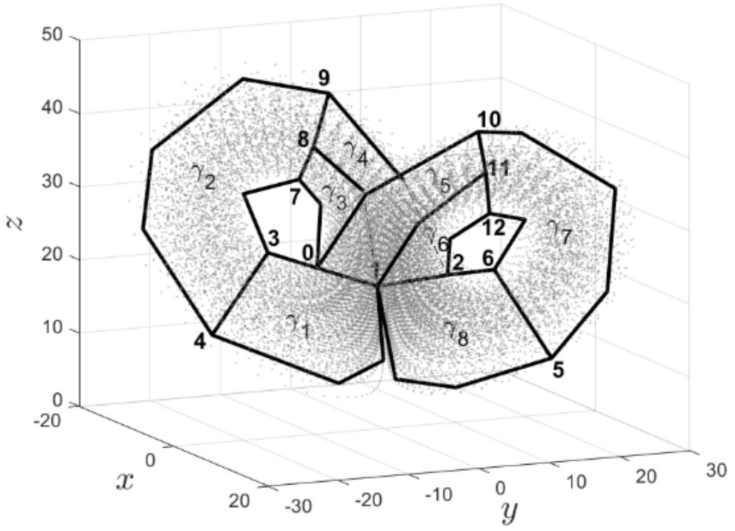

Methods

- Branched Manifold Analysis through Homologies (BraMAH)

How to determine if two spaces are topologically equivalent? → Cell complex covering the cylinder

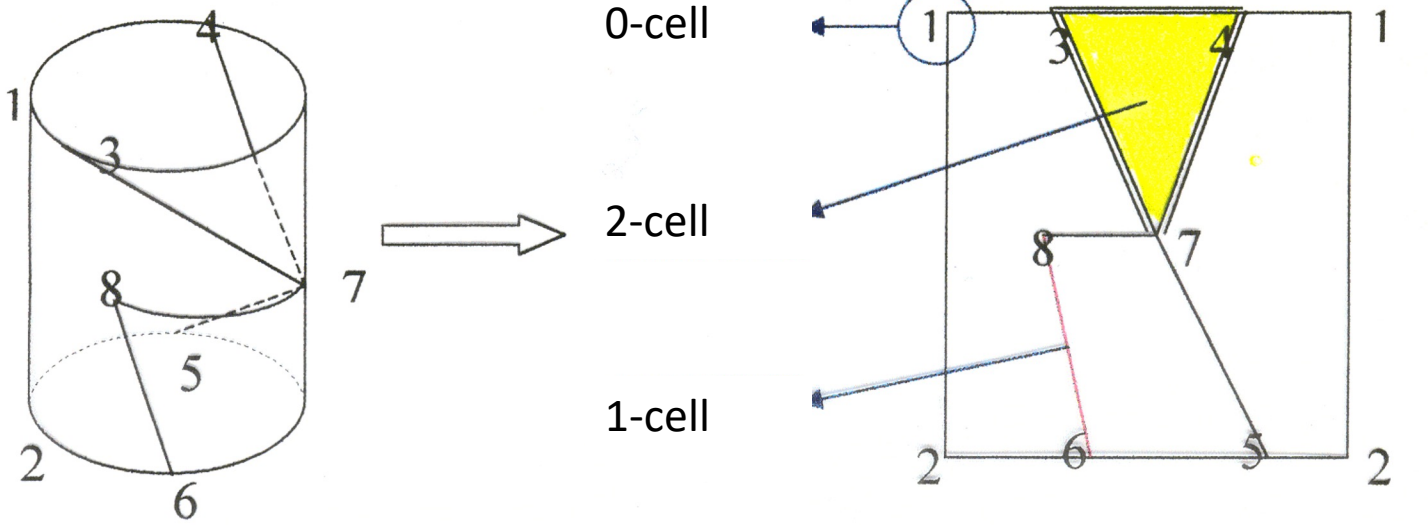

An ***n*-cell** is a set corresponding to the interior of a disk in *n* dimensions whose borders are divided into a number of cells of lower dimension.

An ***n*-complex** is a set of cells such that their borders are elements of the complex with interiors that do not intersect.

Methods

- Branched Manifold Analysis through Homologies (BraMAH)

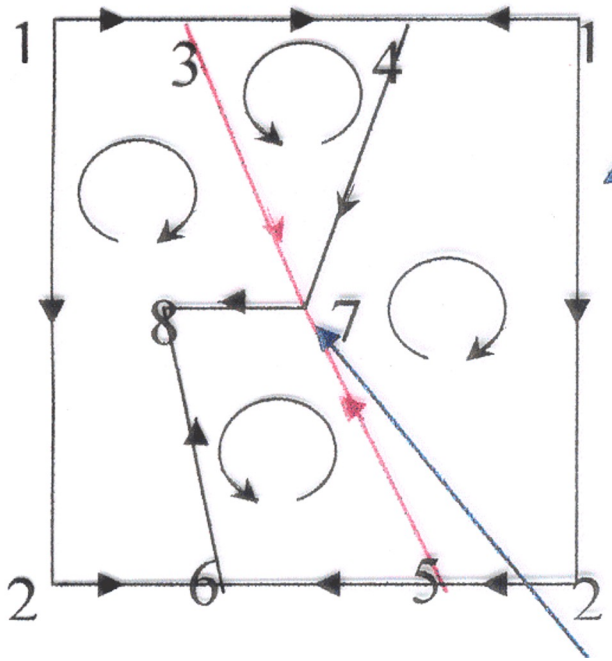

Oriented complexes

Uniformly oriented complex

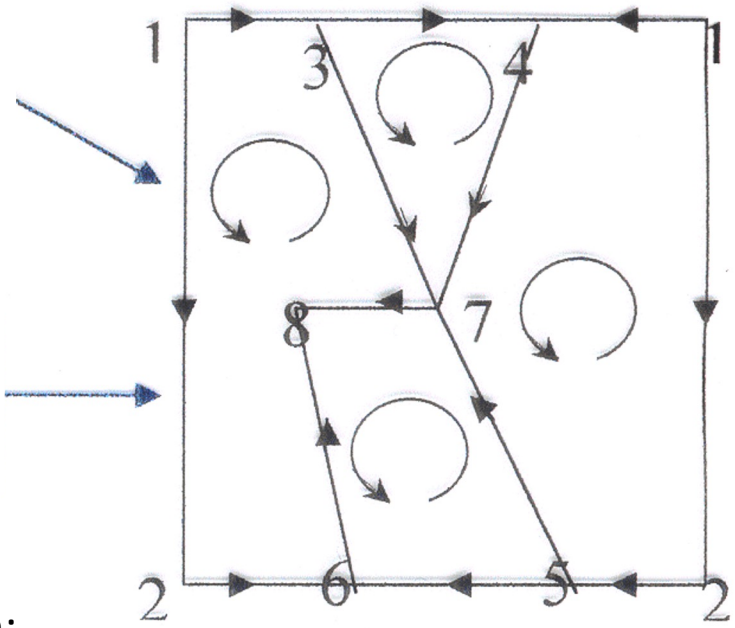

Example of a *1*-chain:
<3,7>-<5,7>

Example of border map:

∂(<3,7,4>)=<3,7>-<4,7>-<3,4>

A ***k*-chain** in a complex *K* is a sum $C = \Sigma a_i \sigma_i$ such that σ_i are the *k*-cells with $a_i \in Z$ and such that $C_k(K)$ = {*k*-chains of *K*} has an abelian group structure.

A **border map** is an operation ∂: $C_k(K) \rightarrow C_{k-1}(K)$ such that $\partial(\Sigma a_i \sigma_i) = \Sigma a_i \, \partial(\sigma_i)$

Methods

- Branched Manifold Analysis through Homologies (BraMAH)

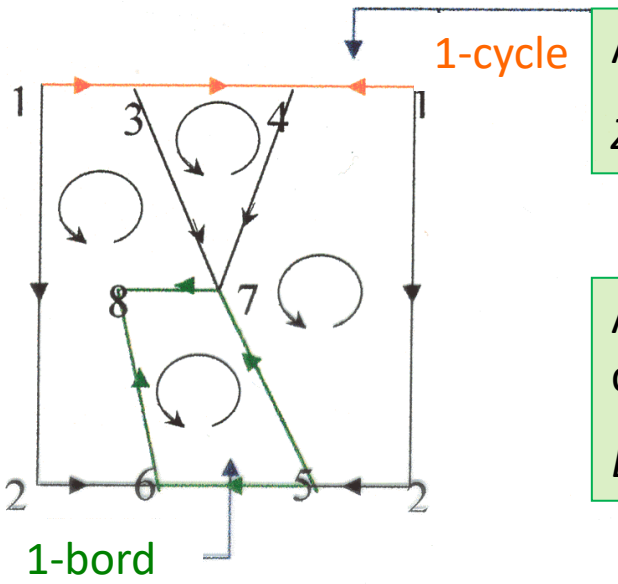

A ***k*-cycle** is a *k*-chain *C* such that $\partial(C)=0$

$Z_k(K)$ = {all *k*-cycles in a complex}

A ***k*-border** is a *k*-chain *C* / there exists a (*k*+1)-chain *D* such tat $\partial(D)=C$

$B_k(K)$ = {all *k*-borders of an *n*-complex}

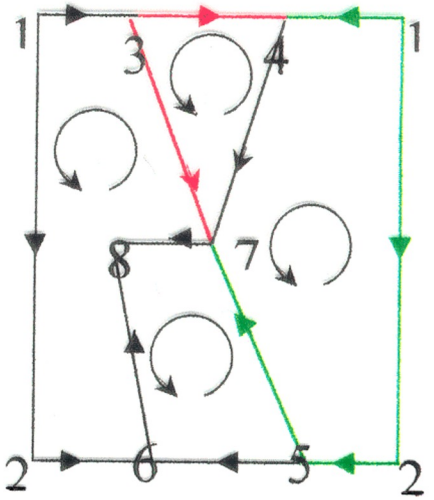

Equivalence relationship:

Two *k*-chains C_1 and C_2 are called homologically equivalent ($C_1 \sim C_2$) if there exists a (*k*+1)-chain *D* such that $\partial(D)=C_1-C_2$

Example: -<3,4>+<3,7> ~ -<1,4>+<1,2>+<2,5>+<5,7>

Methods

- Branched Manifold Analysis through Homologies (BraMAH)

Homology groups

The *n+1* homology groups of an *n*-complex *K* are the sets:

$H_k(K) = Z_k/B_k$ ={the *k*-cycles being homologically independent that are not borders of any (*k*+1)-cell}

Example: the cylinder

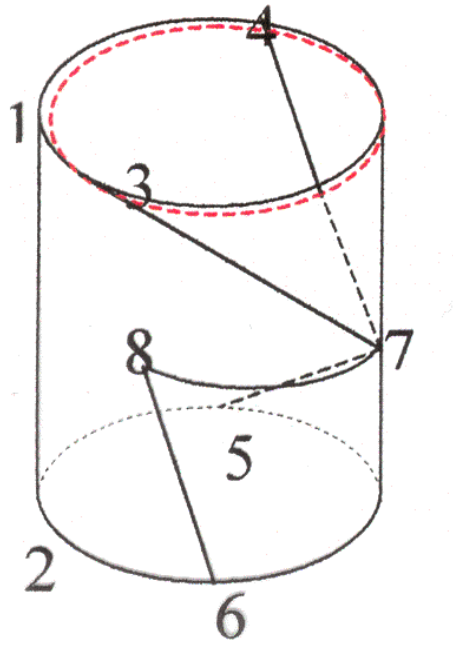

K_1

$H_0(K_1)$=[[<1>]] ~ $Z^1 \Rightarrow$ one connected component

$H_1(K_1)$=[[<1,3>+<3,4>-<1,4>]] ~ $Z^1 \Rightarrow$ one nontrivial loop

$H_2(K_1) = \varnothing \sim 0 \Rightarrow$ **no cavities enclosed**

Methods

- Branched Manifold Analysis through Homologies (BraMAH)

Homology groups

The *n+1* homology groups of an *n*-complex *K* are the sets:

$H_k(K) = Z_k/B_k$ ={the *k*-cycles being homologically independent that are not borders of any (*k*+1)-cell}

Example: the torus

$H_0(K_2)$ =[[<1>]]~ $Z^1 \Rightarrow$ one connected component

$H_1(K_2) \sim Z^2 \Rightarrow$ **two** nontrivial loops

$H_2(K_2) \sim Z^1 \Rightarrow$ **one cavity** enclosed

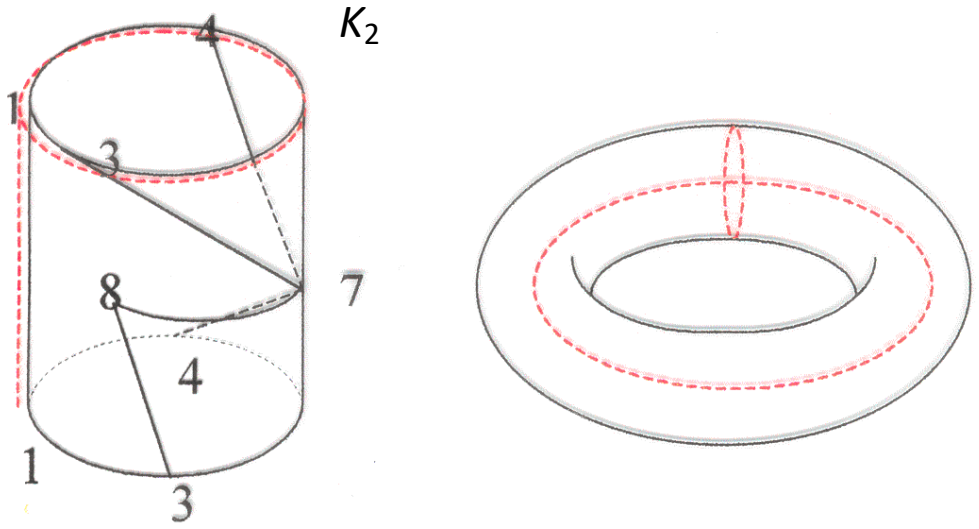

Methods

- Branched Manifold Analysis through Homologies (BraMAH)

Homology groups

The *n+1* homology groups of an *n*-complex *K* are the sets:

$H_k(K) = Z_k/B_k$ ={the *k*-cycles being homologically independent that are not borders of any (*k*+1)-cell}

Example: the Klein bottle

$H_0(K_3)$ =[[<1>]]~ $Z^1 \Longrightarrow$ one connected component

$H_1(K_3) \sim Z^2 \Longrightarrow$ two nontrivial loops

$H_2(K_3) \sim 0 \Longrightarrow$ **no cavity** enclosed

The Klein bottle has a torsioned 1-cycle that is not the boundary of any 2-chain, but that becomes one if travelled 2 times, thus defining a **weak boundary**.

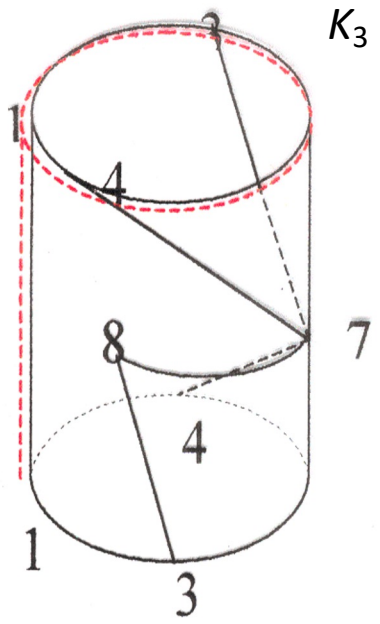

Methods

- Branched Manifold Analysis through Homologies (BraMAH)

An <u>orientability chain</u> in a uniformly oriented complex K with cells b_i is a chain $O = \partial(\Sigma b_i) = \Sigma\, a_j\, t_j$ if there exists at least one coefficient j such that $|a_j| > 1$. We call torsion chains, the consecutive cells t_j preceded by the same multiple in O.

<u>Example</u>: Möbius strip.

$H_0(K_4)$ =[[<1>]]~ $Z^1 \Rightarrow$ one connected component

$H_1(K_4)$ ~ [[L]] $Z^1 \Rightarrow$ one nontrivial loop

$H_2(K_4) \sim 0 \Rightarrow$ no cavities enclosed

$O(K_4) = \partial(\Sigma b_i) = -2\ \langle 1,7 \rangle$

$T(K_4) = \{\langle 1,7 \rangle\} \Rightarrow$ on torsion located at <1,7>.

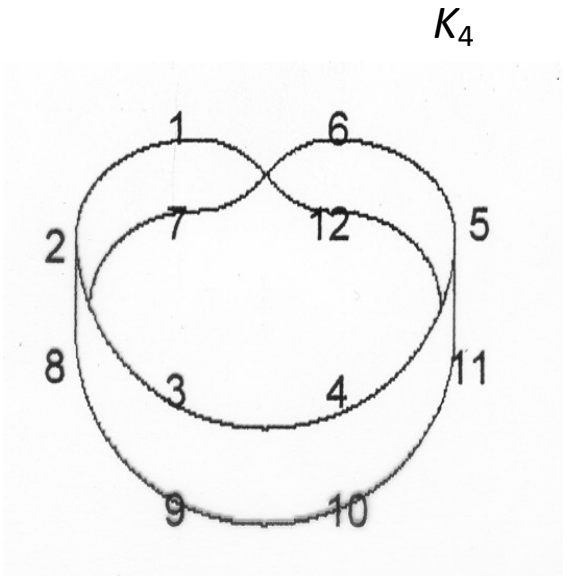

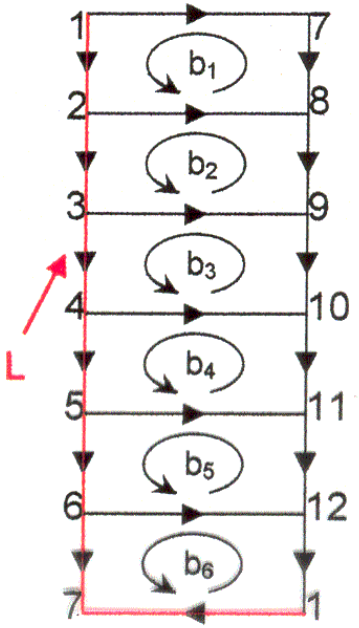

Methods

- Branched Manifold Analysis through Homologies (BraMAH)

3D

$$x' = -(z+2)\, d\, (x-a) + (2-z)\, (\alpha(x-2) - \beta y - \alpha (x-2)\, ((x-2)^2 + y^2 / R^2))$$

$$y' = -(z+2)\, (y-b) + (2-z)\, (\beta (x-2) - \alpha y - \alpha y (x-2)\, ((x-2)^2 + y^2 / R^2))$$

$$\varepsilon z' = (4-z^2)\, (z+2 - m\, (x+2)) - \varepsilon c z$$

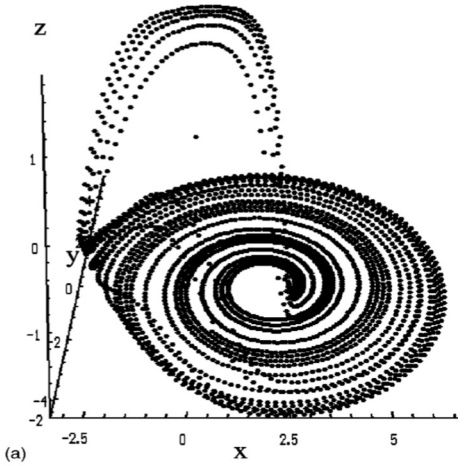

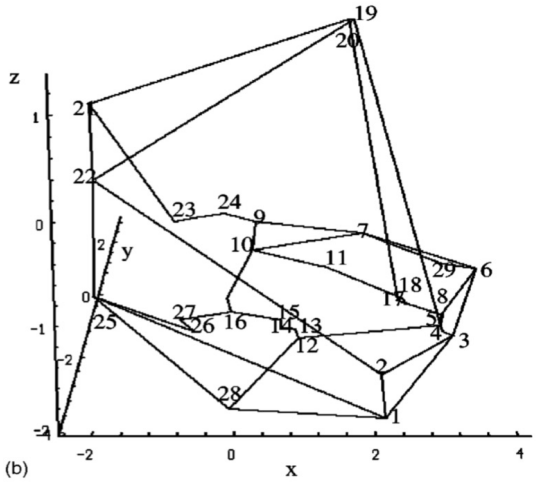

4D

$$x' = -(z+2)\, d\, (x - (a + \varepsilon_3 (2+w))) + (2-z)\, (\alpha(x-2) - \beta y - \alpha (x-2)\, ((x-2)^2 + y^2 / R^2))$$

$$y' = -(z+2)\, (y-b) + (2-z)\, (\beta (x-2) - \alpha y - \alpha y (x-2)\, ((x-2)^2 + y^2 / R^2))$$

$$\varepsilon\, z' = (4-z^2)\, (z+2 - m\, (x+2)) - \varepsilon_1 c z$$

$$\varepsilon w' = (4-z^2)\, (z+2 - m\, (x+2)) - \varepsilon_2 c z$$

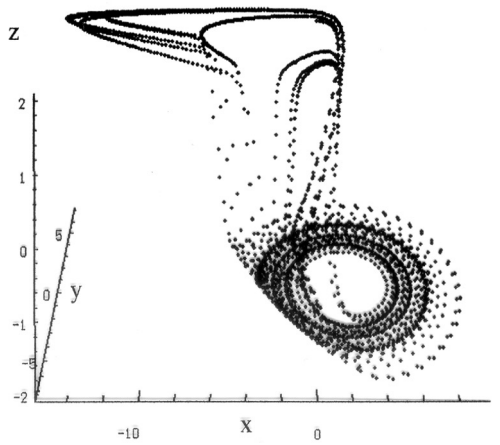

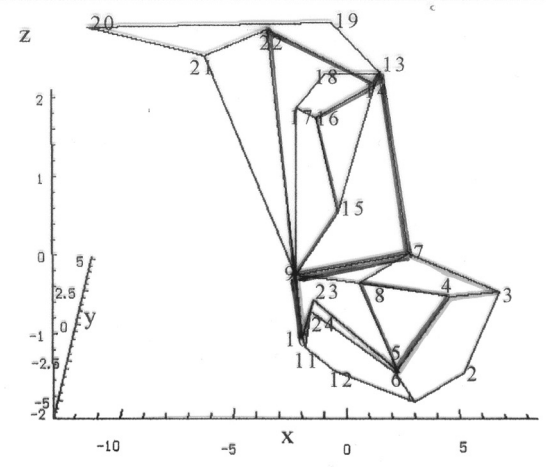

Methods

- Persistent homologies

The concept of persistent homology (PH) emerged independently in Bologna, in Colorado, and within a bio-geometry project North Carolina, towards 2005.

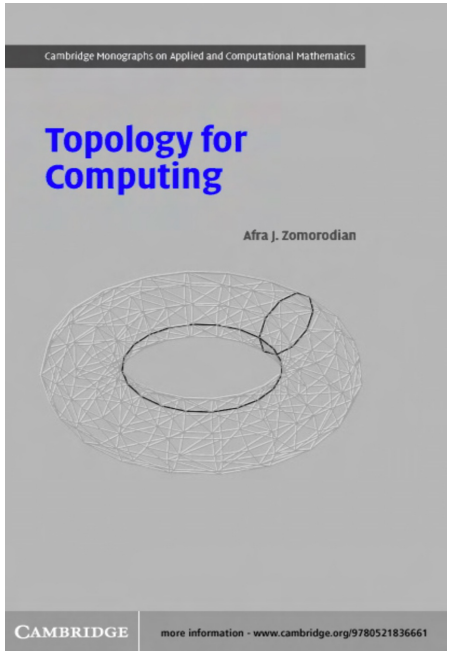

Zomorodian, A. J. *Topology for computing* (Vol. 16). Cambridge university press.

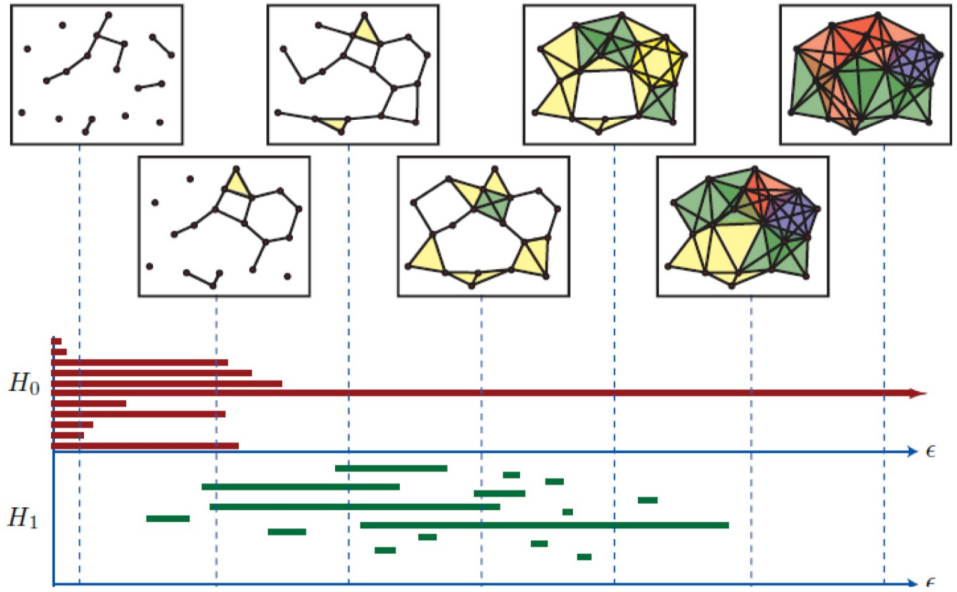

The method constructs a series of complexes as a function of a distance parameter (ε or d).

The connectivity of the point cloud increases as ε or d grows.

PH was conceived to solve pattern recognition problems, mainly in scanned images.

Methods

- Persistent homologies

Software package	Creator	Latest release	Release date	Software license[7]	Open source	Programming language
OpenPH	Rodrigo Mendoza-Smith, Jared Tanner	0.0.1	25 April 2019	Apache 2.0	Yes	Matlab, CUDA
javaPlex	Andrew Tausz, Mikael Vejdemo-Johansson, Henry Adams	4.2.5	14 March 2016	Custom	Yes	Java, Matlab
Dionysus	Dmitriy Morozov			GPL	Yes	C++, Python bindings
Perseus	Vidit Nanda	4.0 beta		GPL	Yes	C++
PHAT	Ulrich Bauer, Michael Kerber, Jan Reininghaus	1.4.1			Yes	C++
DIPHA	Jan Reininghaus				Yes	C++
Gudhi	INRIA	2.1.0	28 January 2018	GPLv3	Yes	C++, Python bindings
CTL	Ryan Lewis	0.2		BSD	Yes	C++
phom	Andrew Tausz				Yes	R
TDA	Brittany T. Fasy, Jisu Kim, Fabrizio Lecci, Clement Maria, Vincent Rouvreau	1.5	16 June 2016		Yes	R
Eirene	Gregory Henselman	1.0.1	9 March 2019	GPLv3	Yes	Julia
Ripser	Ulrich Bauer	1.0.1	15 September 2016	LGPL	Yes	C++
the Topology ToolKit	Julien Tierny, Guillaume Favelier, Joshua Levine, Charles Gueunet, Michael Michaux	0.9.2	25 June 2017	BSD	Yes	C++, VTK and Python bindings
Software package	**Creator**	**Latest Release**	**Release date**	**Software license[7]**	**Open source**	**Programming language**

Methods

- Persistent homologies

Filtrations: the rules used to build cell complexes as the filtration parameter () is varied. The Vietoris-Rips filtration is illustrated in the gif below.

Vietoris-Rips

- A ball of diameter *d* is drawn around these points.

- Two balls intersect (two points are separated by a distance less than *d*) → connect the two points with a segment or 1-cell (simplicial cell of dimension 1).

- The triangles formed are completed by forming 2-cells (simplicial cells of dimension 2), and so on.

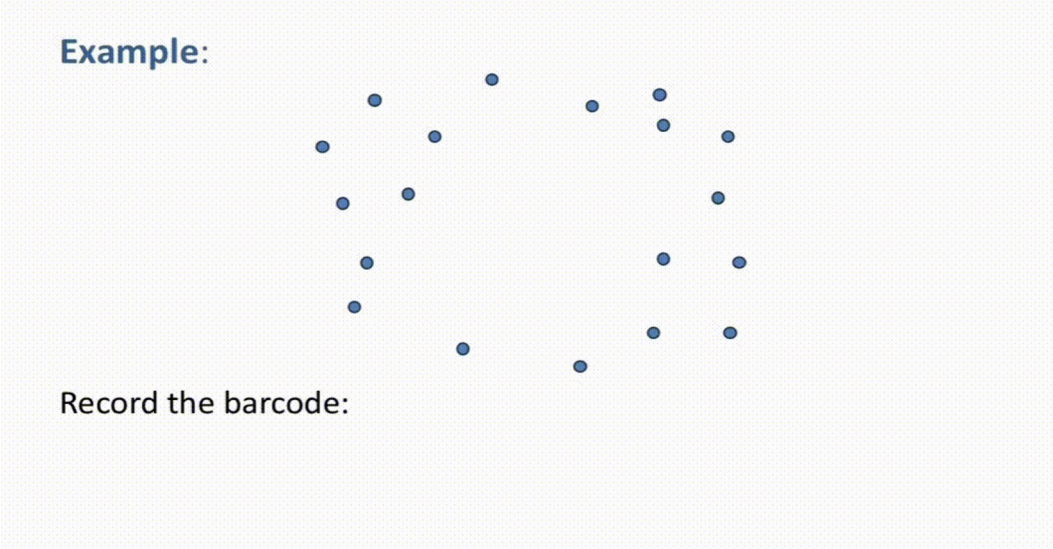

The Vietoris–Rips complex was originally called the Vietoris complex, for Leopold Vietoris, who introduced it as a means of extending homology theory from complexes to metric spaces.

Methods

- Persistent homologies

PH is not a Branched Manifold approximation method but *can* help characterizing state-space point-clouds, serving as guide.

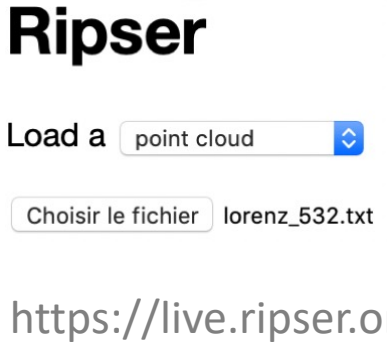

https://live.ripser.org

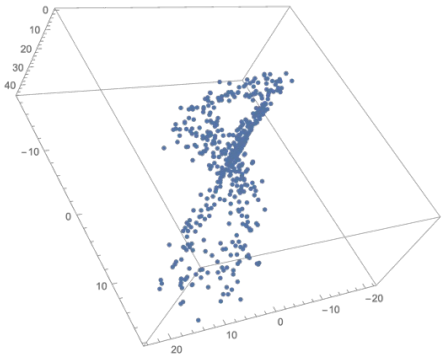

Problems with barcodes:

- Betti numbers (the rank of H_k) depend on the choice of ε_{max} which is always somewhat arbitrary.
- H_k generators not provided as output: branches cannot be identified.
- Orientability properties are not computed.

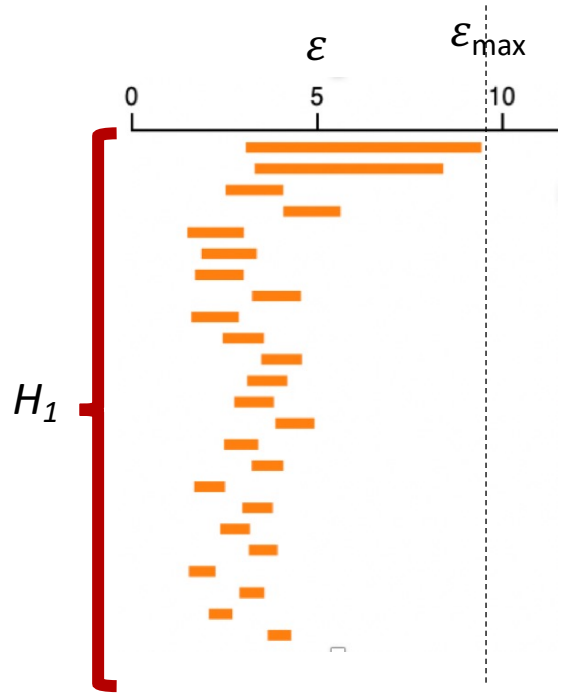

Problems' origin:

- The complexes are constructed in such a way that:
  (1) #cells ≫ #points in the point-cloud ⇒ big point clouds not supported.
  (2) the complexes have k-cells with $k > d$, d being the local dimension.

Applications

- BraMAH can be harnessed for multiple purposes

Voice production

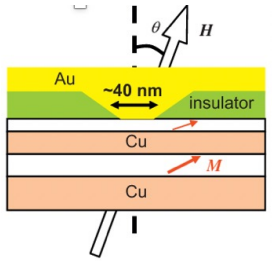

Nano-oscillators

Chemical reactions

Cardiac arrythmia

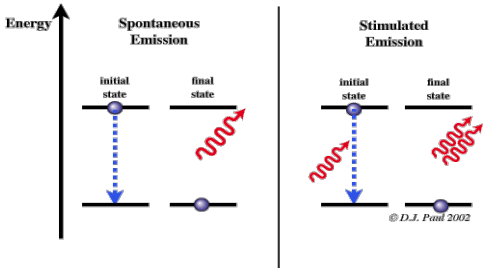

Laser optics

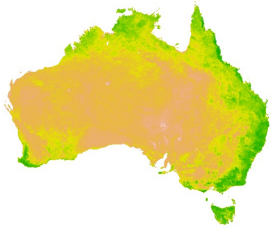

Vegetation index

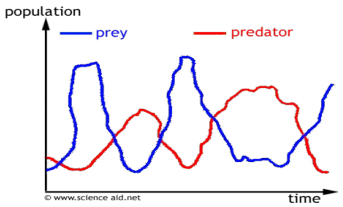

Population dynamics

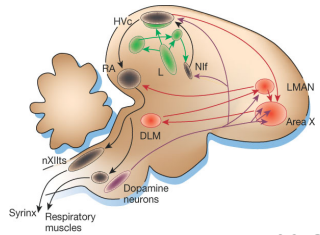

Birdsong motor control

Ocean color (with knots)

Applications

- BraMAH can be harnessed for multiple purposes

> « Topological methods can be used to determine whether or not two dynamical systems are equivalent; in particular, they can determine whether a model developed from time-series data is an accurate representation of a physical system. Conversely, it can be used to provide a model for the dynamical mechanisms that generate chaotic data. »
>
> R. Gilmore, Reviews of Modern Physics, Vol. 70, No. 4, October 1998

- ✓ Validate/refute models – simulations vs. observations.
- ✓ Comparing models – time series generated by different models.
- ✓ Comparing datasets – e.g., *in situ* versus satellite data.
- ✓ Extracting models from data – using global modeling techniques with a topological validation.
- ✓ Characterizing and labeling chaotic behaviors – towards a systematic classification.
- ✓ Classifying sets of time series according to their main dynamical traits – e.g., in Lagrangian Analysis.

Applications

- Lagrangian Analysis

What is Lagrangian analysis?

In fluid mechanics, two viewpoints are possible.

In the Eulerian viewpoint, fluid motion is observed at specific locations in space, as time passes.

In the Lagrangian viewpoint, the observer follows individual fluid particles as they move through the fluid domain.

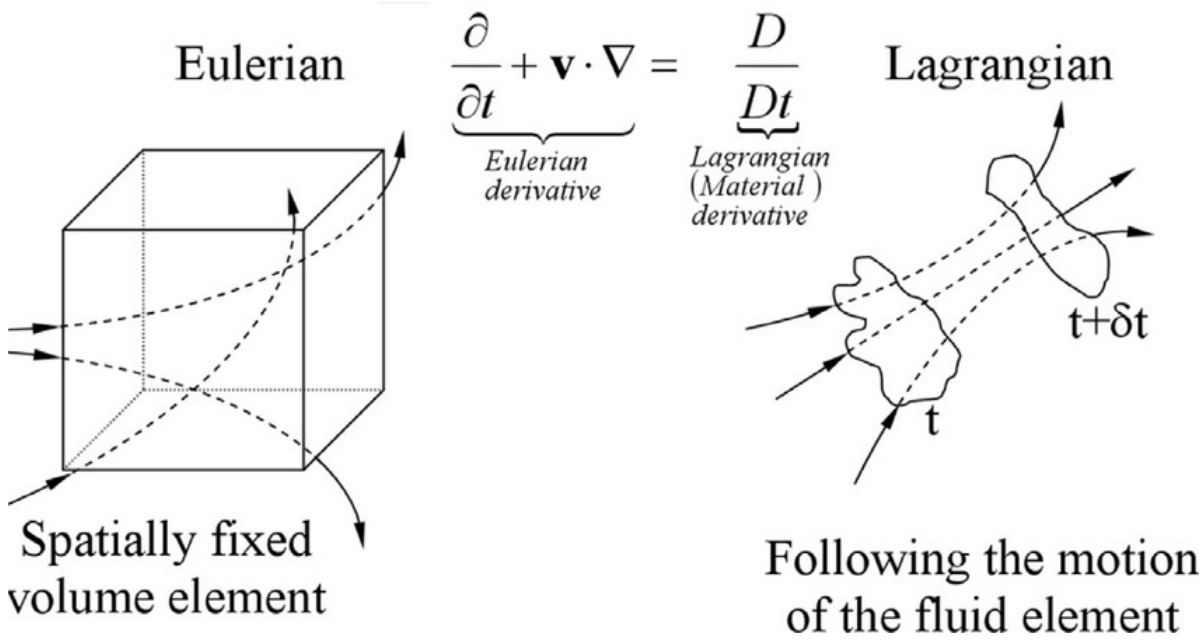

The Driven Double Gyre (DDG) system is an analytic model, often used to show how much Lagrangian patterns may differ from patterns in Eulerian fields.

It was introduced by Shadden et al. (2005) to mimic the motion of two adjacent oceanic gyres enclosed by land and, since Sulalitha Priyankara et al. (2017), it is known to present chaotic transport in some 'regions' of the fluid, even if the Eulerian picture is periodic.

Applications

- Lagrangian Analysis

Let us consider the kinematic model inspired in a pattern that occurs frequently in geophysical flow.

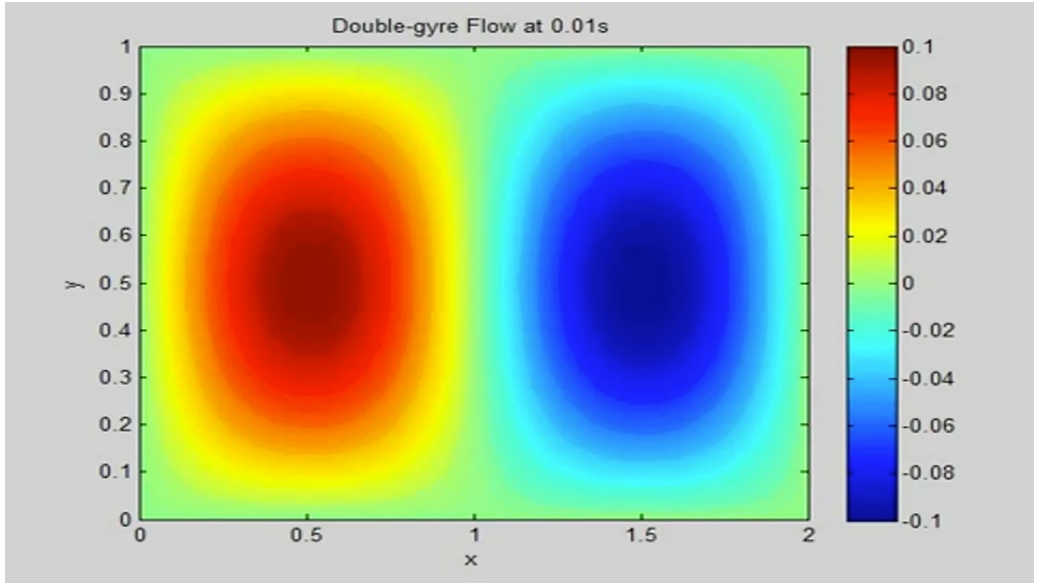

$$(x, y) \in D = [0, 2] \times [0, 1]$$

$$\begin{cases} \frac{dx(t)}{dt} = -\pi A \sin(\pi * forcing) \cos(\pi y) \\ \frac{dy(t)}{dt} = \pi A \cos(\pi * forcing) \sin(\pi y)(2ax + b); \end{cases}$$

$$a = \epsilon \sin(\omega t),\ b = 1 - 2\epsilon \sin(\omega t)$$

$$forcing = ax^2 + bx$$

$$t_0 = 0,\ t_f = 10,\ \epsilon = 0.1,\ A = 0.1,\ \omega = \frac{\pi}{5}$$

From the Eulerian perspective periodically driven Double-Gyre flow has a periodic and simple behaviour. But what about particle behaviour? What happens, for instance, if there is an “oil spill” in the middle of the domain?

Applications

- Lagrangian Analysis

Let us paint in blue the particles that are continuously passing through the centerpoint (streakline) to “visualize” particle behaviour.

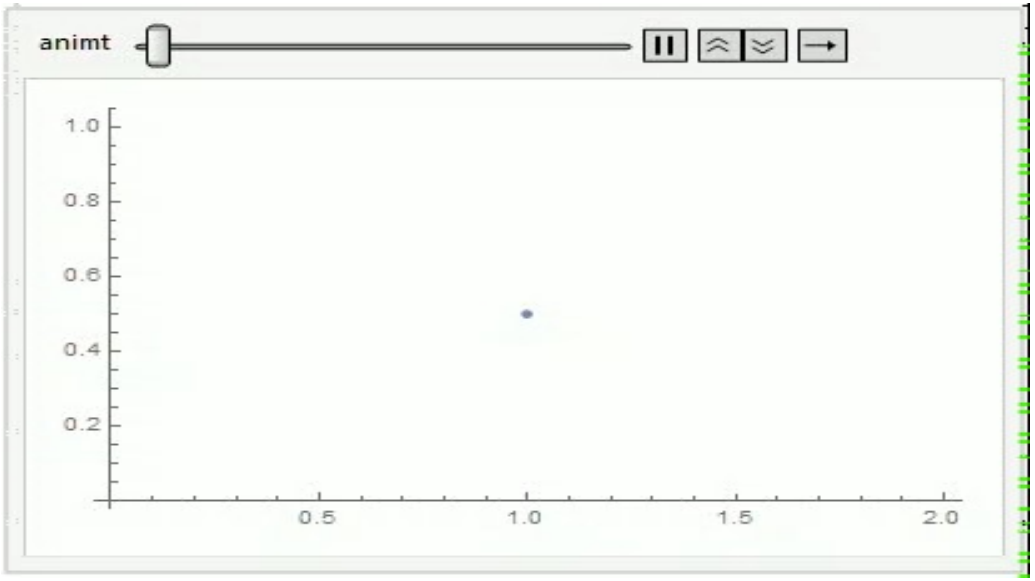

Transport barriers appear, showing that the tracer invades some parts of the domain leaving some other regions blank.

These non-mixing islands move circularly in each half-domain.

What can state-space topology tell us in a problem of this kind?

Lagrangian time series (the position or the velocity of a particle) can be generated and studied in state space with our topological tools.

Applications

- Lagrangian Analysis

A BraMAH topological practised on a collection of 8528 particles (x_1 time series) in a time window of 500 units yields five topological classes. Computations involve complexes constructed from 4-dimensional time-delay embeddings.

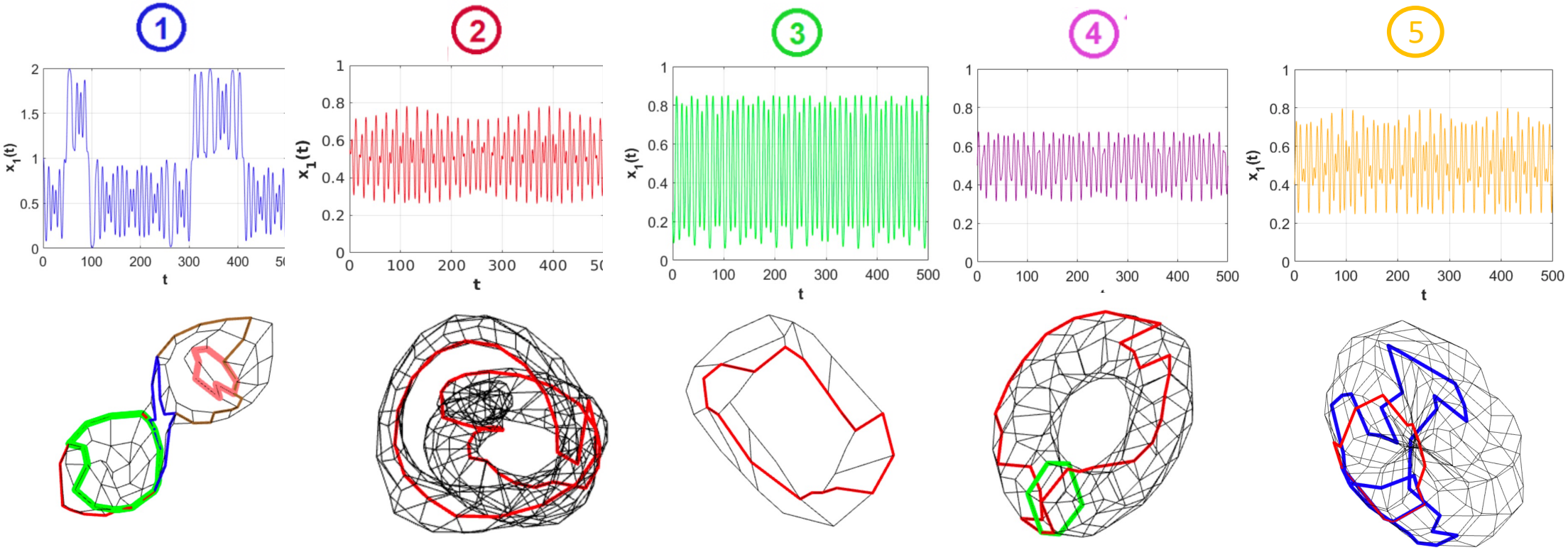

Five-loop structure | Moebius strip | Standard strip | Torus | Klein bottle

Applications

- Lagrangian Analysis

Topological colouring of 8528 advected particles in the driven Double-Gyre flow to visualize topologies are organized in physical space.

Assigning a different color to each topological class, the colors in motion define particle sets that move together forming coherent regions, i.e., without mixing with the surrounding fluid.

Let us use the term ‘separator’ to designate the frontier between differently colored regions.

Such flow separators are associated with ‘Lagrangian coherent structures’, known to separate dynamically distinct regions in fluid flows (Kelley, Allshouse & Ouellette, 2013).

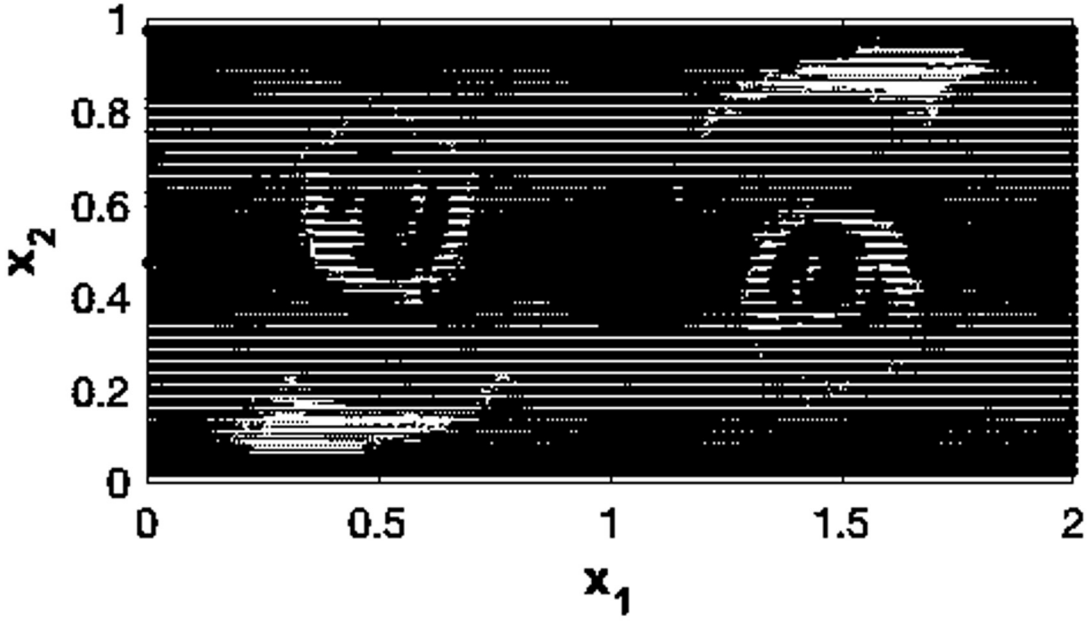

Applications

- Lagrangian Analysis

Topological colouring of 8528 advected particles in the driven Double-Gyre flow to visualize topologies are organized in physical space.

If the advected particles are coloured according to the BraMAH topological analysis, the non-mixing islands come to light.

Classifying topologies (= classifying dynamics) can be used:

i. for an indirect identification of particle sets that do not mix with the surrounding fluid,
ii. to characterize such dynamics within each region,
iii. to compare distant regions behaving similarly,
iv. to compare the behaviour of particles in different flows.

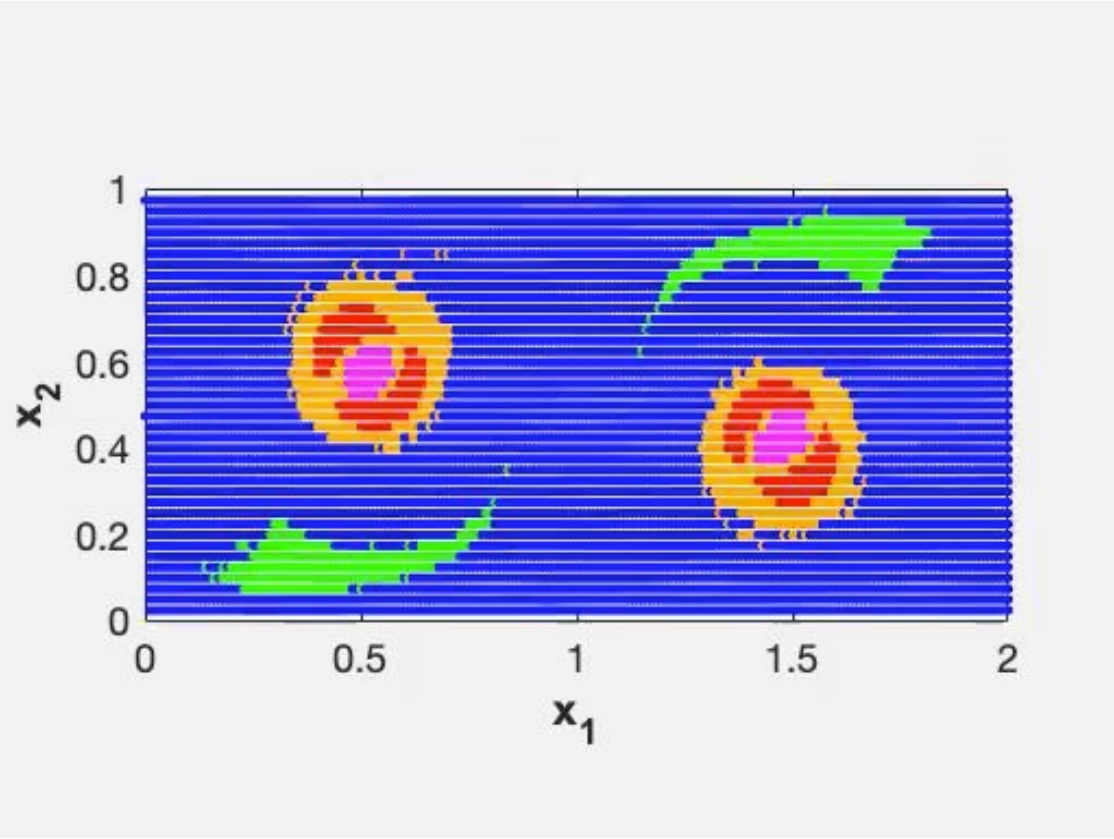

Applications

$$a(t) = \eta \sin\left[\omega t\left(1 + \gamma \sin(\frac{t}{2})\right)\right], b(t) = 1 - 2a(t)$$

- Lagrangian Analysis

What happens if we introduce a perturbation in the driving force of the Double-Gyre in which the particles in the formerly non-mixing islands slowly migrate towards the chaotic sea?

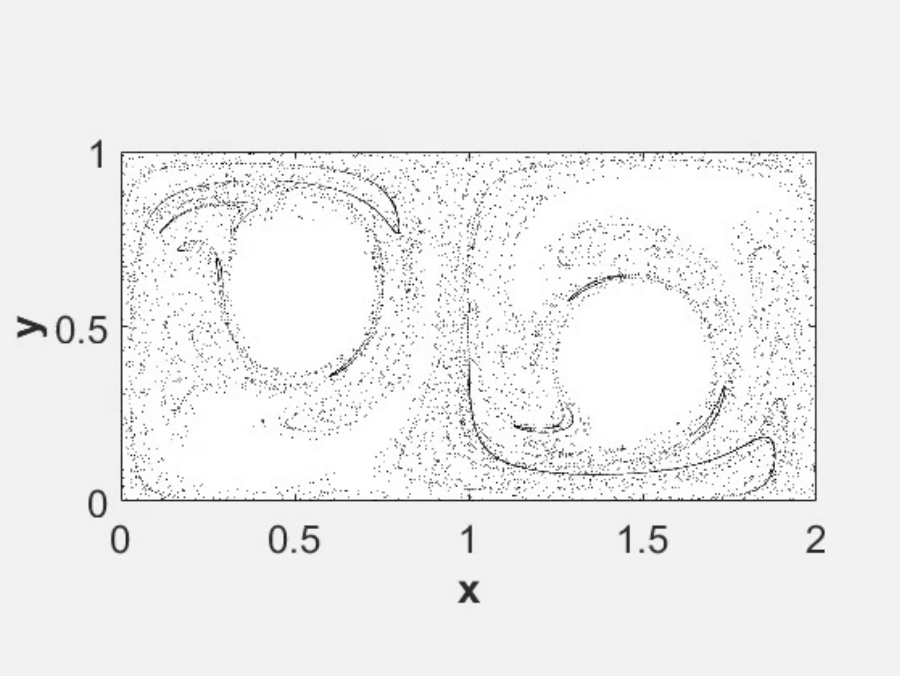

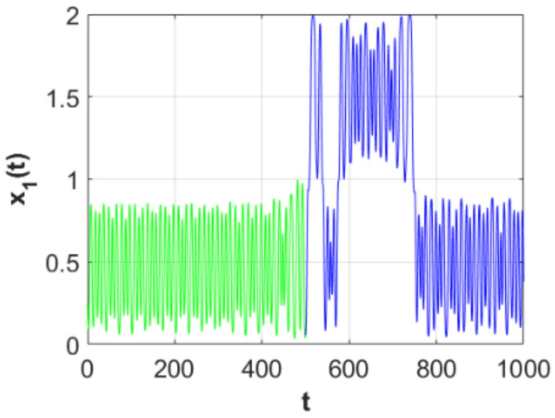

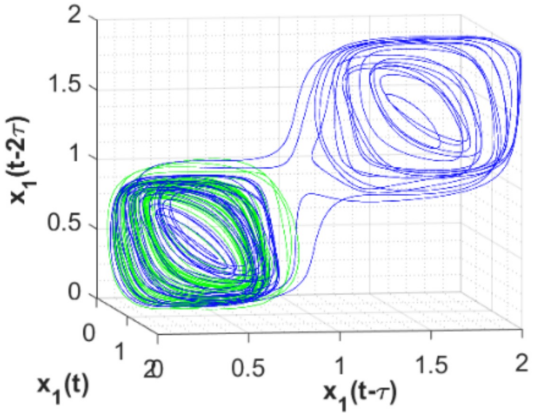

The topology that is computed is always referred to the time window that is chosen for the analysis. A particle that migrates ‘moves’ from one topological class to the other.

Applications

- Lagrangian Analysis

The Bickley Jet: this kinematic flow simulates a zonal sinuous jet flanked by counter-rotating vortices. It corresponds to the idealization of geophysical flows such as the Gulf Stream or the polar-night jet perturbed by a Rossby wave.

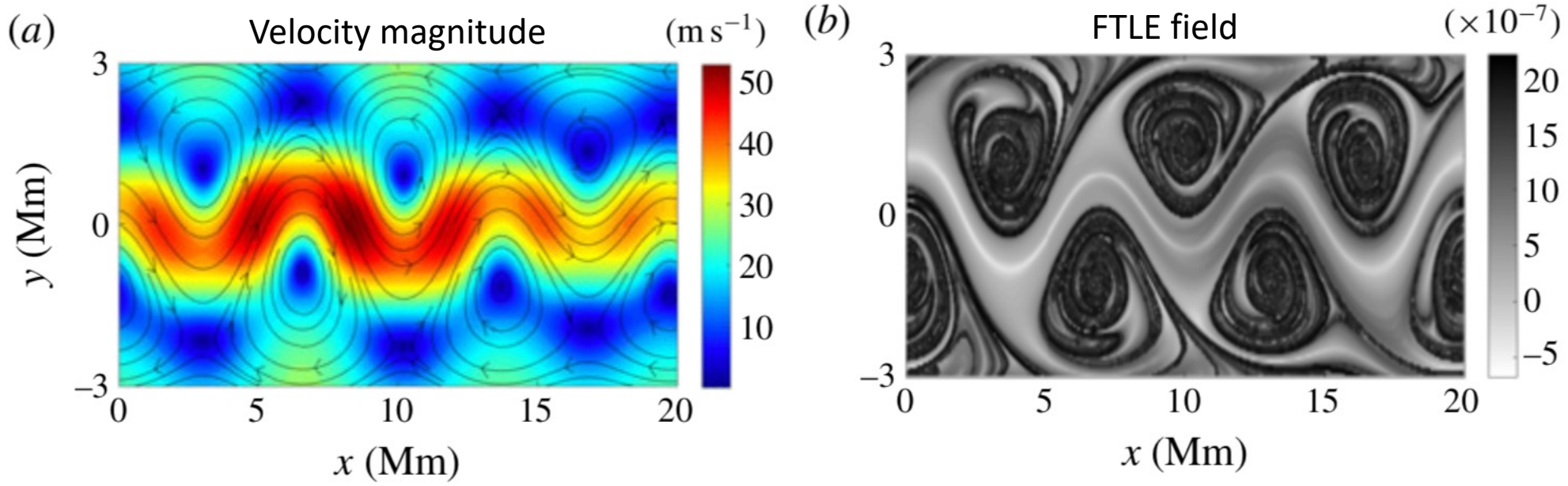

Schlueter-Kuck & Dabiri. *J. Fluid Mech.* (2017), v*ol*. 811, *pp.* 468–486.

Applications

- Lagrangian Analysis

A BraMaH analysis on a collection of 105 time series of sparse particles produces 4 topological classes marked with different symbols. All the flanking vortices share the same structure: a torus “surrounded” by Moebius strips. The background flow has a three-loop structure, and the jet is characterized by a standard strip.

The streakline snapshot is taken at 40 days with injection locations $p = (x_1,x_2) \,/\, x_1 = 1\times10^6 \wedge x_2 \in [-4 : 0.05 : -2] \times 10^6 \cup [2 : 0.05 : 4] \times 10^6$.

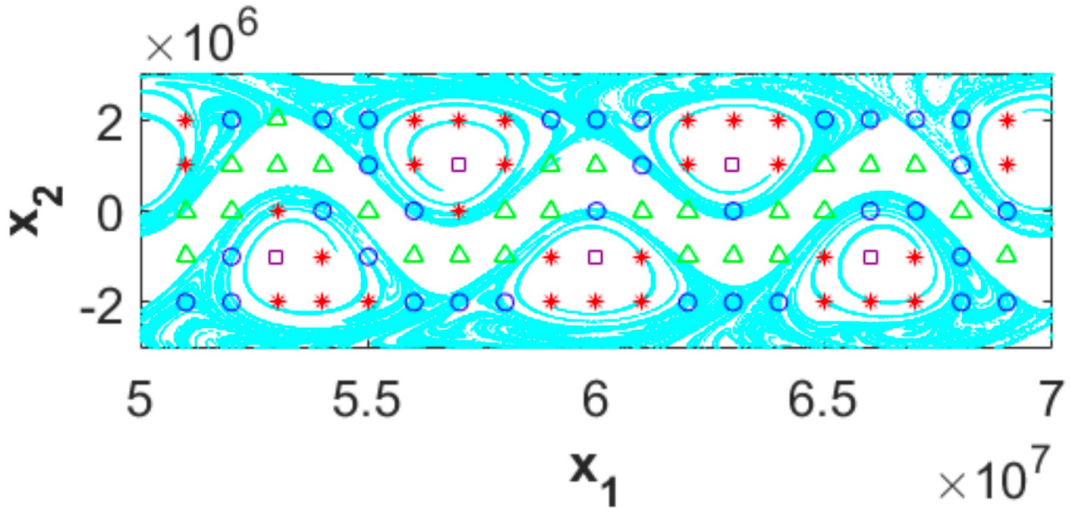

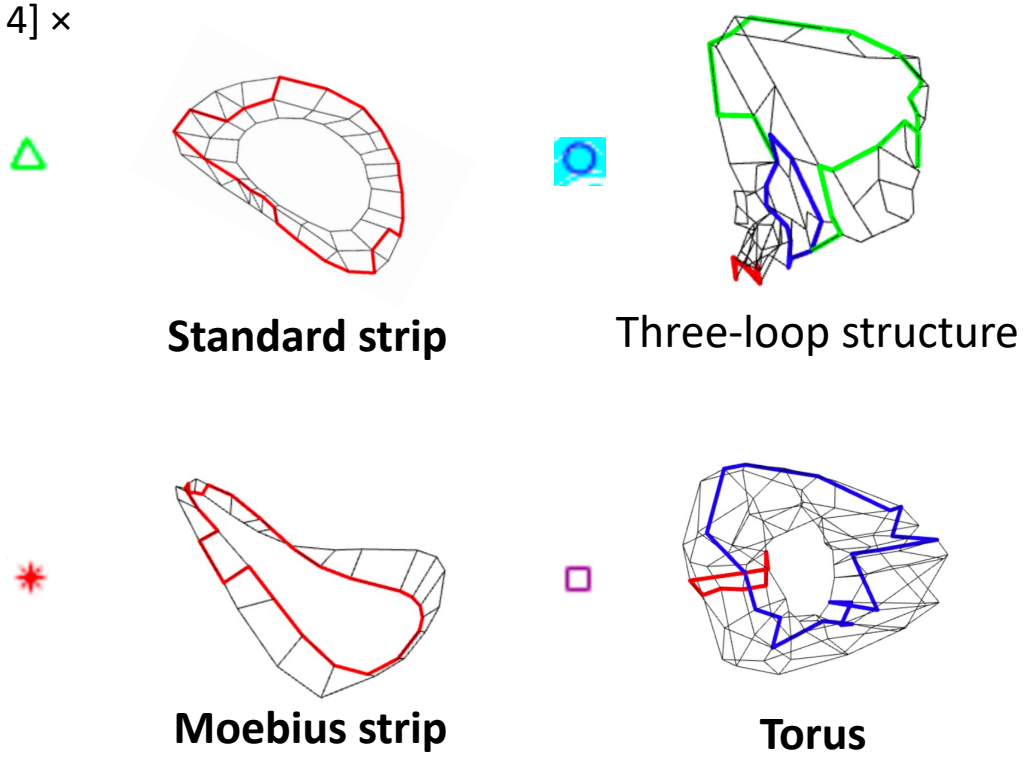

Applications

- Lagrangian Analysis

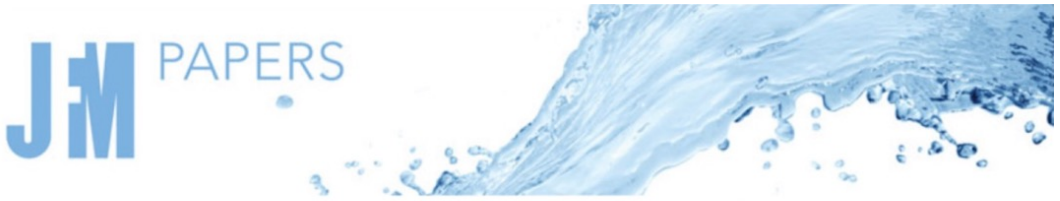

Topological colouring of fluid particles unravels finite-time coherent sets

Gisela D. Charó[1,2,3,†], Guillermo Artana[3,4] and Denisse Sciamarella[2,5]

[1]CONICET – Universidad de Buenos Aires, Centro de Investigaciones del Mar y la Atmósfera (CIMA), Buenos Aires, Argentina

[2]CNRS – IRD – CONICET – UBA, Institut Franco-Argentin d'Études sur le Climat et ses Impacts (IRL 3351 IFAECI), Buenos Aires, Argentina

[3]CONICET – Consejo Nacional de Investigaciones Científicas y Técnicas, C1425FQD CABA, Argentina

[4]Laboratorio de Fluidodinámica, Facultad de Ingeniería, Universidad de Buenos Aires, C1063ACV CABA, Argentina

[5]CNRS – Centre National de la Recherche Scientifique, 75795 Paris, France

(Received 21 December 2020; revised 8 May 2021; accepted 18 June 2021)

"Topological colouring of fluid particles" = using BraMAH to study the individual dynamics of a sparse particle set.

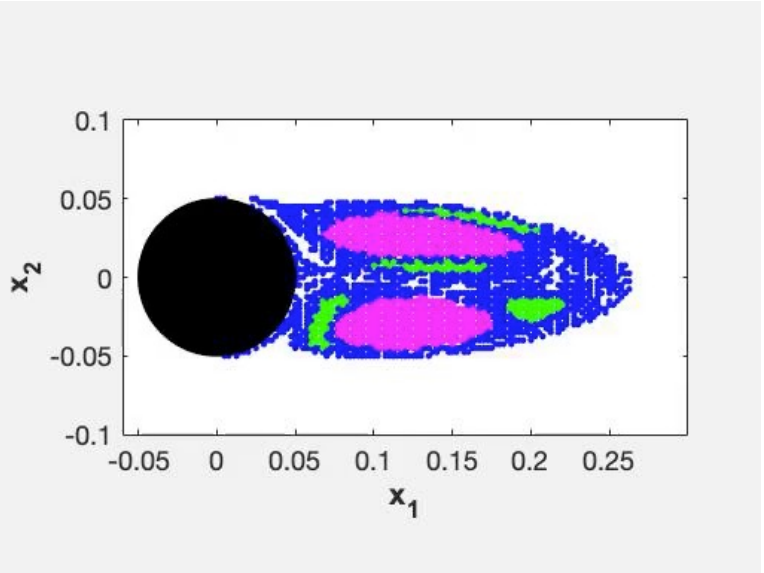

Numerically generated fluid particle behaviour in the wake past a rotary oscillating cylinder (ROC). With these applications, methodological progress is being made: BraMAH is successfully applied to non-dissipative (conservative) systems.

Applications

- Climate dynamics

Can homologies distinguish between simulated climate attractors?

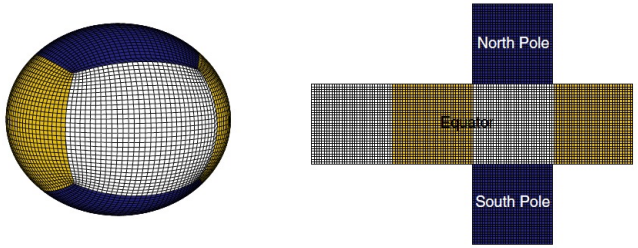

Climate Dynamics
https://doi.org/10.1007/s00382-019-04926-7

Check for updates

Co-existing climate attractors in a coupled aquaplanet

M. Brunetti[1] · J. Kasparian[1] · C. Vérard[2]

Received: 8 March 2019 / Accepted: 2 August 2019

Abstract
The first step in exploring the properties of dynamical systems like the Earth climate is to identify the different phase space regions where the trajectories asymptotically evolve, called 'attractors'. In a given system, multiple attractors can co-exist under the effect of the same forcing. At the boundaries of their basins of attraction, small changes produce large effects. Therefore, they are key regions for understanding the system response to perturbations. Here we prove the existence of up to five attractors in a simplified climate system where the planet is entirely covered by the ocean (aquaplanet). These attractors range from a snowball to a hot state without sea ice, and their exact number depends on the details of the coupled atmosphere–ocean–sea ice configuration. We characterise each attractor by describing the associated climate feedbacks, by using the principal component analysis, and by measuring quantities borrowed from the study of dynamical systems, namely instantaneous dimension and persistence.

Keywords Coupled aquaplanet · Attractors · GCM · Complexity

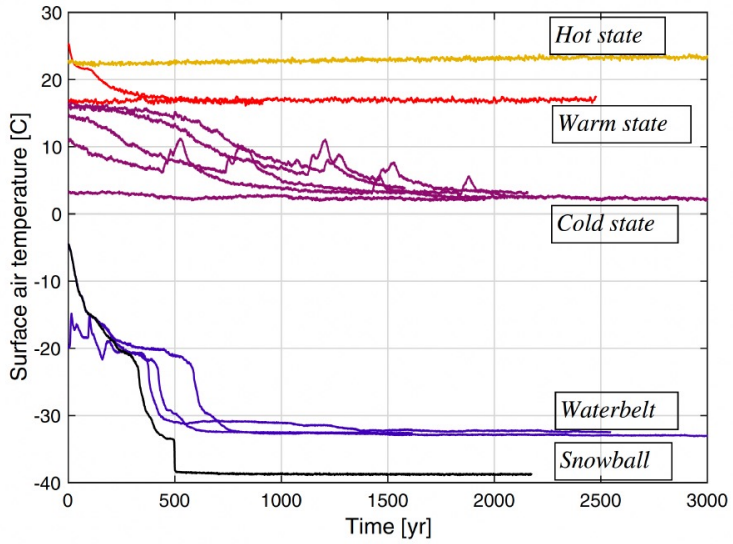

Attractor	Waterbelt	Cold state	Warm state	Hot state
SAT (°C)	-33.00 ± 0.03	2.2 ± 0.1	17.0 ± 0.2	23.4 ± 0.1
Ocean temperature (°C)	-1.6449 ± 0.0008	3.225 ± 0.002	9.877 ± 0.004	17.418 ± 0.006
Sea ice extent (10^6 km^2)	429.51 ± 0.06	160.4 ± 0.9	67 ± 1	0
Latitude of sea ice boundary	9	43	60	90
TOA budget (W/m^2)	1.6 ± 0.1	3.0 ± 0.2	2.6 ± 0.2	2.3 ± 0.2
Ocean surface budget Q_{net} (W/m^2)	0.01 ± 0.14	-0.009 ± 0.217	0.03 ± 0.29	0.05 ± 0.27

https://web.dm.uba.ar/files/tesis_lic/2023/Salvagni.pdf

Applications

- Climate dynamics

The time series of the annual averages are, when embedded, indistinguishable from each other, giving rise to point clouds distributed in the form of spheres or tori.

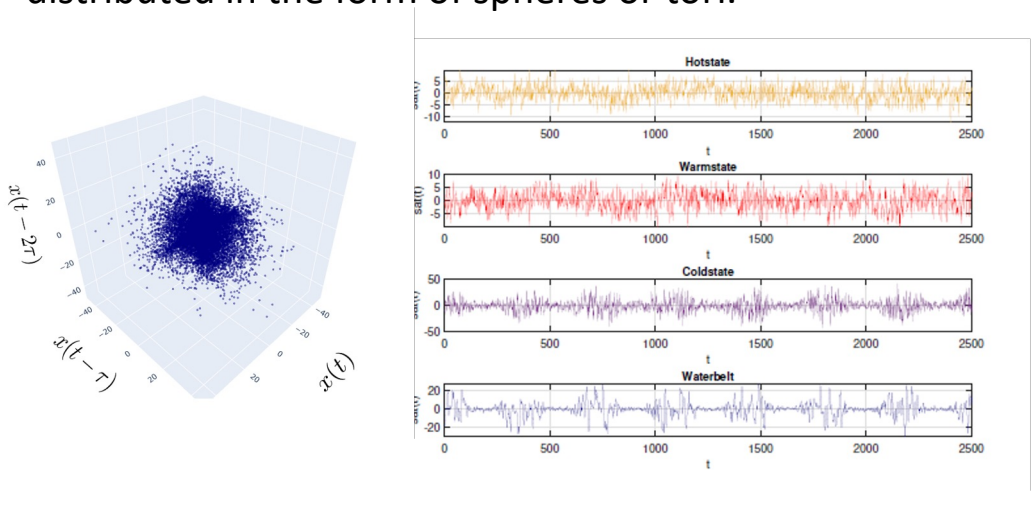

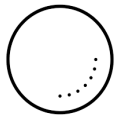

Solid sphere in phase space → statistical version of a fixed point in phase space: transient discarded, the system stabilizes around a given point.

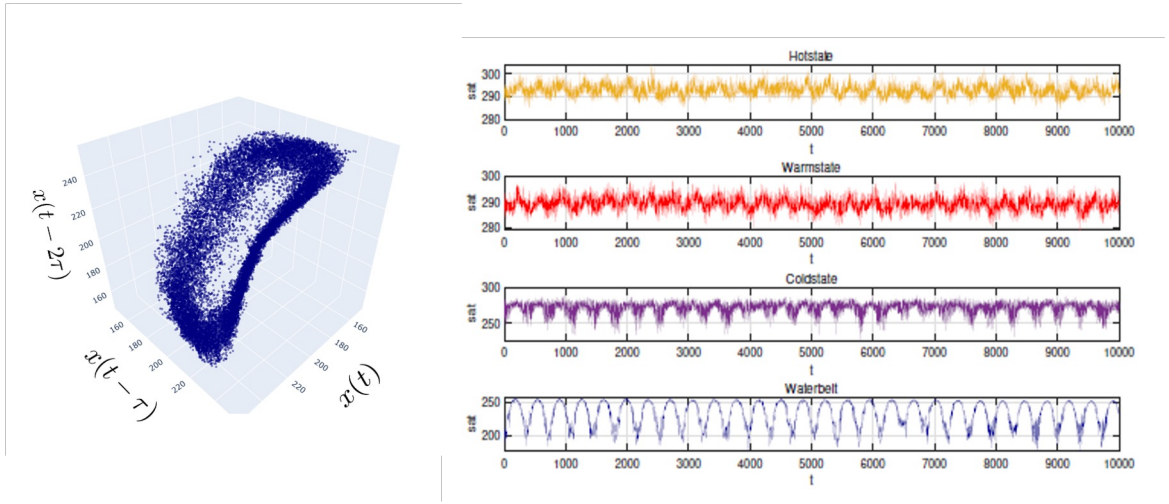

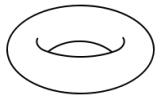

Filled torus in phase space → When the predominant dynamics in the global variability is that of the seasonal cycle Falasca, F., & Bracco, A. (2022). The seasonal cycle will be filtered.

Applications

- Climate dynamics

The dynamical properties of a climate attractor depend on its local and instantaneous properties, rather than its average properties [Lucarini et al, 2016]. Time series for the analysis will have a lower time resolution than that used in [Brunetti et al, 2019], filtering the seasonal cycle.

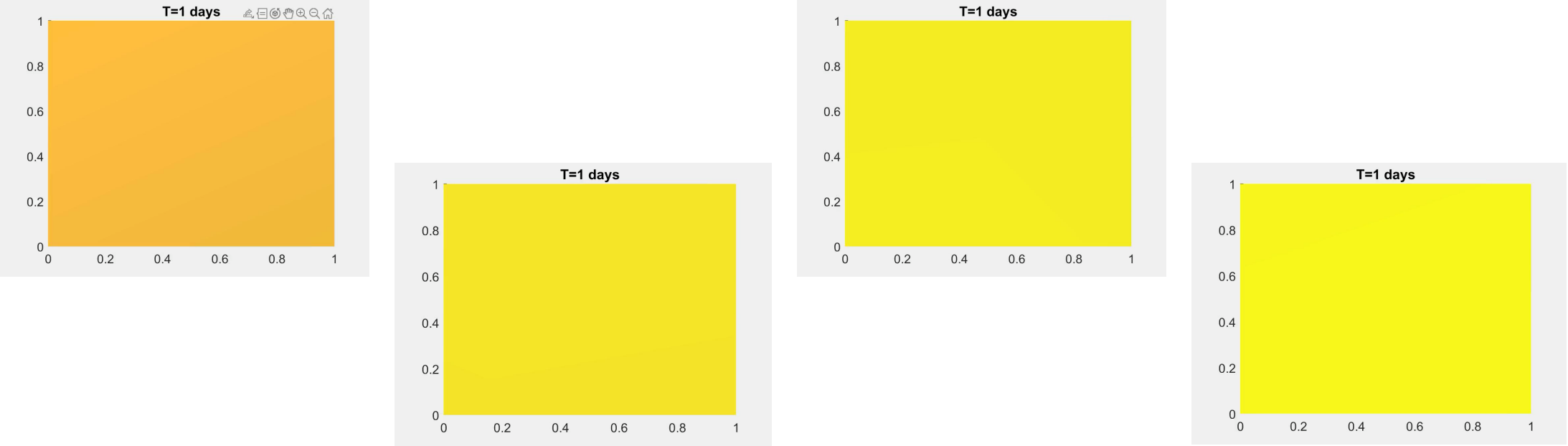

Evolution of four attractors with sliding time windows of 1000 days (range 5000 days) and daily time resolution. The time series were calculated by Maura Brunetti specifically for Luciana Salvagni's bachelor thesis.

Applications

- Climate dynamics

It is common practice to perform multi-channel singular spectrum analysis (M-SSA) separated by variable type (oceanic and atmospheric) to obtain consistent surrogate time series representative of each subsystem.

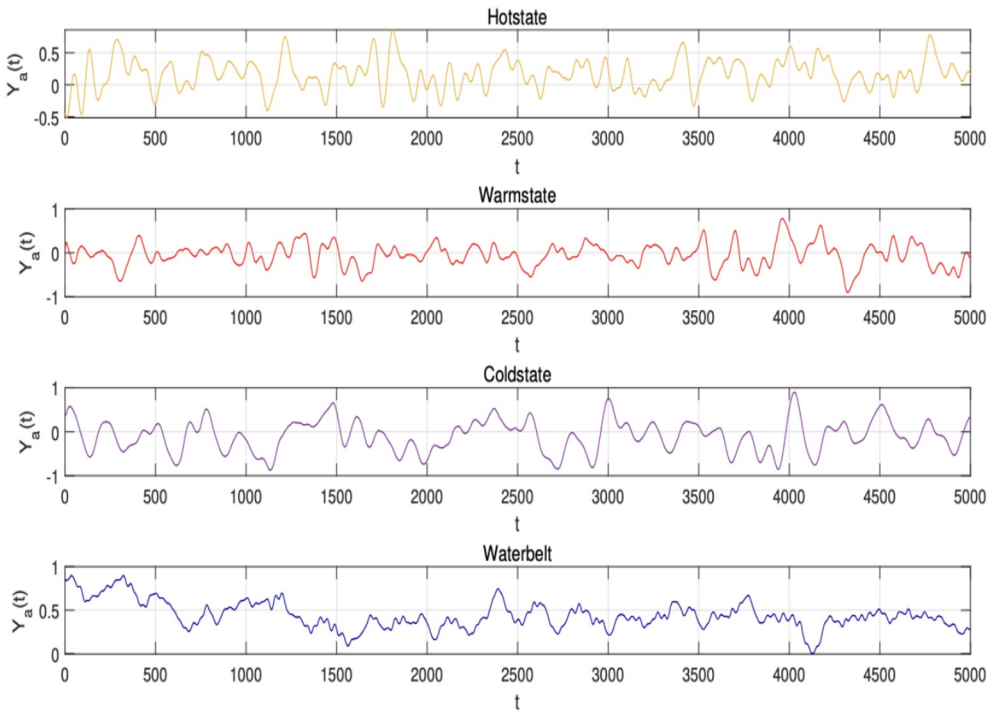

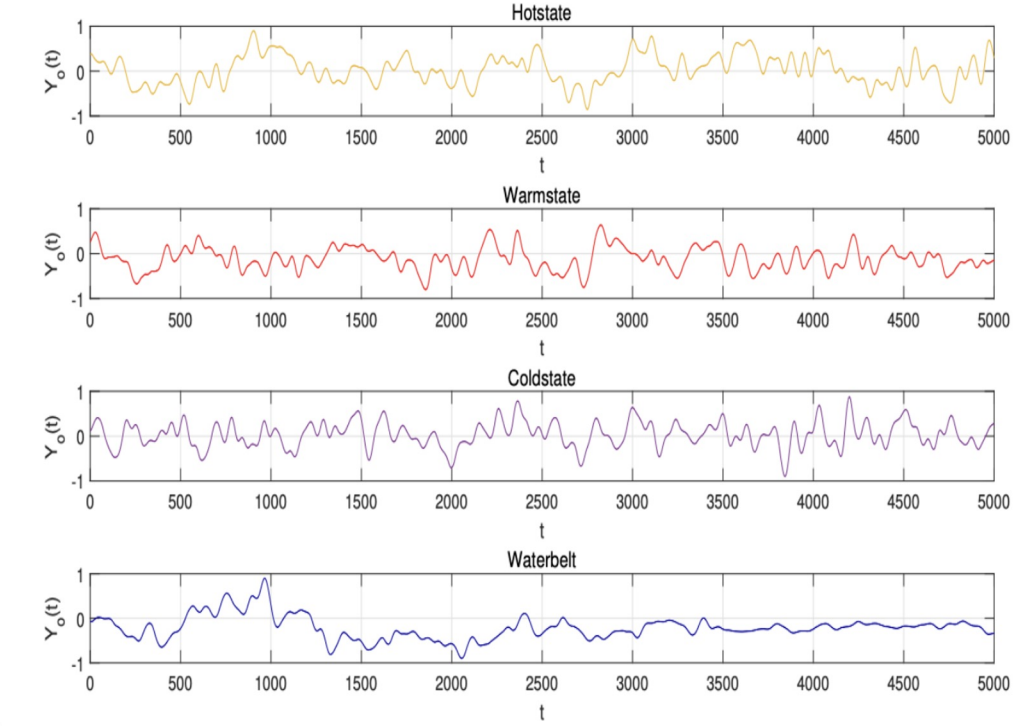

Vautard, R., Yiou, P., & Ghil, M. (1992). Singular-spectrum analysis: A toolkit for short, noisy chaotic signals. *Physica D: Nonlinear Phenomena*, *58*(1-4), 95-126.

Applications

- Climate dynamics

Persistent diagrams

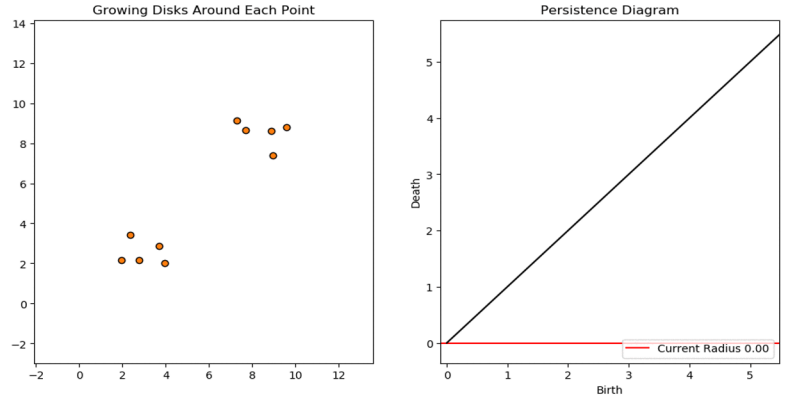

Atmospheric variables $Y_a(t)$

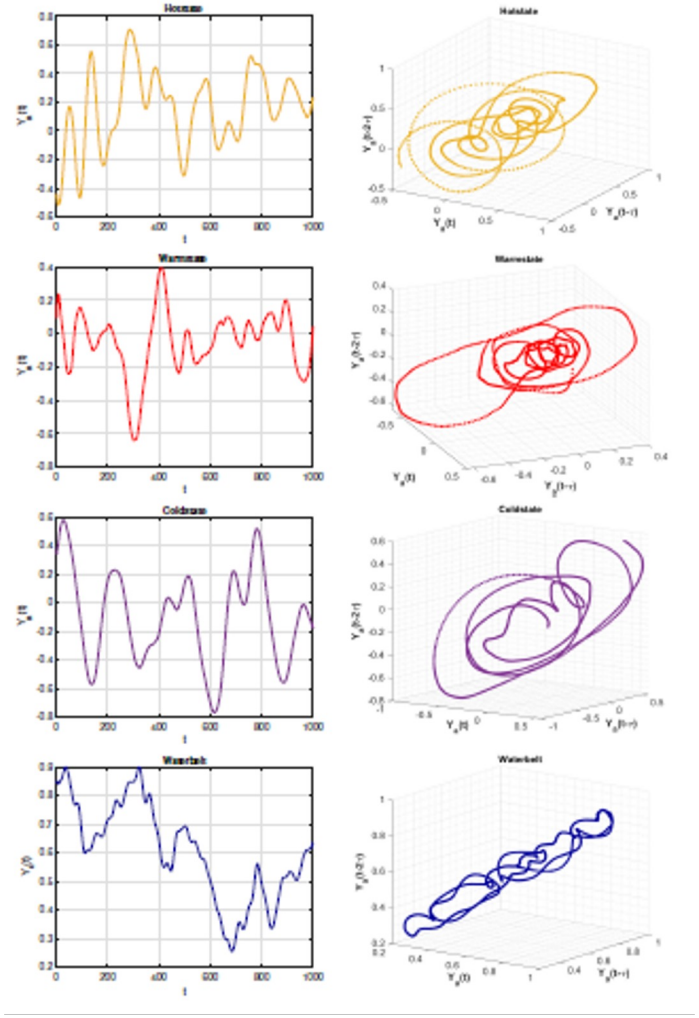

Oceanic variables $Y_o(t)$

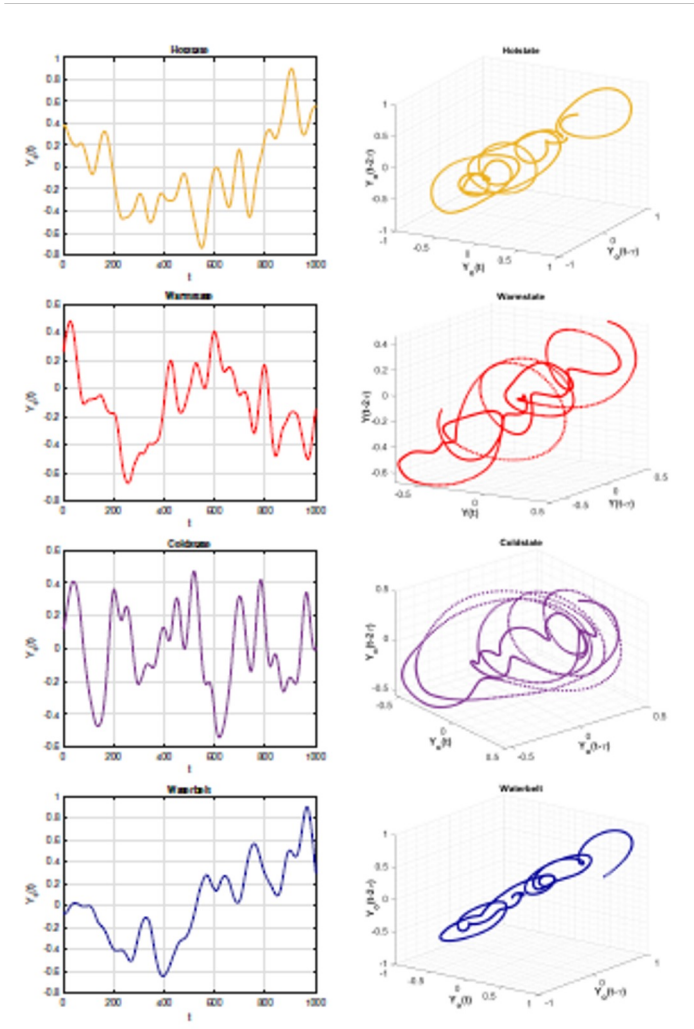

Applications

- Climate dynamics

Plane persistence diagram:

- Points close to the horizontal axis → "noise", born and die fast.
- Points away from the horizontal axis → significant features, persist longer.
- Two orange dots → two 1-hole butterfly wings.

We gather in the same persistence diagram:
0-holes (blue),
1-hole (orange)

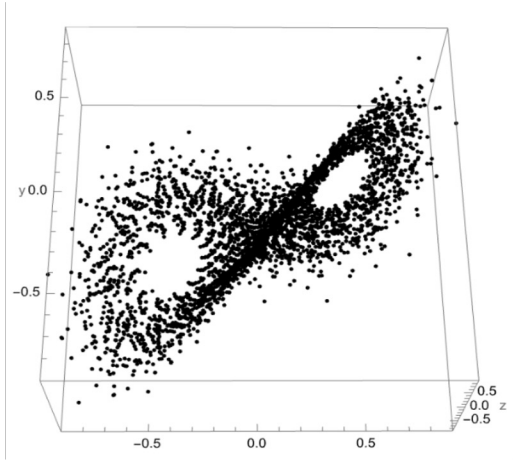

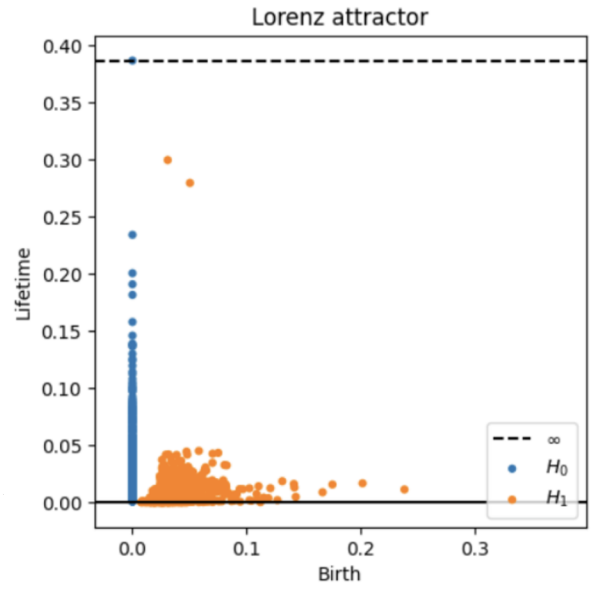

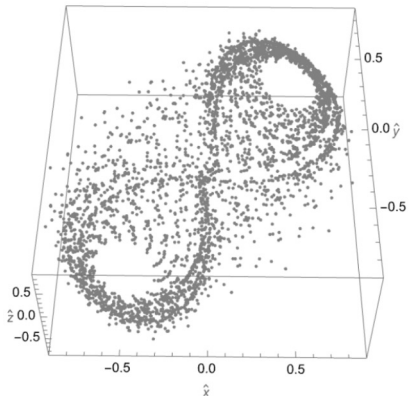

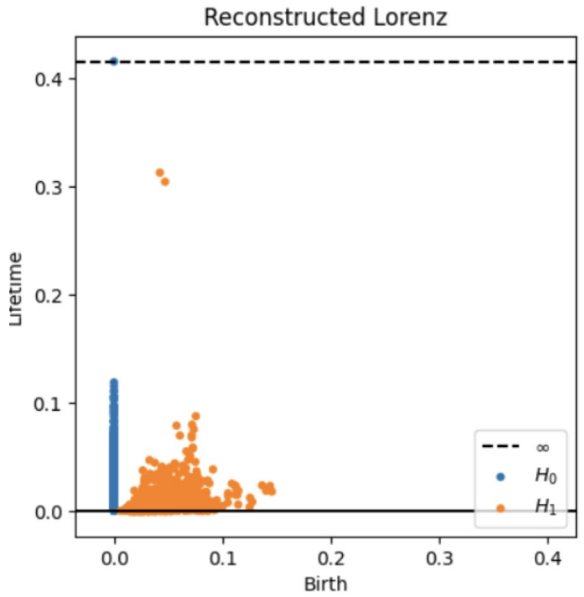

Applications

- Climate dynamics

Four attractors.
Atmospheric & oceanic planar persistence diagrams.

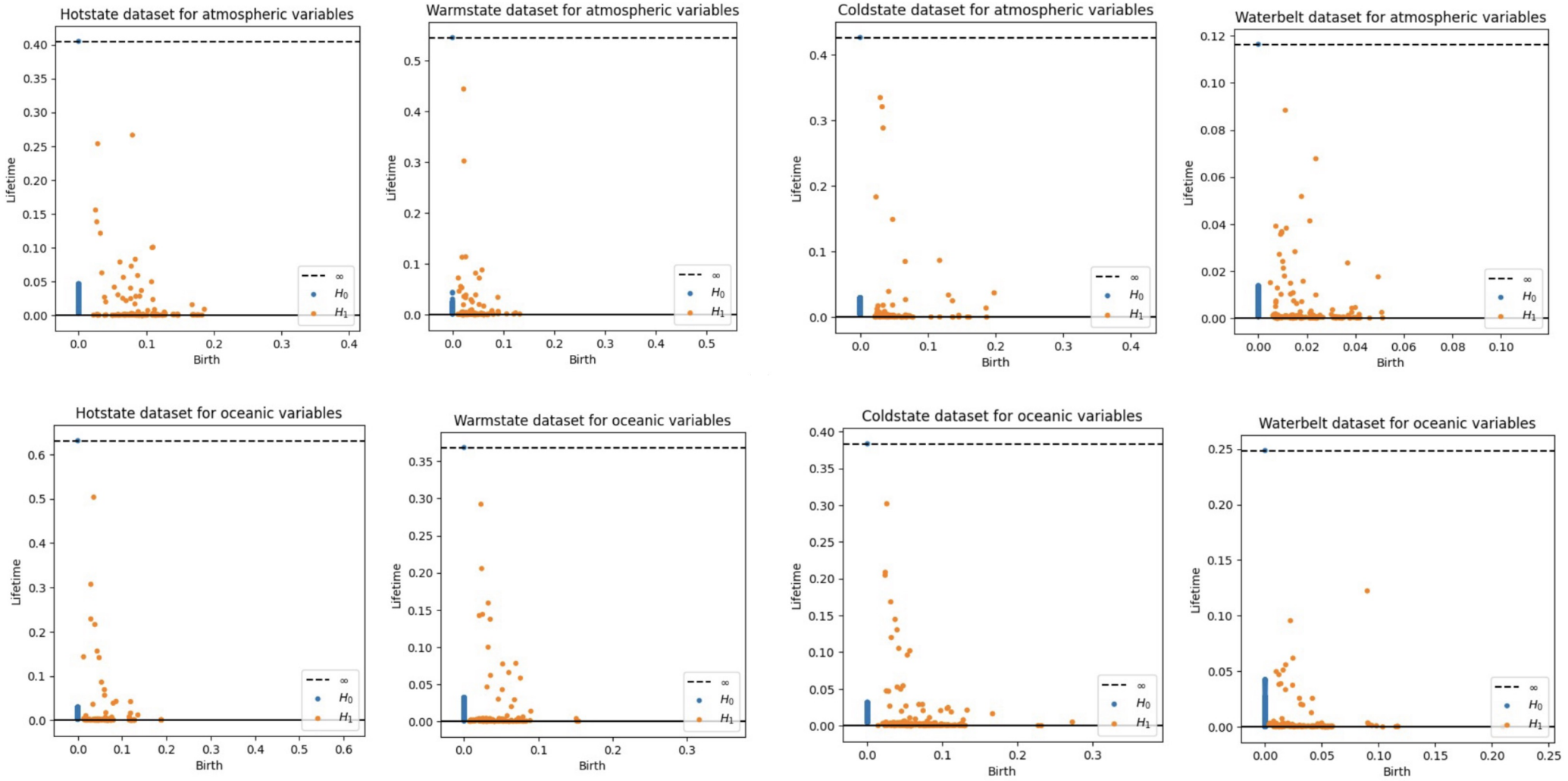

Applications

- Climate dynamics

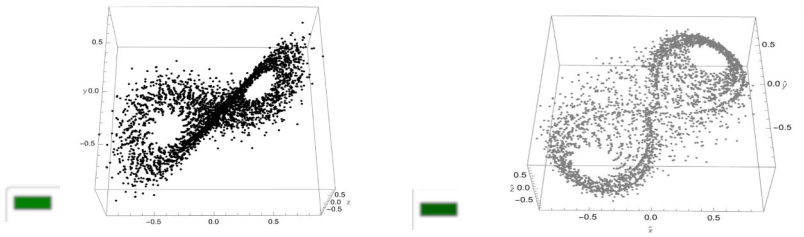

To analyze the persistence diagrams, a set of eight markers or topological indices will be defined to condense the properties of the diagrams and compare them with each other. The markers are based on the vertical coordinates of the blue and orange points of the persistence diagrams.

$F0_1$: vertical coordinate or lifetime of the second most persistent 0-hole (indicates the onset in the filtration where the simplices of the corresponding complex form a connected component).

$F0_2$: vertical coordinate or lifetime of the third 0-hole (indicates the beginning in the filtration where two related components are formed).

$F0_3$: sum of the lifetimes of all 0-holes except those exceeding the maximum filtration value (describes the degree of compactness of the points).

$F0_4$: averaged lifetime of the 0-holes except those exceeding the maximum filtration value.

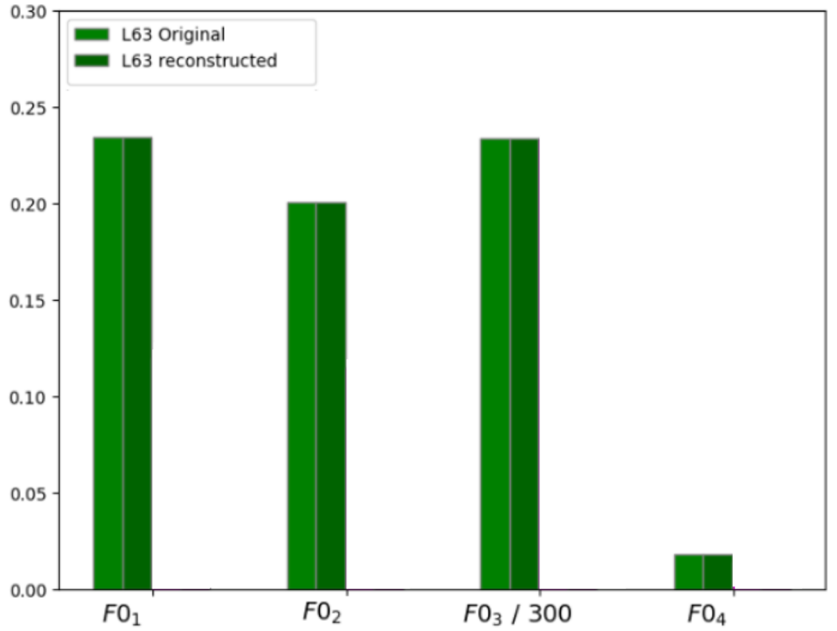

https://web.dm.uba.ar/files/tesis_lic/2023/Salvagni.pdf

Applications

- Climate dynamics

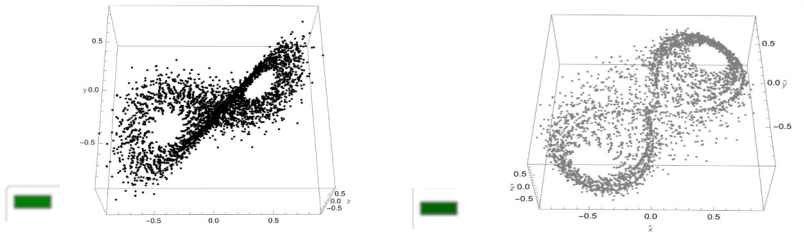

To analyze the persistence diagrams, a set of eight markers or topological indices will be defined to condense the properties of the diagrams and compare them with each other. The markers are based on the vertical coordinates of the blue and orange points of the persistence diagrams.

$F1_1$: the start (birth) value of the largest 1-hole (shows the filtration value at which the largest persistent 1-hole is formed).

$F1_2$: vertical coordinate or lifetime of the largest 1-hole (reflects the size of the geometrically dominant 1-hole).

$F1_3$: sum of the half-lives of all 1-holes except those exceeding the maximum filtration value.

$F1_4$: averaged life time of the 1-holes, except those exceeding the maximum filtration value (indicative of the average size of the 1-holes).

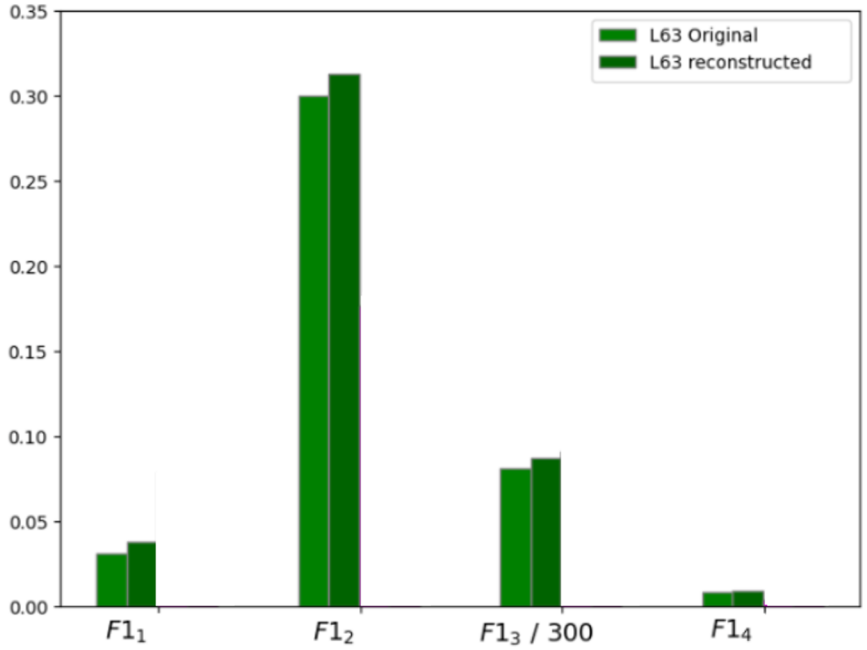

https://web.dm.uba.ar/files/tesis_lic/2023/Salvagni.pdf

Applications

- Climate dynamics

Each attractor has a predominant trait that distinguishes it from the others in time windows of one thousand days.

Persistent homology methods do not allow the topological structure of each attractor to be condensed into a single representative cell complex.

Although persistence diagrams offer a less precise topological characterization, they mark a path toward the construction of cell complexes that represent the topological structure of each climatic attractor, using the markers as a guide.

Topological markers for the four climatic attractors

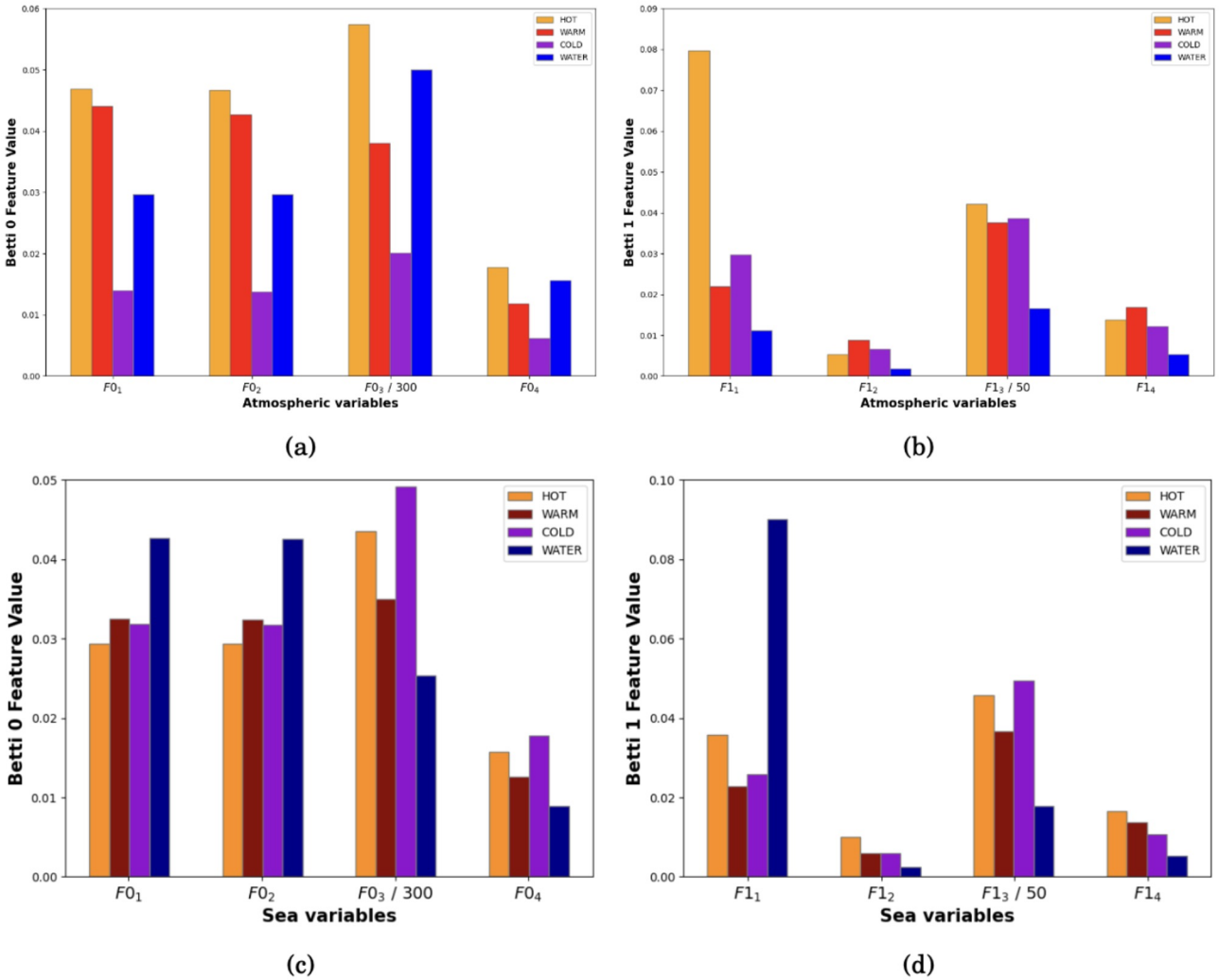

https://web.dm.uba.ar/files/tesis_lic/2023/Salvagni.pdf

Templex

AIP Chaos: An Interdisciplinary Journal of Nonlinear Science

This paper was selected as Featured

Featured

Templex: A bridge between homologies and templates for chaotic attractors

Gisela D. Charó, Christophe Letellier and Denisse Sciamarella

Templex

- Why and how was it conceived?

Homologies cannot distinguish between two different attractors produced by the Rössler dynamical system with different parameter values (spiral Rossler attractor with a = 0.343295 on the left and the funnel Rössler attractor with a = 0.492 on the right).

$$\begin{cases} \dot{x} = -y - z, \\ \dot{y} = x + ay, \\ \dot{z} = b + z(x - c). \end{cases}$$

Spiral Rössler attractor

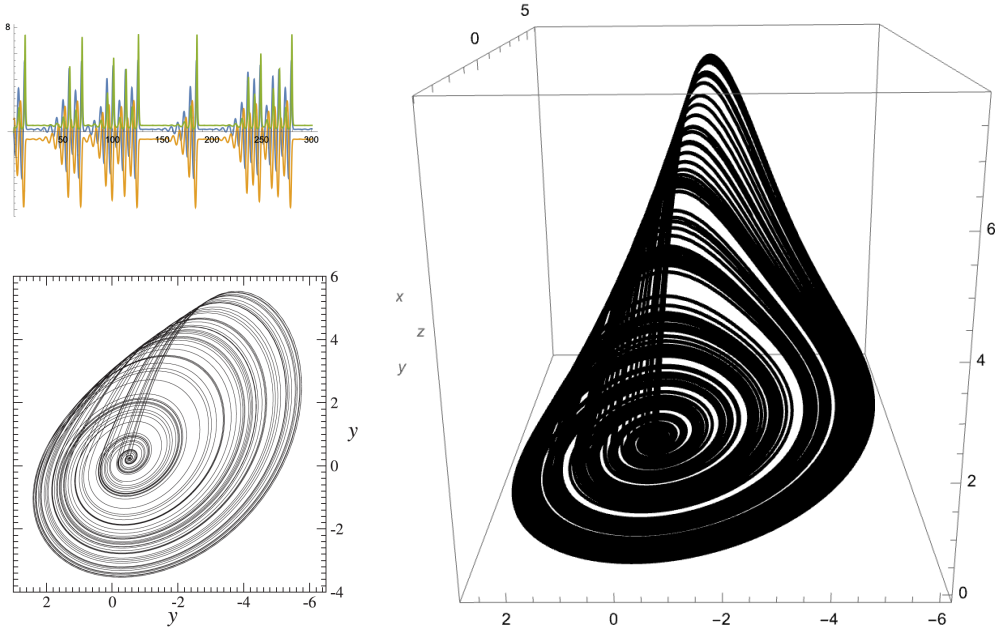

Funnel Rössler attractor

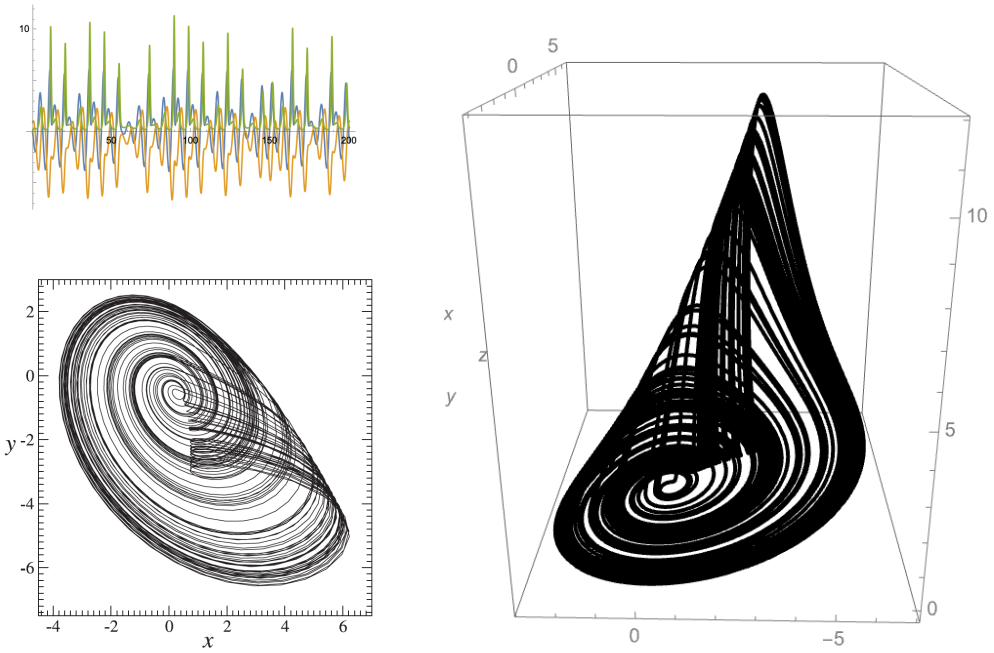

Templex

- Why and how was it conceived?

The template does distinguish between both: the spiral Rössler attractor has two strips (0, 1), while the funnel Rössler attractor has three strips (0,1,2).

Spiral Rössler attractor

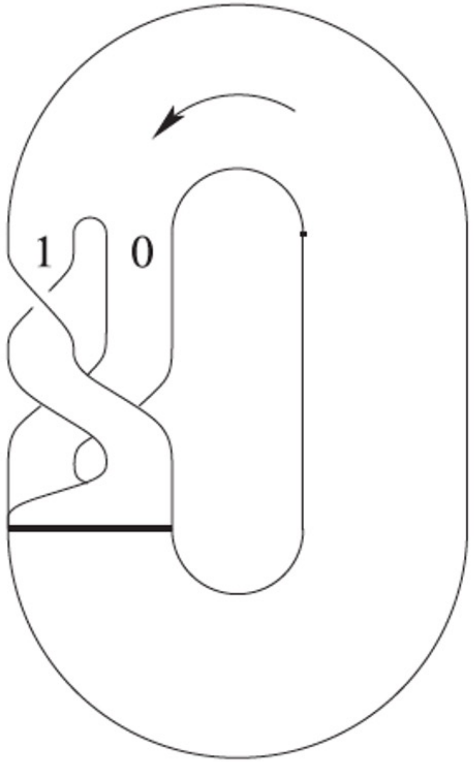

Funnel Rössler attractor

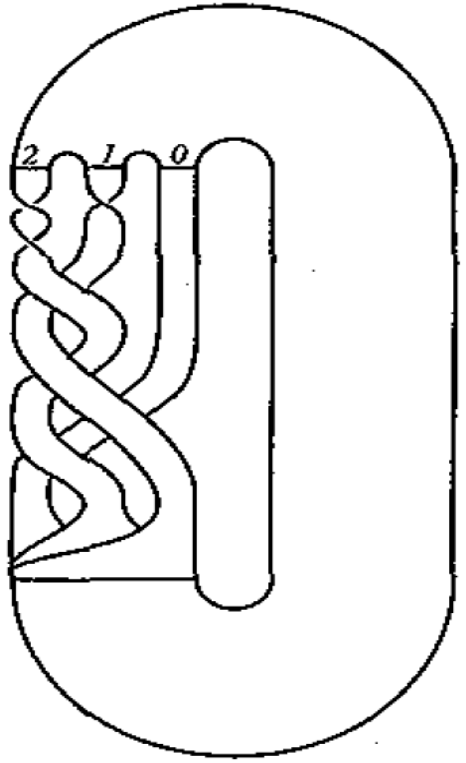

Templex

- Why and how was it conceived?

  The spiral and funnel Rössler attractors are homologically equivalent: **they have both one hole in the centre** ($H_1 = Z^1$).

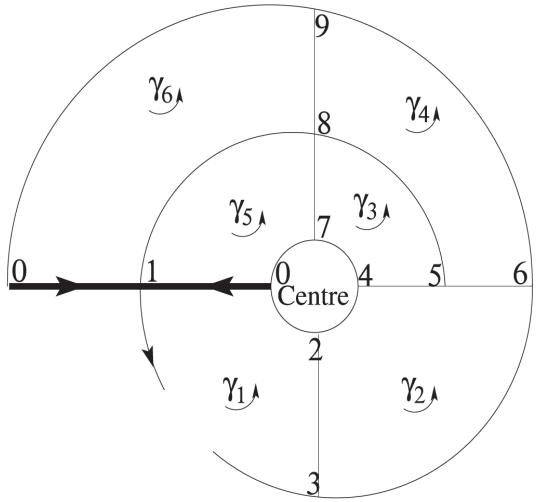

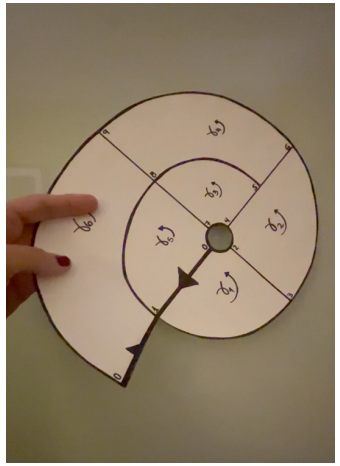

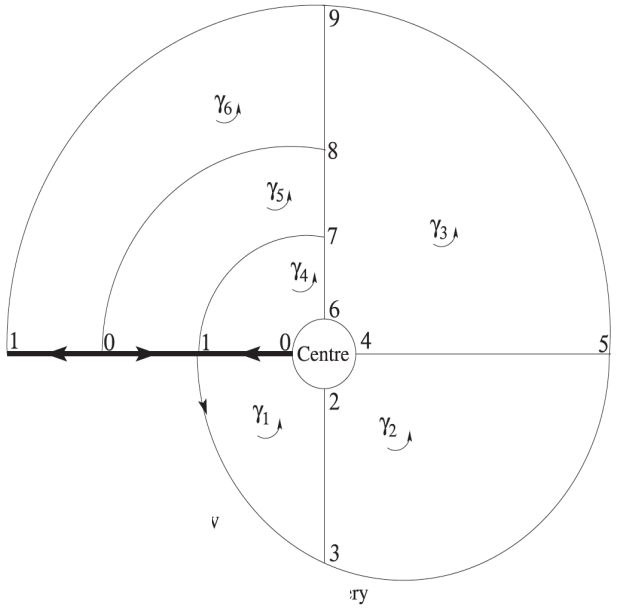

$$\mathcal{H}_1(K(\mathrm{R})) = [[\langle 0,2\rangle - \langle 0,7\rangle + \langle 2,4\rangle + \langle 4,7\rangle]]$$

$$\mathcal{H}_1(K(\mathrm{R}_3)) = [[\langle 0,2\rangle - \langle 0,6\rangle + \langle 2,4\rangle + \langle 4,6\rangle]]$$

But there is more information in a cell complex than the one contained in its homology groups… for instance, the joining lines! They can be detected as the 1-cells shared by at least three 2-cells (thick lines).
Notice that the recipe to scotch the cell complexes is different.

Templex

- Why and how was it conceived?

But there is something else that is very important and that is missing in a cell complex representing a branched manifold.

This is the *flow* or, in other words, *time*!

Homologies do not consider the action of the flow on the cell complex…

In order to take the flow on the complex into account, the cell complex will be endowed with a directed graph that prescribes the flow direction between its highest-dimensional cells.

Definition 1. A **templex** $T \equiv (K, G)$ is made of a complex K of dimension $\dim(K) = \kappa$ and a digraph $G = (N, E)$ whose underlying space is a branched κ-manifold associated with a dynamical system, such that (i) the nodes N are the κ-cells of K and (ii) the edges E are the connections between the κ-cells allowed by the flow.

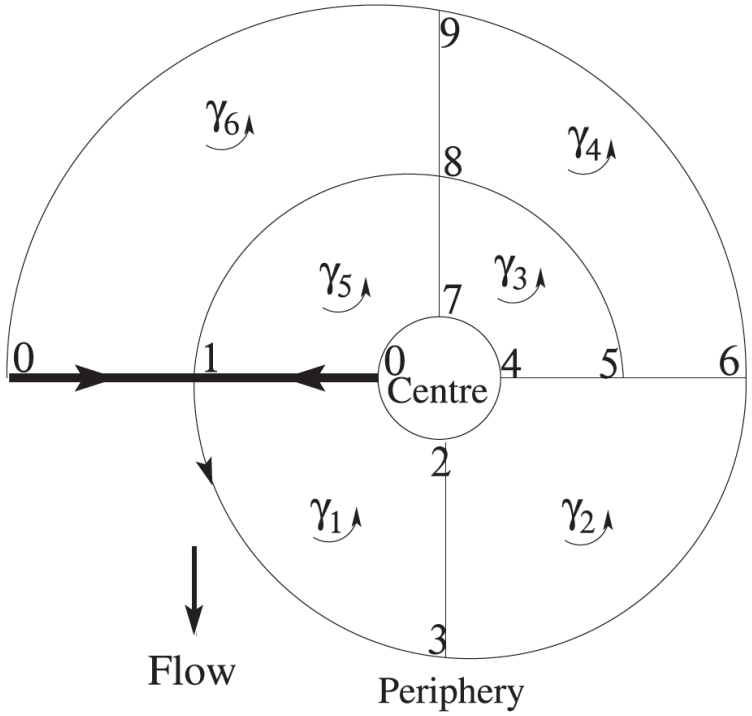

(a)

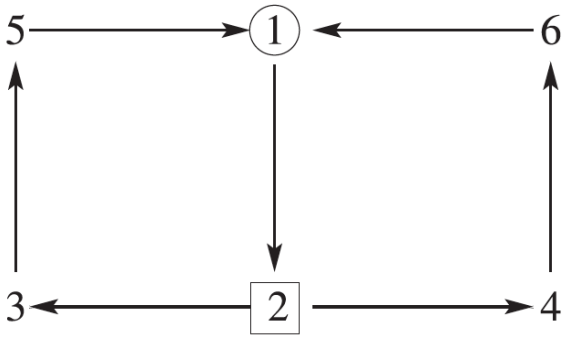

(b)

Templex

- Why and how was it conceived? How is it computed?

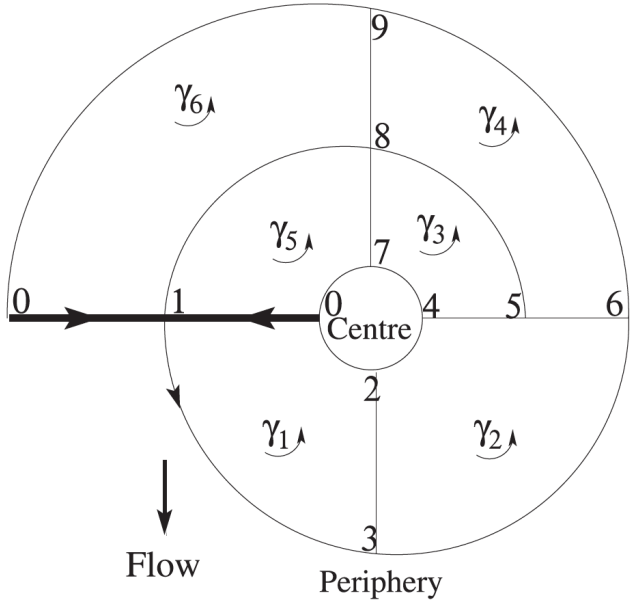

(a)

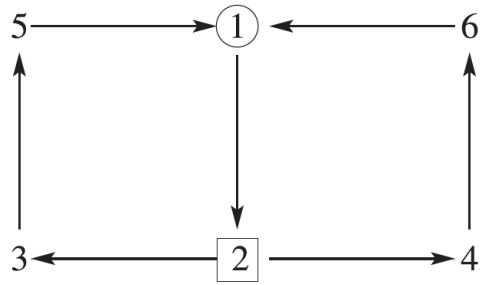

(b)

The thick line indicates the joining 1-cell <0, 1>, which will be used to identify:

- ❑ ingoing nodes (squares)
- ○ outgoing nodes (circles)

in the digraph.

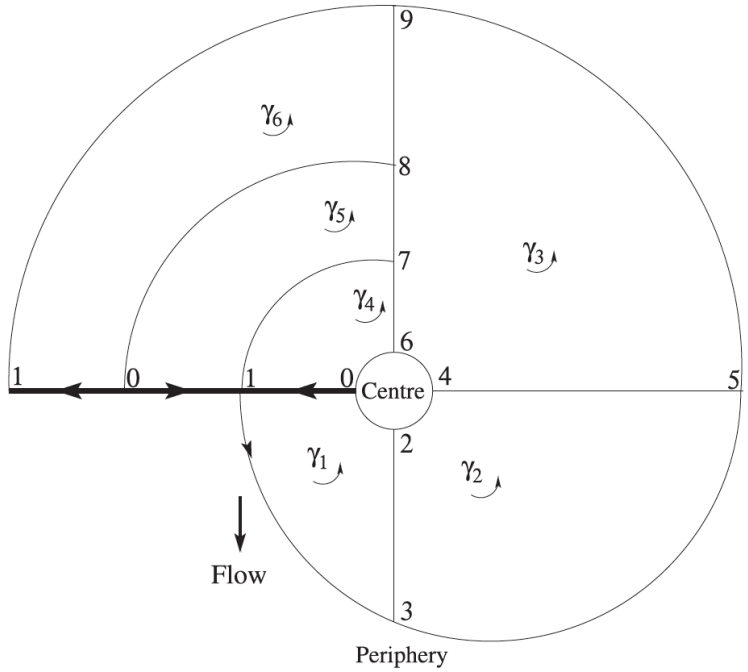

(a)

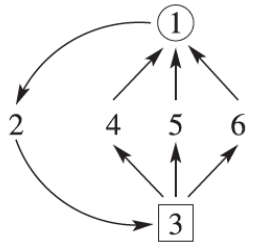

(b)

Templex

- Why and how was it conceived? How is it computed?

Spiral Rössler attractor

T(R)=(K(R),G(R))

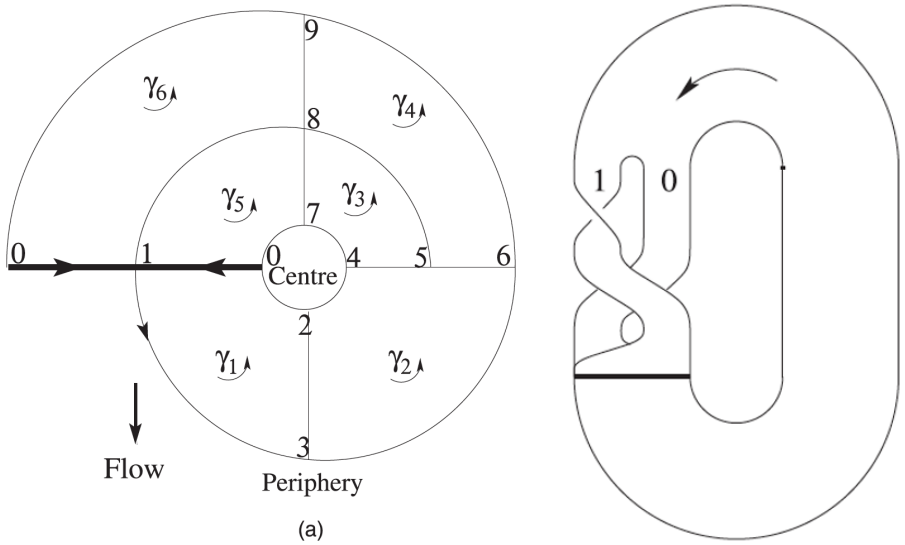

Stripexes in T(R):

twisted $\underline{1} \to 2 \to 4 \to 6 \to \underline{1},$

$\underline{1} \to 2 \to 3 \to 5 \to \underline{1}.$

Funnel Rössler attractor

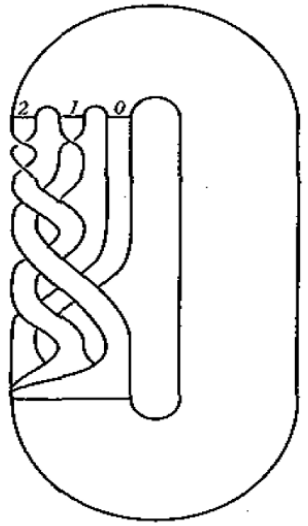

T(R3)=(K(R_3),G(R_3))

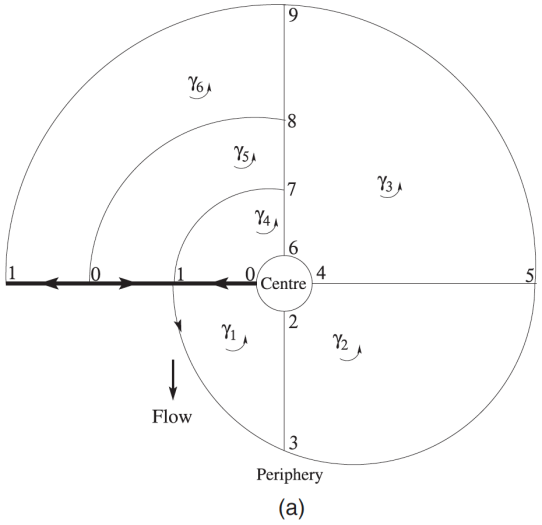

Stripexes in T(R_3):

$\underline{1} \to 2 \to 3 \to 4 \to \underline{1},$

twisted $\underline{1} \to 2 \to 3 \to 5 \to \underline{1},$

$\underline{1} \to 2 \to 3 \to 6 \to \underline{1},$

Templex

- Example I: Lorenz 63 example (autonomous)

T(L)=(K(L),G(L))

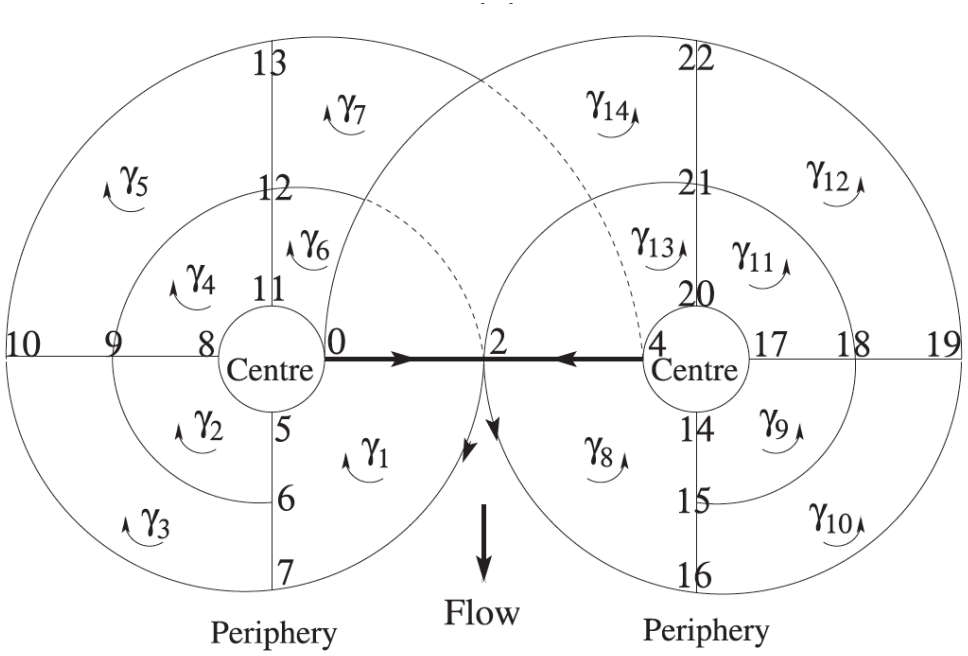

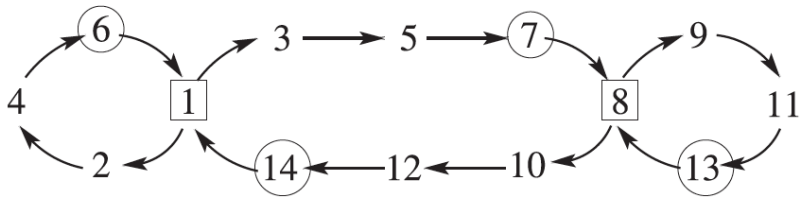

Four stripexes in T(L):

$c_1 \equiv \underline{1} \to 2 \to 4 \to 6 \to \underline{1},$

$c_2 \equiv \underline{8} \to 9 \to 11 \to 13 \to \underline{8},$

} strong cycles

$c_{3_1} \equiv \underline{1} \to 3 \to 5 \to 7 \to \underline{8}$

$c_{3_2} \equiv \underline{8} \to 10 \to 12 \to 14 \to \underline{1}.$

} weak cycles

The weak cycles that form the **two twisted stripexes** correspond to a single generatex of order 2.

This is consistent with the Lorenz template that has four stripexes and a Poincaré section divided into two components.

Templex

- Example II: 4D Deng 94 attractor (autonomous)

A four-dimensional system designed from a three-dimensional system proposed by Deng.

$$
\begin{cases}
\dot{x} = -(z+2)d\,(x - [a + \epsilon_3(2+w)]) + (2-z) \\
\qquad \left[\alpha(x-2) - \beta y - \alpha\,(x-2)\,\dfrac{(x-2)^2 + y^2}{R^2}\right], \\
\dot{y} = -(z+2)\,(y-b) + (2-z) \\
\qquad \left[\beta\,(x-2) + \alpha y - \alpha y \dfrac{(x-2)^2 + y^2}{R^2}\right], \\
\dot{z} = (4 - z^2)\,\dfrac{z + 2 - \mu(x+2)}{\epsilon_1} - cz, \\
\dot{w} = (4 - z^2)\,\dfrac{z + 2 - \mu(x+2)}{\epsilon_2} - cz.
\end{cases}
$$

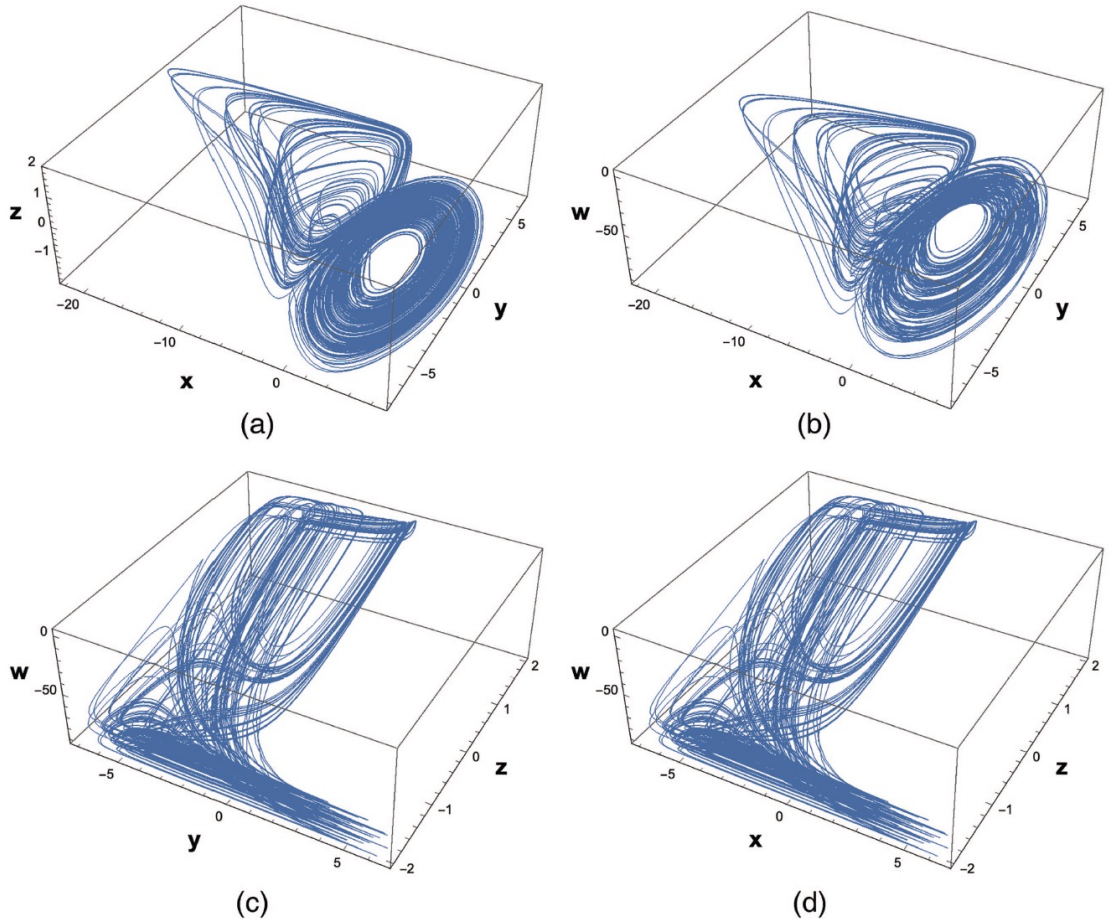

A solution to this system was already investigated with a BraMAH cell complex (but not with a templex) in Sciamarella & Mindlin, 2001.

Templex

- Example II: 4D Deng 94 attractor (autonomous)

The BRAMAH complex K(4D) is built from a cloud of 24999 points (once the transient regime is completed).

The highest-dimensional cells of this complex are the 3-cells γ_i , and the 2-cells σ_i which are not the border of any 3-cell.

The complex has one 0-hole, five 1-holes and no 2-holes (no enclosed empty cavity).

The joining lines are highlighted in colour. They are the 1-cells shared by a set of at least three *k*-cells, with *k*=2,3.

The green and red lines form the main joining locus in the bottom scroll and the second one (violet) is in the upper part of the attractor according to our plot.

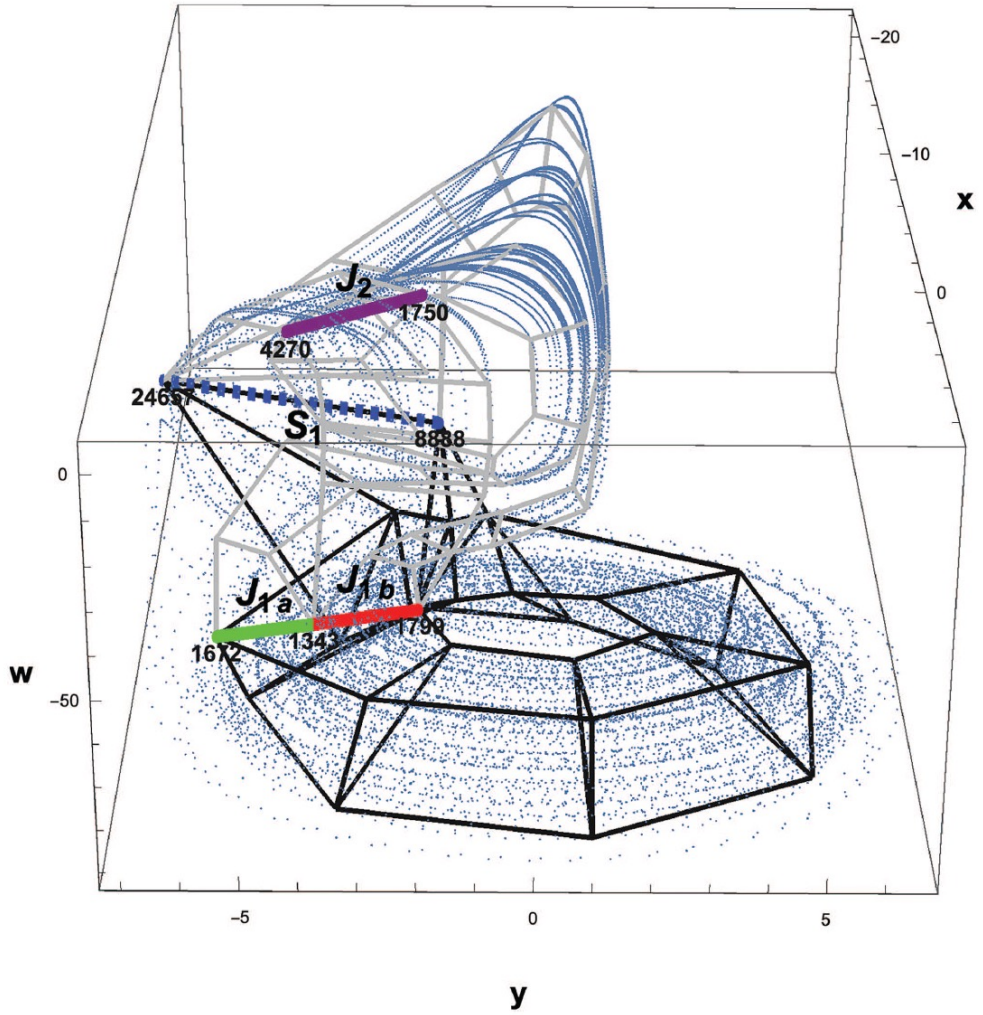

Templex

- Example II: 4D Deng 94 attractor (autonomous)

The dotted blue line is a splitting line between one 3-cell and three 2-cells.

The fact that the ingoing cell is of dimension 3 allows us to preserve the determinism at this splitting locus.

This is a feature that we had not observed for three-dimensional systems.

The simplest deterministic representation of the flow around this splitting locus is to consider that three strips—close to each other as in a foliation within the 3-cell— are sent away from each other.

This specificity will require a novel element for drawing a template.

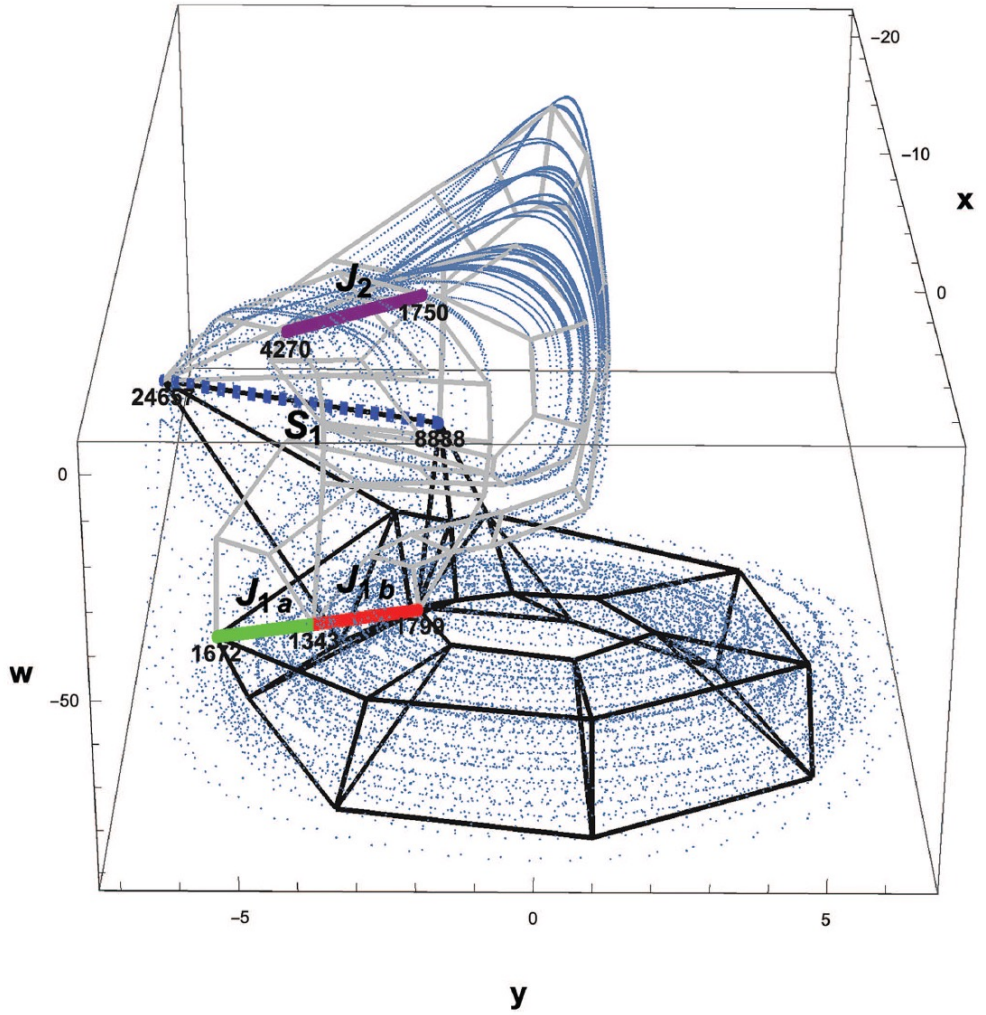

Templex

- Example II: 4D Deng 94 attractor (autonomous)

Digraph on the BRAMAH complex constituting the templex. Ingoing and outgoing nodes are squared and circled, respectively. Splitting loci are not considered for stripex computation.

Three order-1 cycles:

$$c_1 \equiv \underline{1} \to 2 \to 3 \to 4 \to 5 \to 6 \to 7 \to 8 \to \underline{1},$$

$$c_2 \equiv \underline{1} \to 2 \to 3 \to 4 \to 5 \to 6 \to 37 \to 40 \to 36 \to 35 \to 25 \to 26 \to 27 \to 28 \to 29 \to 30 \to 31 \to 32 \to 33 \to 34 \to 1.$$

$$c_3 \equiv \underline{1} \to 2 \to 3 \to 4 \to 5 \to 6 \to 37 \to 40 \to 38 \to 20 \to 19 \to 18 \to 17 \to 21 \to 22 \to 23 \to 24 \to \underline{1},$$

Two order-2 cycles:

$$c_{4_1} \equiv \underline{1} \to 2 \to 3 \to 4 \to 5 \to 6 \to 37 \to 40 \to 38 \to 20 \to 19 \to 18 \to 17 \to 16 \to 15 \to 14 \to \underline{12},$$

$$c_{4_2} \equiv \underline{12} \to 11 \to 10 \to 9 \to \underline{1}.$$

$$c_{5_1} \equiv \underline{1} \to 2 \to 3 \to 4 \to 5 \to 6 \to 37 \to 40 \to 39 \to 13 \to \underline{12},$$

Five stripexes in T(4D)=(K(4D),G(4D)):

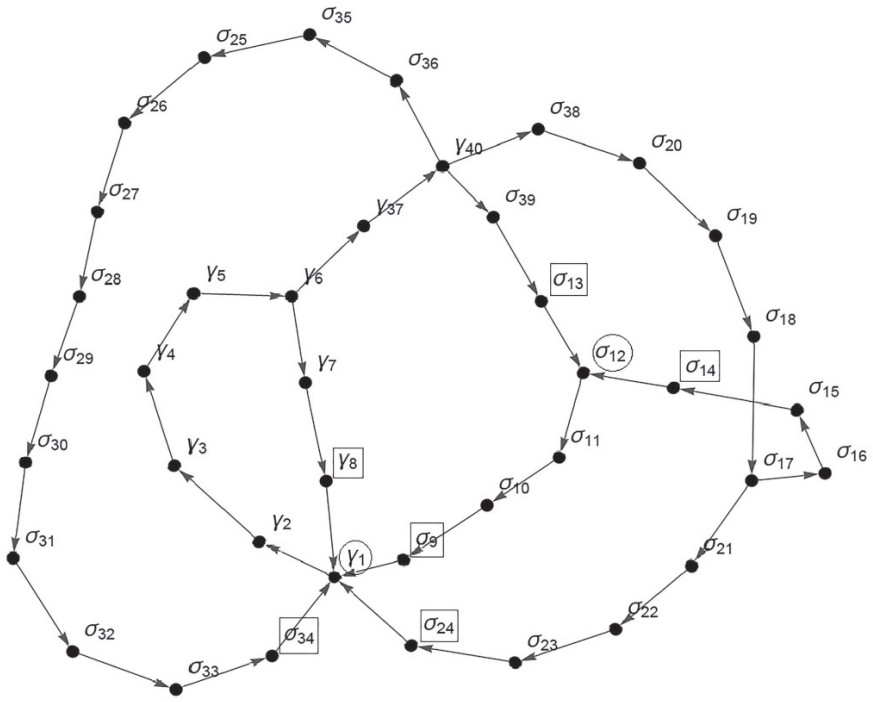

Templex

- Example II: 4D Deng 94 attractor (autonomous)

The four-dimensional attractor can be described with five stripexes, that is, with a five symbol dynamics. A paper model of the attractor is constructed, similar to the *xyz* projection of the system.

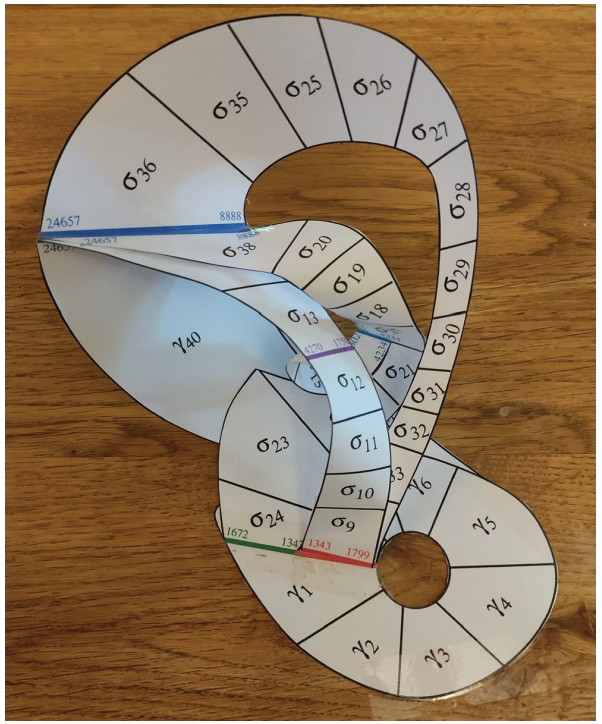

The volume formed by the ten 3-cells of K(4D) is topologically equivalent to a solid (filled) torus.

Homologies of a filled torus are equivalent to those of a cylinder, and so, the paper model is homologically equivalent to K(4D).

A direct template can be drawn for the four-dimensional system from the templex analysis.

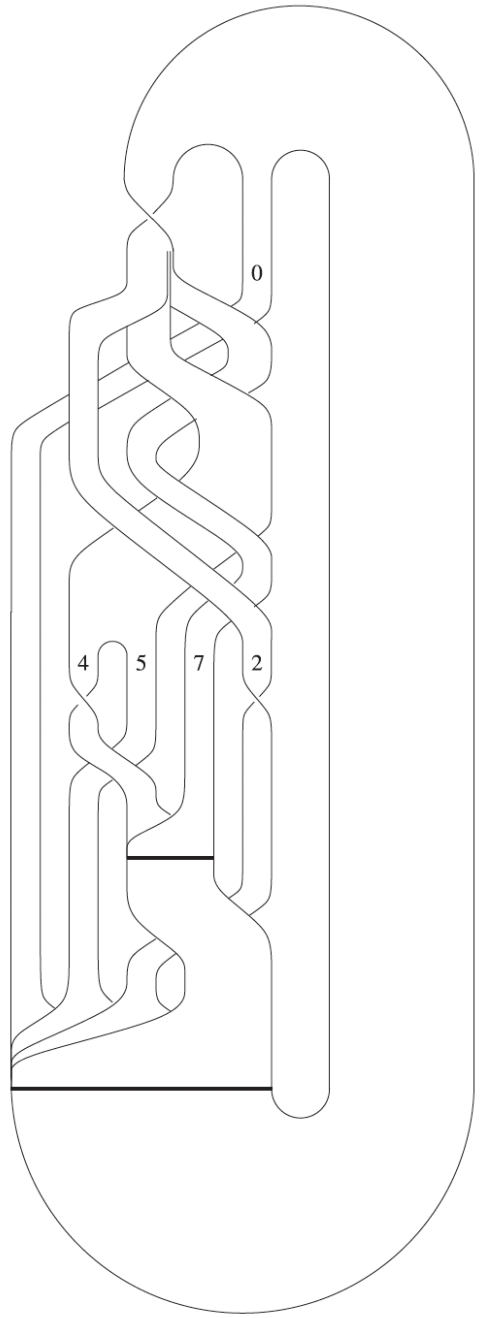

Templex

- Example II: 4D Deng 94 attractor (autonomous)

The templex dissects the phase-space structure into several identifiable components, connected at certain joints. Closed non-redundant pathways are cell sequences encoded by the digraph.

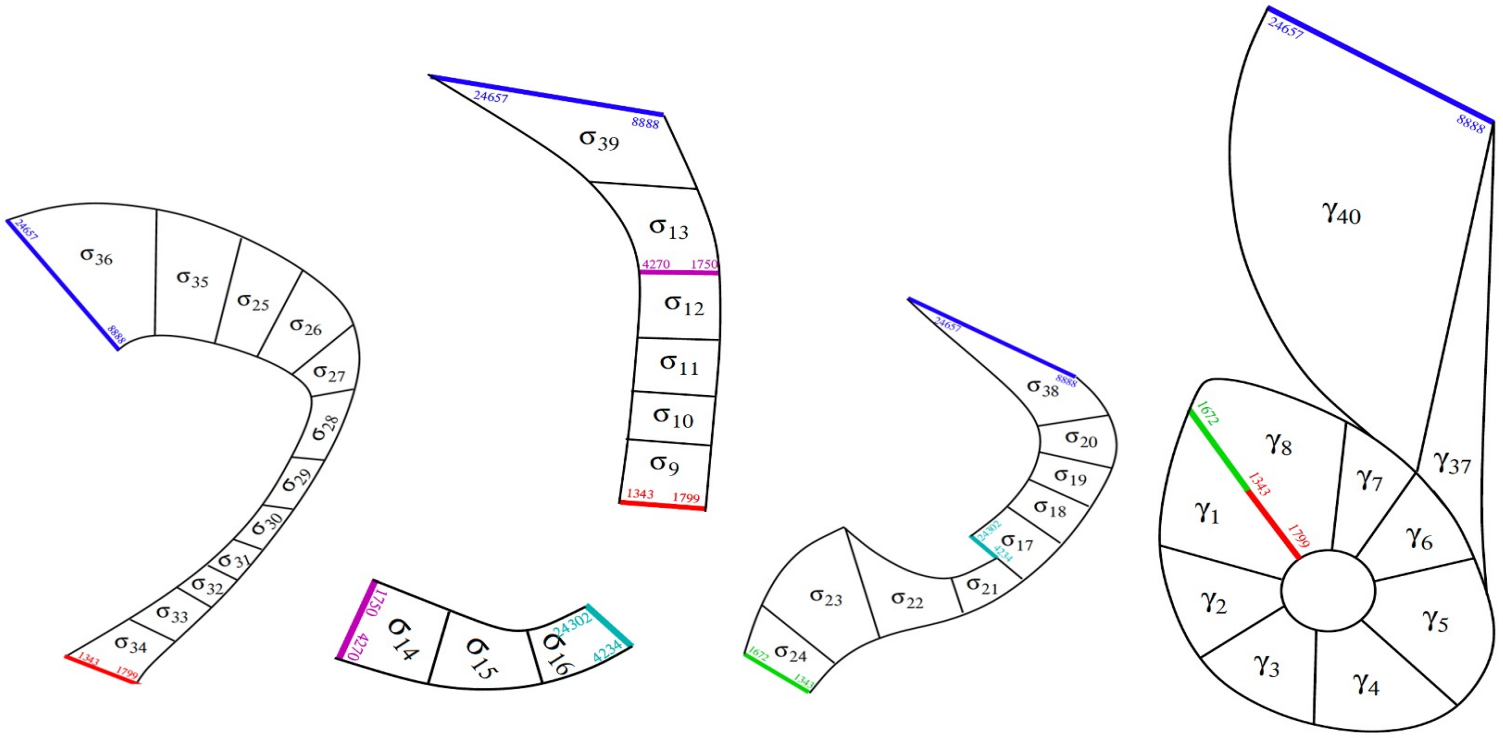

The templex properties: some describe the spatial structure alone (homology groups, torsion groups, weak boundaries) and a subset for the topology of flow along the structure (generatex, stripex, twists).

Templex

- Example III: 3D AMOC example (autonomous)

Let us now consider an autonomous 3D model of the Atlantic Meridional Overturning Circulation (AMOC) : Sévellec et Fedorov, *J. Clim.*, 2014) reproducing the chaotic dynamics of the glacial periods.

$$d_t\omega = -\lambda\omega - \epsilon\beta S_{NS},$$
$$d_t S_{BT} = +\Omega S_{NS} - K S_{BT} + F_{BT},$$
$$d_t S_{NS} = -\Omega S_{BT} - K S_{NS} + F_{NS}.$$

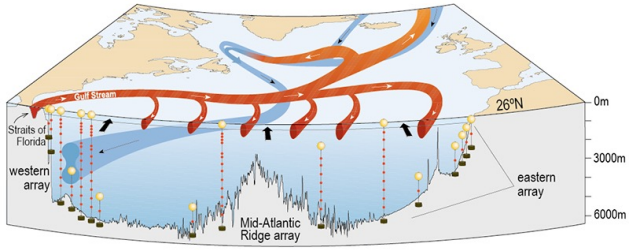

The most simple AMOC model has the same set of stripexes as the spiral Rössler attractor.

T(AMOC3D) = (K(AMOC3D), G(AMOC3D))

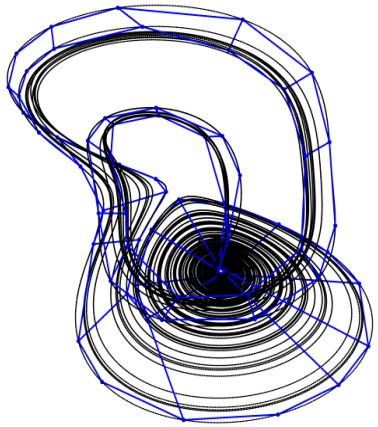

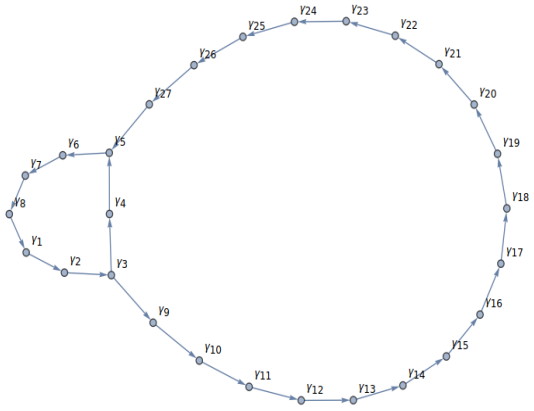

K(AMOC3D) has two 1-holes
T(AMOC3D) has two stripexes.

Stripexes in T(AMOC3D)

twisted $\underline{1} \to 2 \to 4 \to 6 \to \underline{1},$

$\underline{1} \to 2 \to 3 \to 5 \to \underline{1}.$

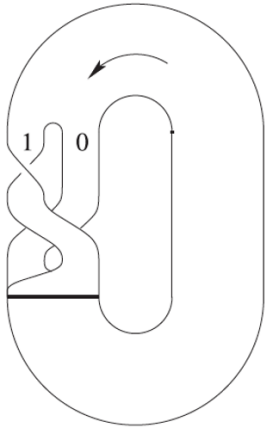

Work in progress with C. Mosto et J. Ruiz (IFAECI) en collaboration avec F. Sévellec et al. (Brest)

Templex

- Example IV: Unstable AMOC (non autonomous)

Let us consider the imposed temporal changes in the position of the edge of sea ice (ESI) to account for the chaotic behavior during the glacials and for the stable ocean conditions during the interglacials.. F_{BT} and F_{NS} are the Fourier projections of surface salt flux.

$$d_t\omega = -\lambda\omega - \epsilon\beta S_{NS},$$
$$d_t S_{BT} = +\Omega S_{NS} - K S_{BT} + F_{BT},$$
$$d_t S_{NS} = -\Omega S_{BT} - K S_{NS} + F_{NS},$$
$$\text{where } F_{BT} + iF_{NS} = \frac{S_0}{2\pi h}\int_0^{2\pi} F e^{-i\theta} d\theta.$$

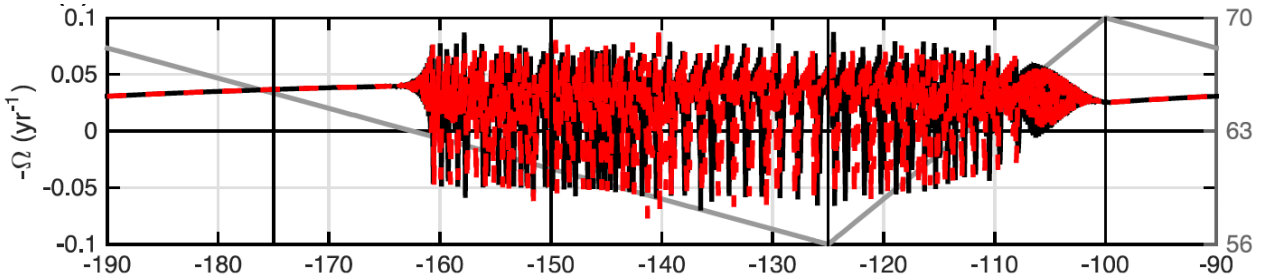

Simulated variations in the overturning rate (−Ω) for two slightly different sets of initial conditions (solid black and red dashed lines) for a single glacial–interglacial cycle.

The grey sawtooth line indicates the imposed temporal changes in the position of the edge of sea ice (ESI).

The four vertical lines indicate the freezing times (t0) used later to compute the Pullback attractor (**PBA**) [Ghil et al, 2008 ; Chekroun et al, 2011].

Templex

- Example IV: Unstable AMOC (non autonomous)

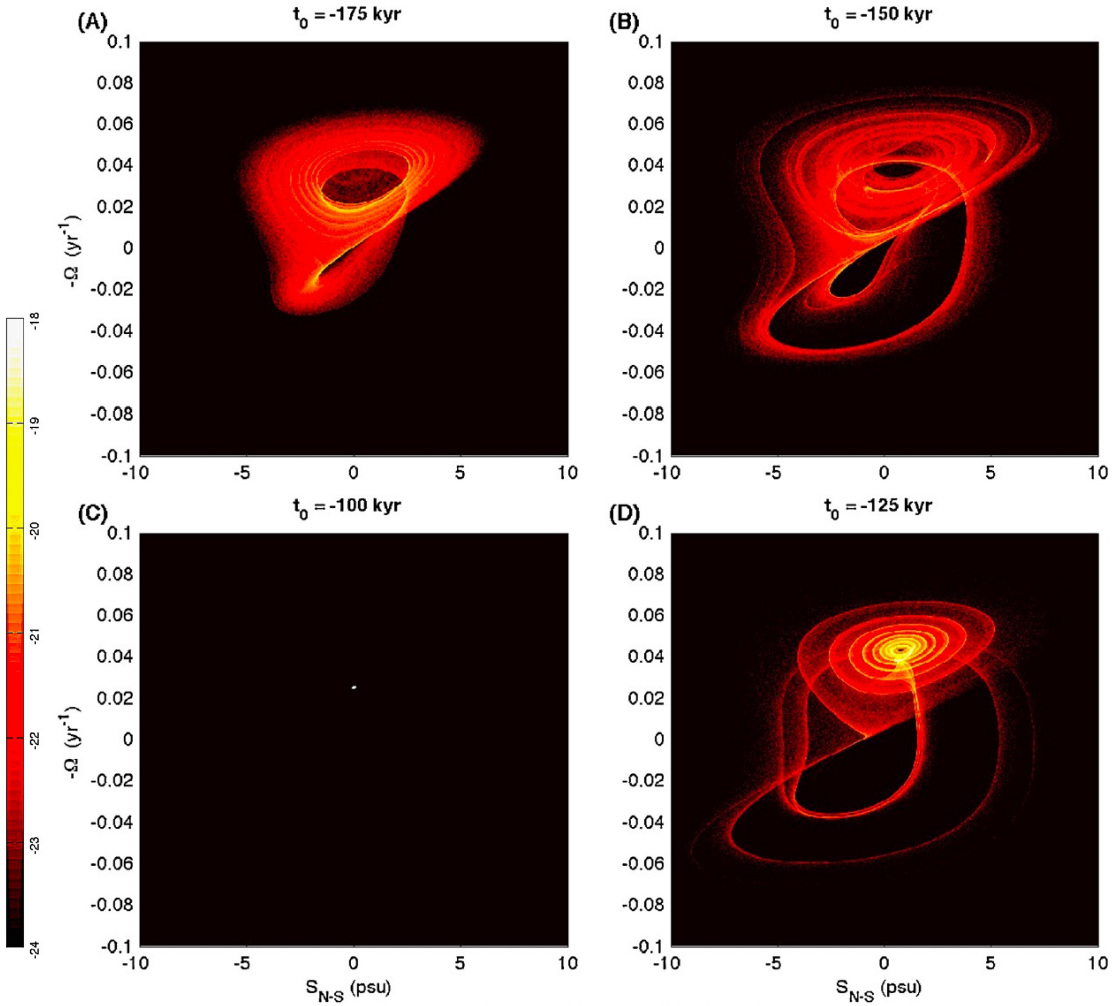

Earth and Planetary Science Letters 429 (2015) 60–68

Contents lists available at ScienceDirect

Earth and Planetary Science Letters

www.elsevier.com/locate/epsl

Unstable AMOC during glacial intervals and millennial variability: The role of mean sea ice extent

Florian Sévellec [a,*], Alexey V. Fedorov [b]

[a] Ocean and Earth Science, National Oceanography Centre Southampton, University of Southampton, Southampton, UK
[b] Department of Geology and Geophysics, Yale University, New Haven, CT, USA

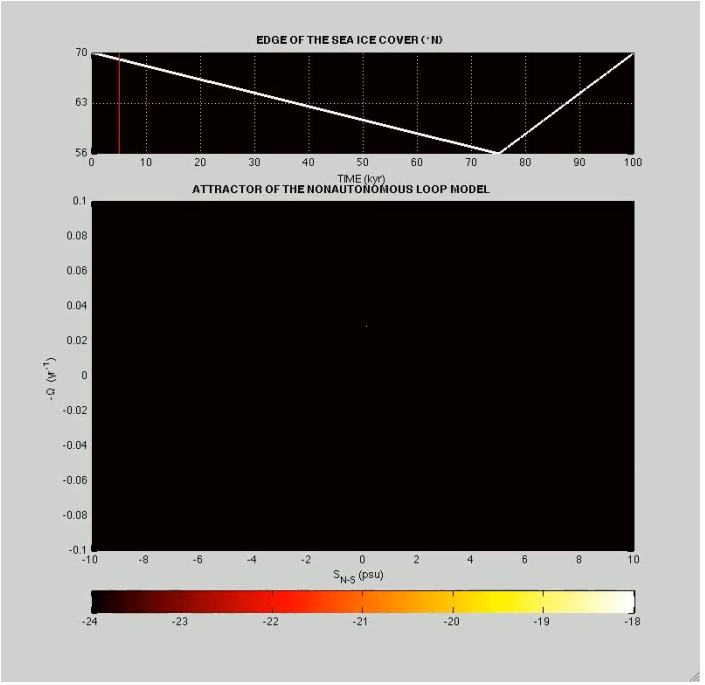

Templex

- Example IV: Unstable AMOC (non autonomous)

4D solutions: we obtain a cloud of four-dimensional points. We construct the **BraMAH** complex from this point cloud. The four-dimensional point cloud does not have false neighbors: it is related to an atonomous writing of the AMOC equations and can be used to build a templex.

```
-1.204390949016654645e-02 -3.755666436397816499e-01 1.306518394821738482e+00 1.348398174857631283e-02
-1.224216393305090946e-02 -4.105094258159222020e-01 1.302943763424306400e+00 1.348421537371332669e-02
-1.243740567030636977e-02 -4.455459503156868895e-01 1.297985263600033523e+00 1.348444899293549729e-02
-1.262932547193569219e-02 -4.806182011675594890e-01 1.291628288655764401e+00 1.348468260624273440e-02
-1.281761394464031763e-02 -5.156665152828940890e-01 1.283860898299330700e+00 1.348491621363492356e-02
-1.300196222019738522e-02 -5.506297133049842252e-01 1.274673984047107300e+00 1.348514981511196587e-02
-1.318206265102916247e-02 -5.854452473115573374e-01 1.264061403415025930e+00 1.348538341067376072e-02
-1.335760953344140682e-02 -6.200493585640195482e-01 1.252020112163938492e+00 1.348561700032020402e-02
-1.352829982505172543e-02 -6.543772419896768389e-01 1.238550270411638454e+00 1.348585058405119691e-02
-1.369383396027380913e-02 -6.883632413582051468e-01 1.223655375731521167e+00 1.348608416186663009e-02
-1.385391662238839167e-02 -7.219410390573020031e-01 1.207342364900948040e+00 1.348631773376640641e-02
-1.400825754992730994e-02 -7.550438634653665604e-01 1.189621705883329605e+00 1.348655129975042180e-02
-1.415657236815926791e-02 -7.876047132207103507e-01 1.170507470205472522e+00 1.348678485981857564e-02
-1.429858339870929487e-02 -8.195565760147025536e-01 1.150017391270899081e+00 1.348701841397076037e-02
-1.443402050473086007e-02 -8.508326700754310634e-01 1.128172909629967080e+00 1.348725196220687365e-02
-1.456262192774995280e-02 -8.813666883084957382e-01 1.104999200382378088e+00 1.348748550452682354e-02
-1.468413509473222647e-02 -9.110930350798221999e-01 1.080525186846978958e+00 1.348771904093049555e-02
-1.479831746114401020e-02 -9.399470891449953625e-01 1.054783525091836704e+00 1.348795257141779599e-02
-1.490493731082714705e-02 -9.678654534644385299e-01 1.027810576471543280e+00 1.348818609598861386e-02
-1.500377453792354869e-02 -9.947862054894188732e-01 9.996463597398603795e-01 1.348841961464285373e-02
-1.509462142964136840e-02 -1.020649159083170110e+00 9.703344758810172888e-01 1.348865312738041326e-02
-1.517728339478972496e-02 -1.045396106763873956e+00 9.399220267897770986e-01 1.348888663420118143e-02
-1.525157967480668918e-02 -1.068971066939994996e+00 9.084595025506267962e-01 1.348912013510506283e-02
-1.531734402118566096e-02 -1.091320526419735426e+00 8.760006462164051655e-01 1.348935363009195684e-02
-1.537442532355817737e-02 -1.112393665222866090e+00 8.426023160366005182e-01 1.348958711916175765e-02
-1.542268819799532883e-02 -1.132142579929327209e+00 8.083243076167658803e-01 1.348982060231436464e-02
```

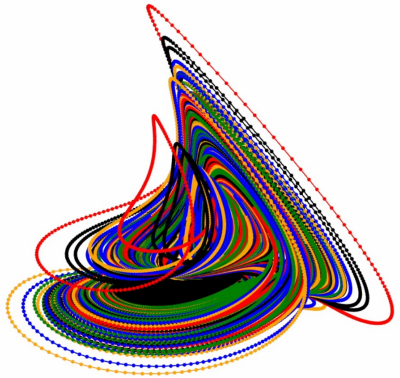

Templex

- Example IV: Unstable AMOC (non autonomous)

T(AMOC4D) = (K(AMOC4D), G(AMOC4D))

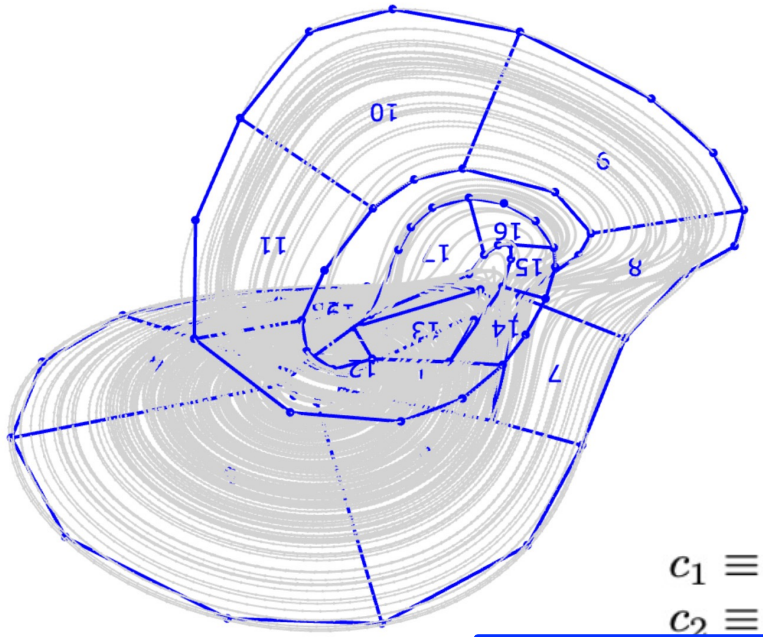

K(AMOC4D) has 3-cells
(basis: solid torus)

Three 1-holes in the BraMAH complex

3 stripexes
(1 twisted)

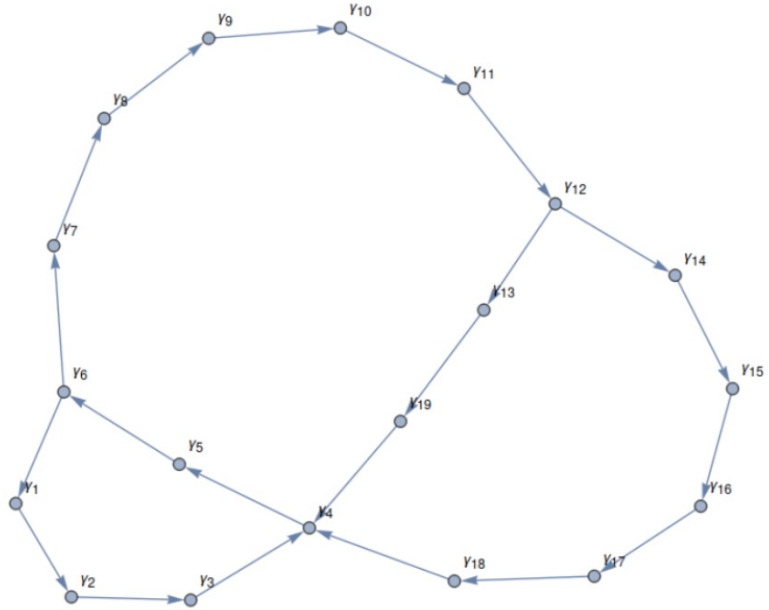

$$c_1 \equiv \underline{4} \to 5 \to 6 \to 1 \to 2 \to \underline{3}$$

$$c_2 \equiv 4 \to 5 \to 6 \to 7 \to 8 \to 9 \to 10 \to 11 \to 12 \to 13 \to 19$$

twisted $$c_3 \equiv \underline{4} \to 5 \to 6 \to 7 \to 8 \to 9 \to 10 \to 11 \to 12 \to 14 \to 15 \to 16 \to 17 \to \underline{18}$$

What is the relationship between the PBA approach and the 4D Templex structure?

Templex

- Example IV: Unstable AMOC (non autonomous)

The **templex** can be considered as a single static object of higher dimension, combining all the « parts » of the structure observed in the snapshot sequence in a PBA approach as a fonction of (t_0,t).

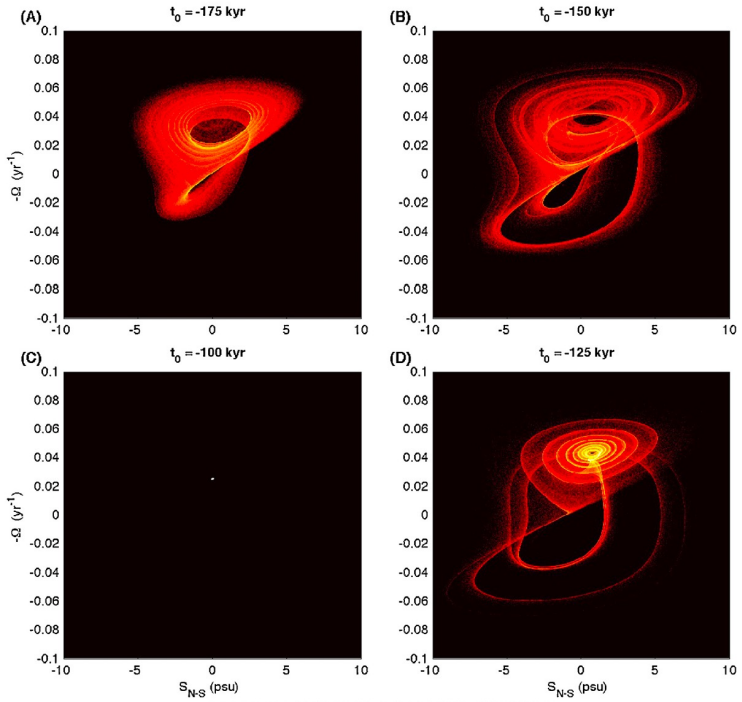

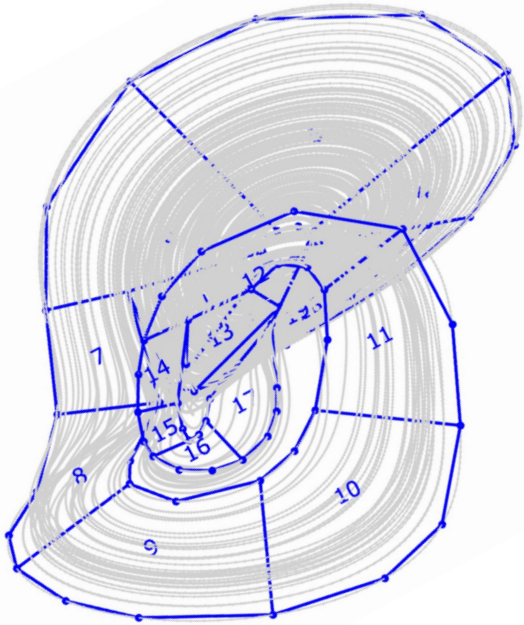

Working in higher dimensions may provide an alternative to working with the PBA approach.

Random Templex

- How is it defined?

The topological characterization of noise-driven chaos is a challenging issue that is crucial in the understanding of complex systems, where part of the dynamics remains unresolved and is modelled as noise.

While additive noise in a system of equations will blur the topological structure, multiplicative noise may radically change it [Chekroun et al, 2011].

[Charó et al, 2021] extended the concept of a branched manifold to account for the integer-dimensional set in phase space that robustly supports the system's invariant measure at each instant.

Such a branched manifold, however, does not contain any information about the future or the past of the invariant measure. The branched manifold is now itself time-dependent.

Random Templex

- How is it defined?

Home > Chaos: An Interdisciplinary Journal of Nonlinear Science > Volume 31, Issue 10 > 10.1063/5.0059461

Open • Submitted: 09 June 2021 • Accepted: 15 September 2021 • Published Online: 12 October 2021

Noise-driven topological changes in chaotic dynamics

Chaos **31**, 103115 (2021); https://doi.org/10.1063/5.0059461

Gisela D. Charó[1,2,a)], Mickaël D. Chekroun[3], Denisse Sciamarella[2,4], *and* Michael Ghil[5,6]

One cell complex per snapshot!

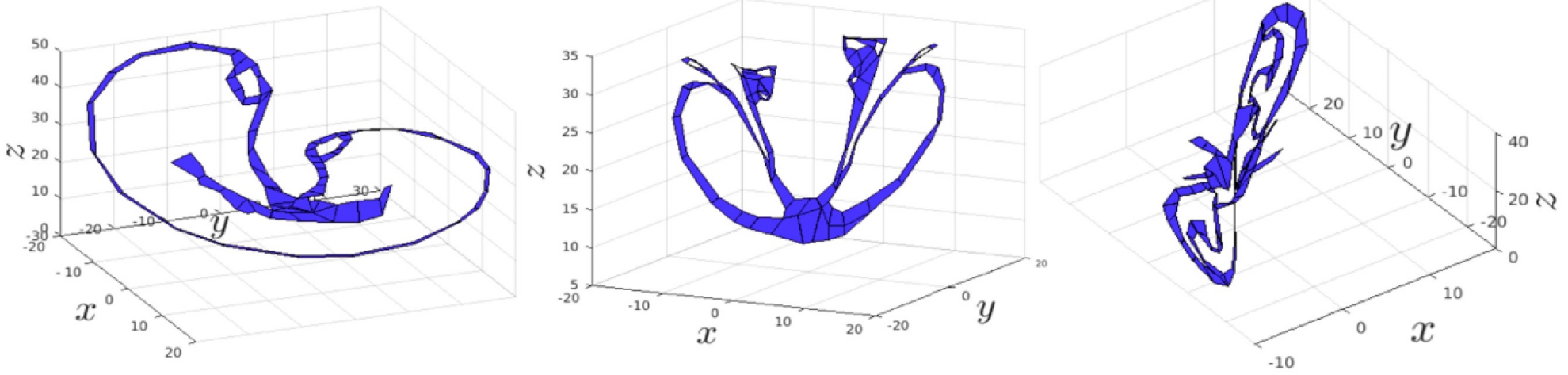

Random Templex

- How is it defined?

How can we track changes between different cell complexes? Tracking holes!

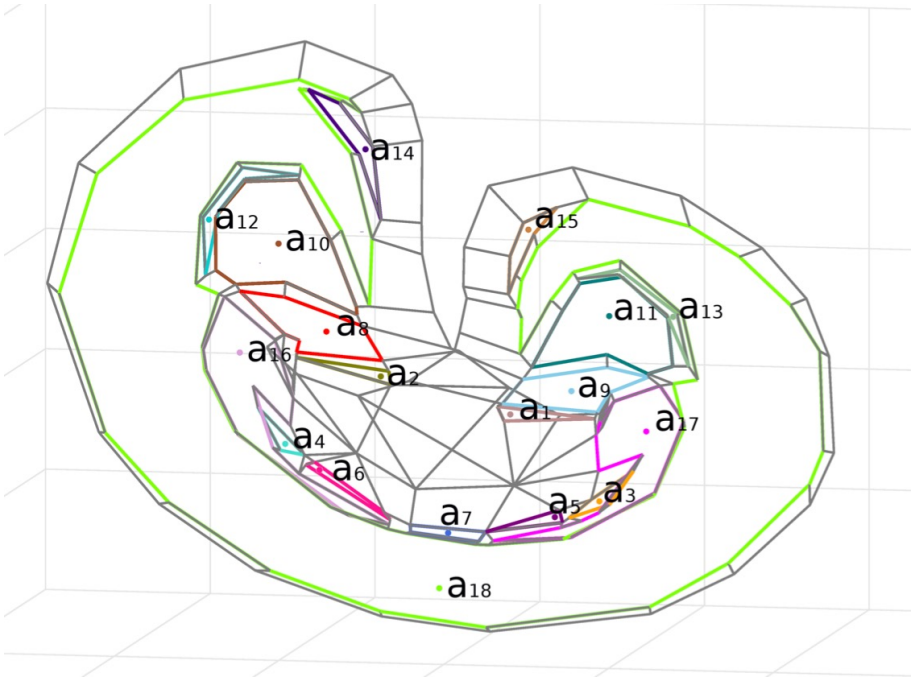

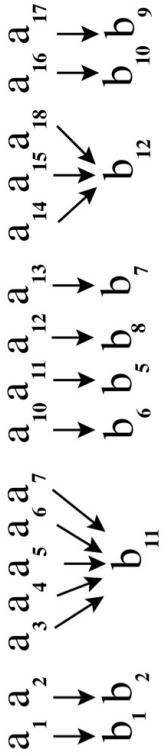

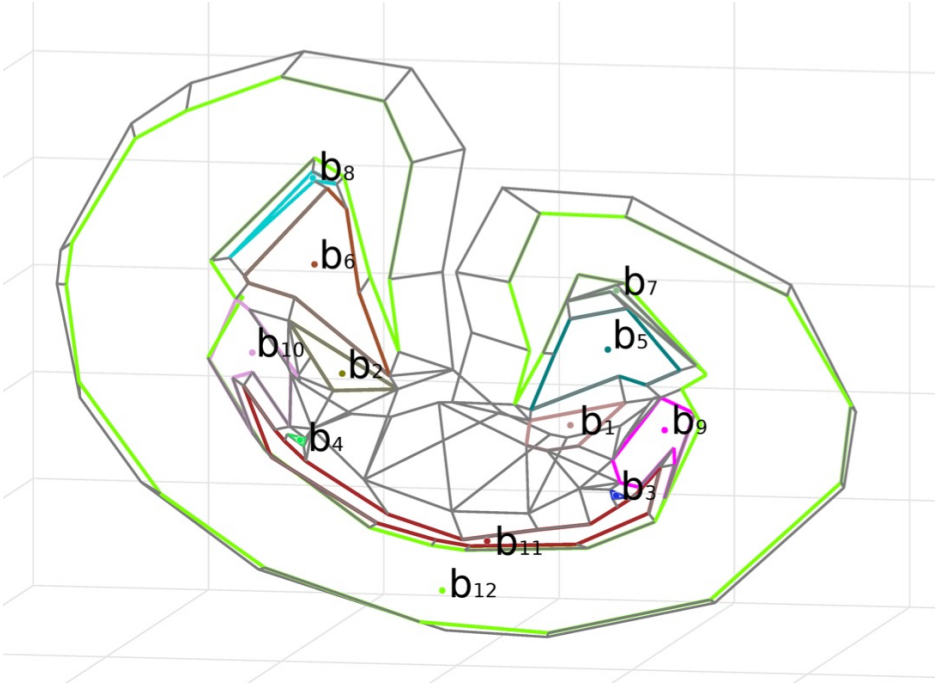

For a random attractor, the digraph does not connect cells, but holes of successive time cell complexes.

Random Templex

- How is it defined?

***A* random 2-templex R = (K, D) *is an indexed family* K *of BraMAH 2-complexes and a digraph* D.**

The digraph D is presented as a tree plot on the left. It has 15 singly connected components, each of which tells the story of one or several holes.

Tipping points can be identified and classified using the digraph.

They are highlighted in different colours according to the type of event: creation in green, destruction in black, splitting in red, merging in blue, and merging followed immediately by splitting in magenta.

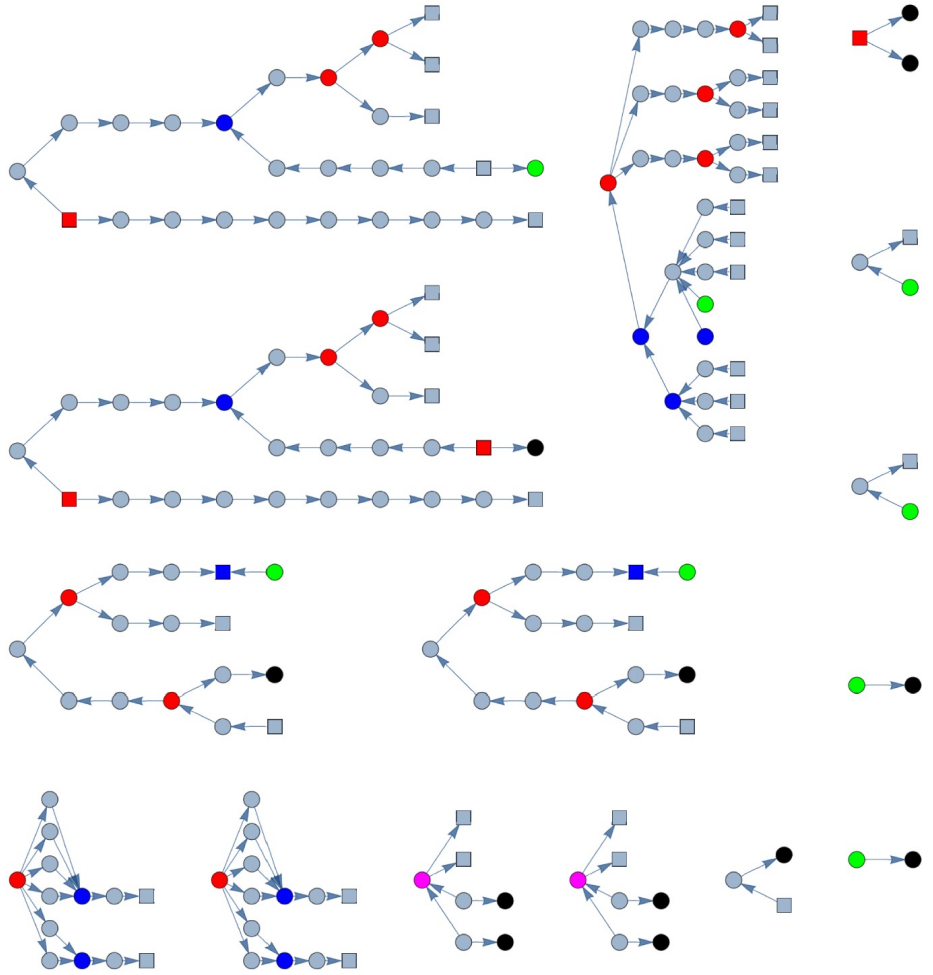

Random Templex

- How does it encode topological tipping points?

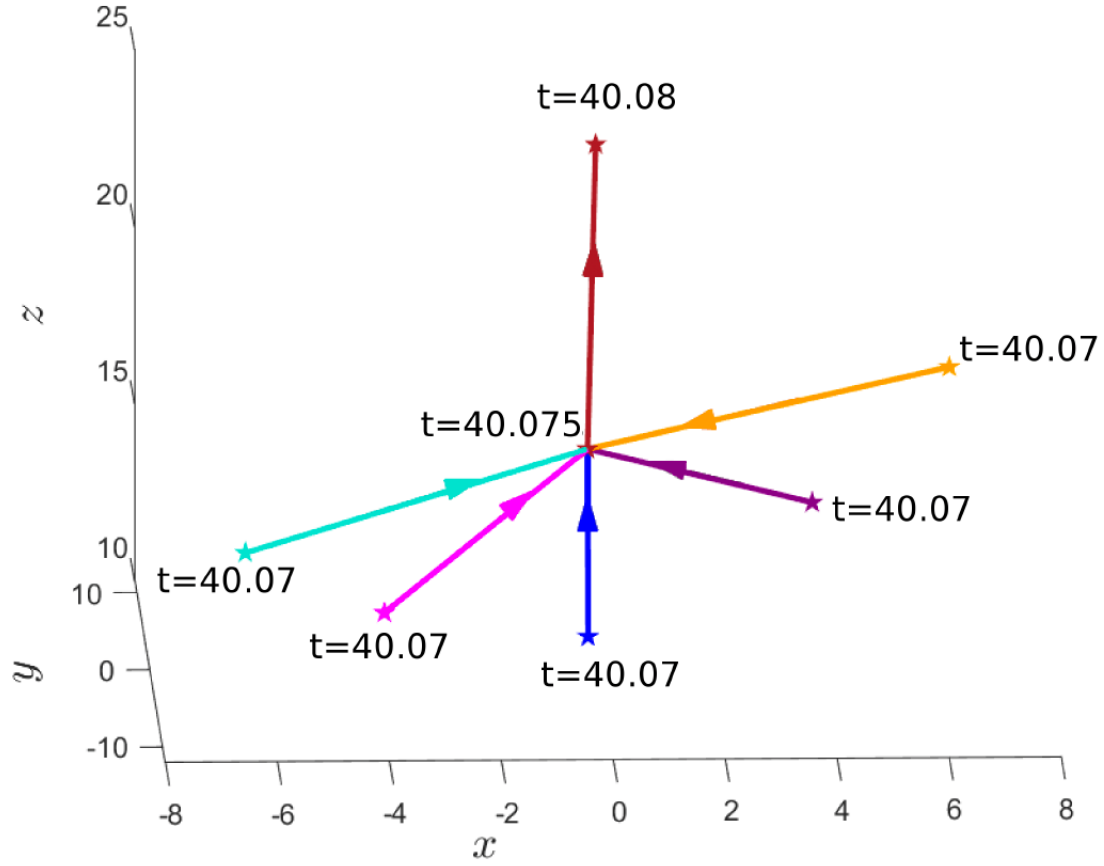

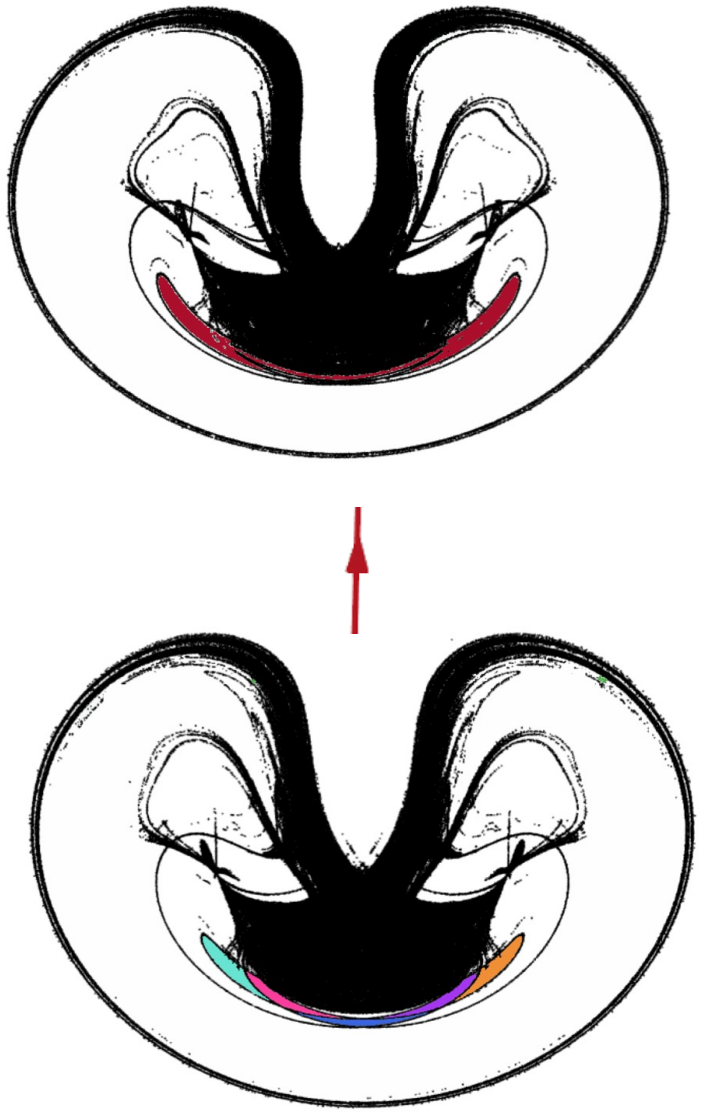

Merging event: a type of topological tipping point

Random Templex

- How does it encode topological tipping points?

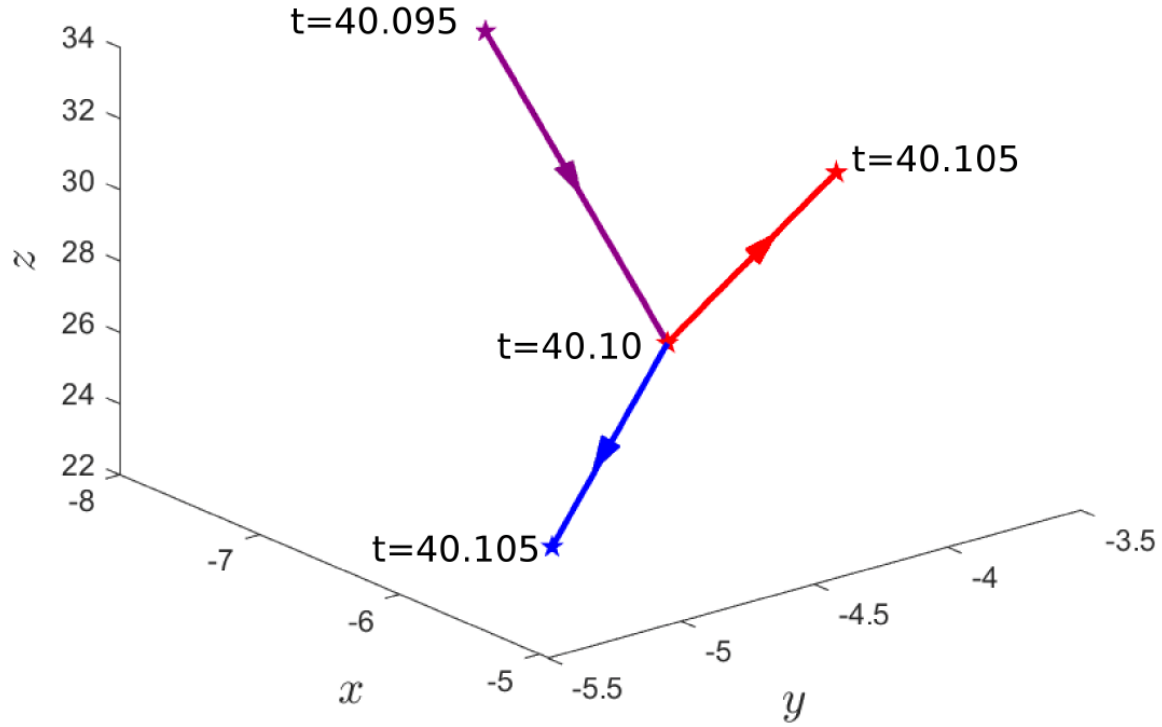

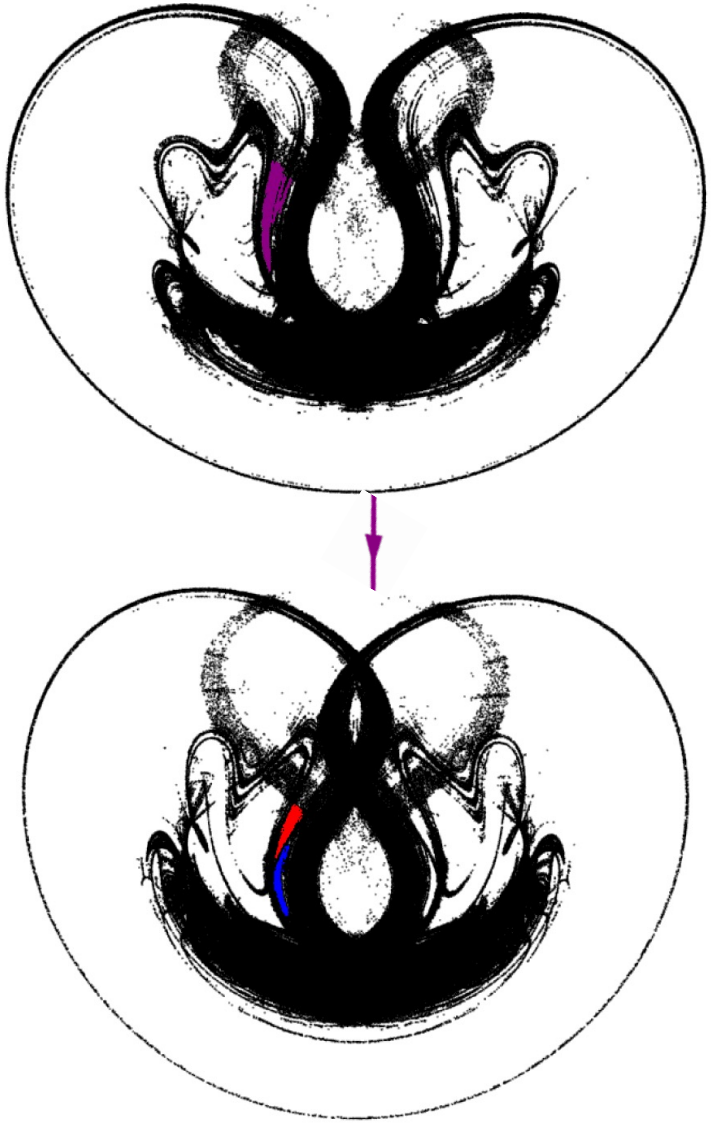

Splitting event: a type of topological tipping point

Random Templex

- How does it encode topological tipping points?

A better picture of how the holes are evolving in the system's phase space can be gained by using the coordinates of the barycenters of the holes for an embedding of D into this space. We call the embeddings of D's distinct connected components into phase space constellations.

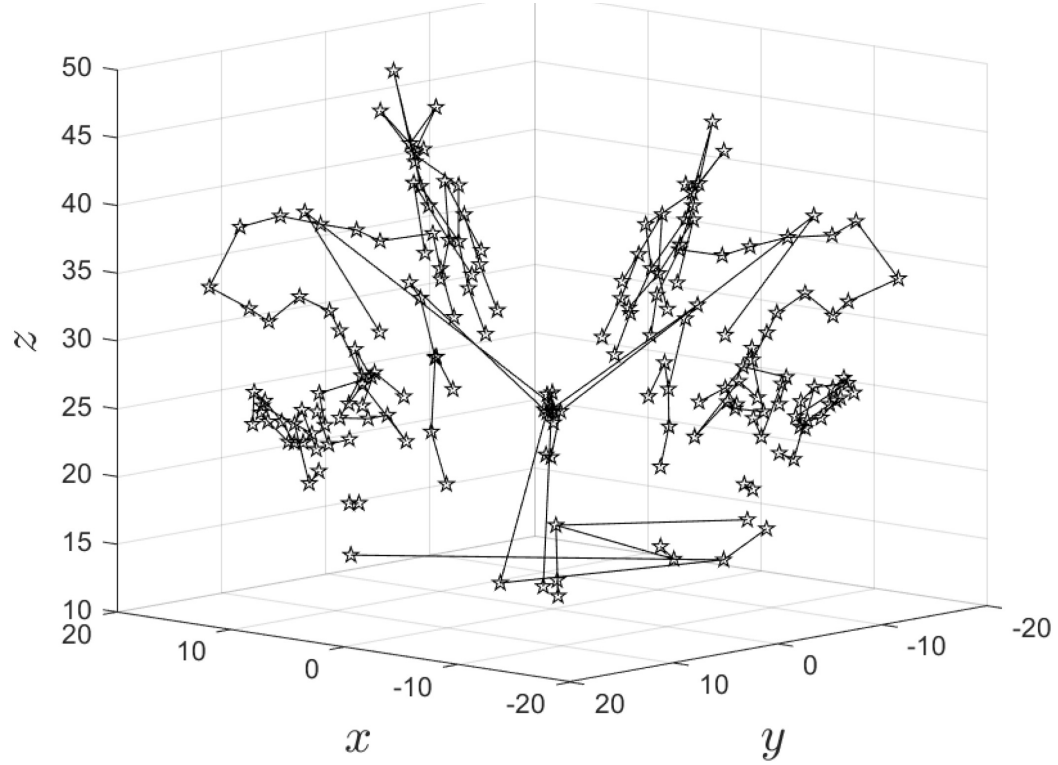

A constellation C is the set of immersed nodes and edges forming a connected component in the digraph D of a random templex.

Each node is immersed in the phase space using the coordinates of the corresponding hole's barycenter.

Concluding remarks

In this talk, we introduce novel tools into algebraic topology and used them to provide insights into the behaviour of deterministic and stochastically perturbed chaotic attractors.

- Attractors in state space can be studied using Branched Manifold Analysis through Homologies: this strategy constructs a cell complex from a cloud of points in state space and uses homology groups to characterize its topology.
- The approach, however, does not consider the action of the flow on the cell complex. The procedure is here extended to take this fundamental property into account, as done with templates.
- The goal is achieved endowing the cell complex with a directed graph that prescribes the flow direction between its highest-dimensional cells.
- The tandem of cell complex and directed graph, baptized templex, is shown to allow for a sophisticated characterization of chaotic attractors and for an accurate classification of them.
- In a random templex, there is one complex per snapshot of the random attractor and the digraph connects the generators or “holes” of successive cell complexes.
- Tipping points appear in a random templex as drastic changes of its holes in motion, namely their birth, splitting, merging, or death.

Max Planck Institute for the Physics of Complex Systems

SELECTED REFERENCES

Charó, G. D., Sciamarella, D., Mangiarotti, S., Artana, G., & Letellier, C. (2019) Observability of laminar bidimensional fluid flows seen as autonomous chaotic systems. Chaos, 29(12), 123126.

Charó, G. D., Artana, G., & Sciamarella, D. (2020) Topology of dynamical reconstructions from Lagrangian data. Physica D: Nonlinear Phenomena, 405, 132371.

Charó, G. D., Artana, G., & Sciamarella, D. (2021a) Topological colouring of fluid particles unravels finite-time coherent sets. Journal of Fluid Mechanics, 923.

Charó, G. D., Chekroun, M. D., Sciamarella, D., & Ghil, M. (2021b). Noise-driven topological changes in chaotic dynamics. Chaos, 31(10), 103115

Charó, G. D., Letellier, C., & Sciamarella, D. (2022a) Templex: A bridge between homologies and templates for chaotic attractors. Chaos, 32(8), 083108

Charó, G. D., Ghil, M., & Sciamarella, D. (2023) Random templex encodes topological tipping points in noise-driven chaotic dynamics, accepted, arXiv:2212.14450 [nlin.CD]

Chekroun, M. D., Simonnet, E., & Ghil, M. (2011). Stochastic climate dynamics: Random attractors and timedependent invariant measures. Physica D: Nonlinear Phenomena, 240(21), 1685-1700

Ghil, M., Chekroun, M. D., & Simonnet, E. (2008) Climate dynamics and fluid mechanics: Natural variability and related uncertainties, Physica D, 237, 2111–2126,

Ghil, M., & Lucarini, V. (2020) The physics of climate variability and climate change. Reviews of Modern Physics, 92(3), 035002

Ghil, M. and Sciamarella, D. (2023) Review Article: Dynamical Systems, Algebraic Topology, and the Climate Sciences, EGUsphere [preprint], Nonlinear Processes in Geophysics, in press.

Gilmore, R. (1998). Topological analysis of chaotic dynamical systems. Reviews of Modern Physics, 70(4), 1455.

Kelley, D. H., Allshouse, M. R., & Ouellette, N. T. (2013) Lagrangian coherent structures separate dynamically distinct regions in fluid flows. Physical Review E, 88(1), 013017.

Letellier, C., Stankevich, N. & Rössler, O. E. (2022) Dynamical Taxonomy: some taxonomic ranks to systematically classify every chaotic attractor. International Journal of Bifurcation & Chaos, 32 (2), 2230004.

Sciamarella, D., & Mindlin, G. B. (1999) Topological structure of chaotic flows from human speech data. Physical review letters, 82(7), 1450.

Sciamarella, D., & Mindlin, G. B. (2001) Unveiling the topological structure of chaotic flows from data. Physical review E, 64(3), 036209.

ACKNOWLEDGMENTS

Some of the ideas that led to the consideration of the *templex,* and its stochastic version came from stimulating discussions with Iván Sadofschi Costa (DM-UBA), Sylvain Mangiarotti (CESBIO) and Mickael D. Chekroun (Weizmann Institute of Science).

This work is supported by the French National program LEFE (Les Enveloppes Fluides et l'Environnement) and by the CLIMAT- AMSUD 21-CLIMAT-05 project.

Gislea D. Charó gratefully acknowledges her postdoctoral scholarship from CONICET.

This project has received funding from the EU Horizon 2020 research and innovation program under grant agreement No. 820970, and it helps support the work of Michael Ghil.

Denisse Sciamarella and Gisela D. Charó are personally grateful to the Visitor's program of the Max Planck Institute for the Physics of Complex Systems.

Special thanks to Claudia Domaschke, Michael Genkin and to the scientific coordinators, Peter Aswhin, Ulrike Feudel and Michael Ghil.